2013

Modeling temporal and spatial variations in dissolved oxygen in Amite River

Vahid Zahraeifard
Louisiana State University and Agricultural and Mechanical College, v.zahraee@gmail.com

MODELING TEMPORAL AND SPATIAL VARIATIONS IN DISSOLVED OXYGEN IN AMITE RIVER

A Dissertation

Submitted to the Graduate Faculty of the
Louisiana State University and
Agricultural and Mechanical College
in partial fulfillment of the
requirements for the degree of
Doctor of Philosophy

in

The Department of Civil and Environmental Engineering

by
Vahid Zahraeifard
B.Sc., Tabriz University, 2003
M. Sc., Shiraz University, 2006
M. E., Louisiana State University, 2011
August 2013

ACKNOWLEDGMENTS

First, I would like to extend my sincere gratitude to my major advisor Dr. Zhi-Qiang Deng for his supervision, support, and encouragement during my graduate studies at Louisiana State University. His critical suggestions and ideas made my research more interesting.

I would like to acknowledge and express gratitude to Prof. Dean Adrian and Prof. Clinton S. Willson for their time and constructive comments and suggestions which strengthened my dissertation. I also thank Dr. Aixin Hou for her serving on my dissertation committee and her comments. I am indebted to Prof. Malone for his time and efforts put into the review of my dissertation.

I also appreciate instructive discussions I had with Dr. Frank Tsai during my research work. I would like to thank all faculty and staff who helped me during my Ph.D. study here at LSU.

My wife, Sareh deserves huge appreciation for her unrestricted love, support, and inspiration. She is absolutely great. I would like to extend my deepest regards to my parents, sisters, and in-laws for their love and guidance.

Thanks to all friends for their company and affection.

TABLE OF CONTENTS

ACKNOWLEDGMENTS ii

LIST OF TABLES vi

LIST OF FIGURES vii

ABSTRACT x

CHAPTER 1 INTRODUCTION 1

1.1. Background 1

1.2. Study Area 3

1.3. Goals and Objectives 4

1.4. Scope and Organization of Dissertation 5

1.5. References 10

CHAPTER 2 VART MODEL-BASED METHOD FOR ESTIMATION OF INSTREAM DISSOLVED OXYGEN AND REAERATION COEFFICIENT 12

2.1. Introduction 12

2.2. Materials and Methods 14

2.2.1. VART Model for DO Simulation 14

2.2.2. Inverse Modeling 17

2.2.3. Observed Data 19

2.2.4. Sensitivity Analysis 20

2.3. Results 23

2.3.1. Scenario I: Reaeration Coefficient with E=0 23

2.3.2. Scenario II: Reaeration Coefficient with Strong Longitudinal Dispersion 25

2.3.3. Scenario III: Reaeration Coefficient with Weak Longitudinal Dispersion 25

2.4. Discussion 26

2.5. Comparison of VART-DO with other models and main contributions of this chapter 31

2.6. Conclusion 34

2.7. References 35

CHAPTER 3 WATERSHED MODELING OF AMITE RIVER FOR ESTIMATION OF BOD LOADING 39

3.1. Introduction 39
3.2. Materials and Methods 40
3.2.1. Better Assessment Science Integrating point and Non-point Sources (BASINS) 40
3.2.2. Hydrological Simulation Program- FORTRAN (HSPF) 43
3.3. Results 48
3.3.1. Simulation of flow discharge in the Amite River 48
3.3.2. Simulation of dissolved oxygen and biochemical oxygen demand in the Amite River 48
3.3.3. Land use and land cover changes across the Amite River watershed 49
3.4. Discussion and Conclusion 49
3.5. References 53

CHAPTER 4 MODELING SEDIMENT RESUSPENSION-INDUCED DO VARIATION IN FINE-GRAINED STREAMS 55
4.1. Introduction 55
4.2. Materials and Methods 58
4.2.1. Conceptual Model for In-Stream Dissolved Oxygen 58
4.2.2. Numerical Model for In-Stream Dissolved Oxygen 58
4.2.3. Study Area 62
4.2.4. Data Collection 63
4.2.5. Determination of model parameters 64
4.2.6. Sensitivity Analysis of VART-DOS Model 66
4.3. Applications of VART-DOS model to Amite River 68
4.4. Comparison of VART-DOS with other DO models and main contributions of this chapter 71
4.5. Conclusions 73
4.6. References 74

CHAPTER 5 MODELING SPATIAL VARIATIONS IN DISSOLVED OXYGEN IN FINE-GRAINED STREAMS UNDER UNCERTAINTY 77
5.1. Introduction 77
5.2. Materials and Methods 79
5.2.1. Study River Reach – Lower Amite River 79
5.2.2. Triple-Layer Conceptual Model for Instream DO Fluxes and Processes 81
5.2.3. Mathematical Model for Spatial Variations in DO: VART DO-3L Model 84

5.2.4. Estimation of VART DO-3L Model Parameters 86
5.2.5. Sensitivity Analysis of Model Input Parameters 88
5.2.6. Computation of Sediment Oxygen Demand (SOD) 92
5.3. Results 93
5.3.1. Sensitivity Analysis Results 93
5.3.2. Simulation Results for DO under High R Value Cases (Scenario 1) 96
5.3.3. Simulation Results for DO under Moderate R Value Cases (Scenario 2) 97
5.3.4. Simulation Results for DO under Low R Value Cases (Scenario 3) 98
5.3.5. Simulation Results for DO under Additional Cases 99
5.3.6. Simulation Results for Spatial Variations in DO and SOD 100
5.3.7. Mapping Longitudinal Variations in DO and SOD along Amite River 102
5.4. General Discussion 105
5.5. Conclusions 108
5.6. References 109

CHAPTER 6 SUMMARY OF MAJOR FINDINGS AND DISCUSSION 114
6.1. Summary 114
6.2. Discussion of Future Work 116

VITA 118

LIST OF TABLES

Table 2-1- Results of sensitivity analysis in terms of RMSE/percent change of RMSE..... 23

Table 2-2- Results of sensitivity analysis for reaeration coefficient..... 23

Table 2-3- Selected values for different river reaches based on optimization..... 27

Table 2-4- Processes considered by different models..... 34

Table 4-1- Geometry and sediment parameters of Amite River..... 64

Table 4-2- Sensitivity analysis of sediment resuspension parameters..... 67

Table 4-3- Effects of BOD and SOD on DO change along the Amite River..... 68

Table 5-1- Results of cases in scenario 1..... 97

Table 5-2- Results of cases in scenario 2..... 98

Table 5-3- Results of cases in scenario 3..... 99

LIST OF FIGURES

Figure 1.1- Percentage impairment of river reaches for different states calculated according to information from EPA website. (*) defines the percentage based on impaired reach length (mile) to the total length examined; otherwise, the number of DO-related impairments to the total number of impairments was used to calculate the percentage of impairment 2

Figure 1.2-Amite River watershed location and monitoring stations 4

Figure 1.3- Flowchart showing relationship among dissertation chapters 5

Figure 1.4- Causal relationship among DO changes and stressors with system response to changes 7

Figure 2.1- Typical Cross-Section of a Stream and its Storage Zones 15

Figure 2.2- DO deficit data calculated for a reach along Clinch River using measured data by Churchill et al. (1996). 21

Figure 2.3- Comparison of reaeration coefficient of VART and empirical equations when dispersion is neglected; E=0.0. 24

Figure 2.4- Comparison of reaeration coefficient of VART and empirical equations considering the dispersion coefficient with $\psi=15$ in the *Eq. 15.* 26

Figure 2.5- Comparison of reaeration coefficient of VART and empirical equations considering dispersion coefficient with $\psi=1$ *in the Eq. 15.* 26

Figure 2.6- Comparison of RMSEs corresponding to K_2 from Churchill equation and inverse-VART 29

Figure 2.7- Comparison of RMSEs corresponding to the K_2 of Owens equation and inverse VART calculation 29

Figure 2.8- Comparison of RMSEs corresponding to the K_2 of Dobbins equation and inverse VART calculation 30

Figure 2.9- Comparison of RMSEs corresponding to the K_2 of Langbein equation and inverse VART calculation 30

Figure 2.10- Comparison of RMSEs corresponding to the K_2 of Bansal equation and inverse VART calculation 31

Figure 3.1- Right: Amite River model in BASINS; Left: various data layers 41

Figure 3.2- Amite River watershed and river systems in BASINS4 43

Figure 3.3- Soil, land use/cover across Amite River watershed in BASINS4..... 44

Figure 3.4- Digital elevation map of Amite River watershed in BASINS4 45

Figure 3.5- Sub-watersheds delineated across Amite River watershed and outlets in BASINS4 46

Figure 3.6- Meteorological stations across Amite River watershed and Baton Rouge station encircled in BASINS4..... 47

Figure 3.7- Upper panel: simulated and observed flow in Amite River. Lower panel: flow duration curves after calibration 50

Figure 3.8- Simulated DO concentration at Denham Springs; up: for July 1990 and down: for the year 1990 51

Figure 3.9- BOD input from Amite River watershed: a) for January 1990; b) for July 1990 52

Figure 3.10- Comparison of land use/land covers across the Amite River watershed 53

Figure 3.11- Land use/land cover changes in the Amite River watershed 53

Figure 4.1- Flow, erosion rate, and DO concentration at Port Vincent Station during July 1990 in Amite River..... 56

Figure 4.2- Mechanisms that affect DO changes along a river..... 58

Figure 4.3- Map of Amite River watershed showing the study reach from Denham Springs to Port Vincent 64

Figure 4.4- BOD Input from Amite River watershed: a) for January 1990; b) for July 1990 65

Figure 4.5- DO change at Port Vincent for January 1990 70

Figure 4.6- DO change at Port Vincent for July 1990 71

Figure 5.1- Map of Amite River watershed showing the study reach from Denham Springs to Port Vincent 80

Figure 5.2- Land use and land cover in the Amite River watershed..... 81

Figure 5.3- (a) Vertical profile of a typical streams including water column, advection-dominate storage zone and diffusion-layer and (b) Longitudinal profiles and the processes that affect DO changes 83

Figure 5.4- Probability density function for storage zone size 91

Figure 5.5- Probability density function for residence time T_V (hours) 91

Figure 5.6- First order sensitivity indices based on DO data from first six days of July 1990 94

Figure 5.7- Total sensitivity indices based on DO data from first six days of July 1990 95

Figure 5.8- Vertical DO concentration ratio relative to DO concentration in water column at Denham Springs station (a-Case 5), Port Vincent station (c- Case 34), and a third station in between (b). 101

Figure 5.9- SOD variation along Amite River under different conditions 102

Figure 5.10- Spatial variation of DO along Amite River for case 2 103

Figure 5.11- Watershed-scale map showing DO variation along Amite River 104

Figure 5.12- Reach-scale map showing DO variation along Amite River 104

Figure 5.13- Spatial variations of SOD along Amite River between Denham Springs and Port Vincent Stations 105

ABSTRACT

A watershed-based modeling framework is developed in this dissertation for simulating temporal and spatial variations in DO in lowland rivers with organic-rich fine-grained sediment. The modeling framework is based on three major contributions/new models, including (1)VART-DO model for improved estimation of reaeration coefficient (K_2) in natural streams, (2)VART-DOS model for simulation of temporal variations in DO in response to sediment resuspension, and (3)VART DO-3L model for simulation of spatial variations in DO.

A major advantage of VART-DO model is the capability of simulating DO exchange across the water-sediment interface through the hyporheic exchange mechanism in addition to the air-water exchange. Simulation results from VART-DO model revealed that hyporheic exchange can reduce K_2 by 30% while longitudinal dispersion increases K_2 by 50%.

VART-DOS model is developed for simulation of temporal variations in DO particularly due to sediment resuspension effect during high flow. Application results of VART-DOS model to the Amite River in Louisiana showed that 83% of DO consumption in water column in July 1990 was because of sediment resuspension.

A novel feature of VART DO-3L model is that a fine-grained stream with the flocculent layer can be vertically modeled with three layers: overlying water column, an advection-dominated storage zone, and a diffusion-dominated storage zone in relatively consolidated stream bed-sediment. While the importance of flocculent layer to instream DO has been widely reported, VART-DO-3L model is the first modeling tool that incorporates the flocculent layer into DO modeling. This is a unique feature of VART-DO-3L model, making it possible for determining both longitudinal and vertical profiles of DO in streams. Results of VART-DO-3L for the Amite River indicated that the DO level decreases longitudinally from 7.9mg/L at the

Denham Springs station to 2.89mg/L at the Port Vincent station. Vertically, DO level drops rapidly from overlying water column to the advection-dominated storage zone and further to the diffusive layer. The DO level in the advective layer is about 40% of that in water column. The thickness of the diffusive layer varies between 0-10mm, depending on effective diffusion coefficient.

Developed models in this dissertation are also applicable to sandy/gravel rivers.

CHAPTER 1
INTRODUCTION

1.1. Background

Dissolved Oxygen (DO) concentration is the most important water quality indicator for aquatic environments that support aquatic life. DO in rivers and streams is produced and consumed dynamically. Therefore, DO concentration within stream systems fluctuates based on rates of its production and consumption (USEPA, 2010). In order to maintain aquatic life in rivers, estuaries and coastal waters, EPA recommend water quality criteria for DO. Based on these criteria, EPA has identified the river reaches impaired by oxygen consuming pollutants. Figure 1.1 depicts the percentage of river reaches impairment identified so far for different states across the United States. It can be seen from the figure that DO impairment is a serious threat to rivers in almost all states.

The main mechanism responsible for oxygen production in river environments is reaeration at the atmosphere-water interface. Plant photosynthesis also produces oxygen in the water column. Unlike production processes, DO consumption mechanisms may vary significantly from respiration of living species within the water to decomposition of organic materials through biochemical reactions and further by reactions at the water-sediment interface. Thus, a comprehensive study on DO variations in rivers should include transfer of oxygen across atmosphere-water and water-sediment interfaces. Numerical modeling of water quality has been used to describe spatial and temporal variations in constituent of concern (Motta et al., 2010). For DO concentration evaluation, the simplified Streeter-Phelphs (1925) model has been further improved over the past decades to get more realistic results by incorporation of additional terms and mechanisms (Motta et al., 2010).

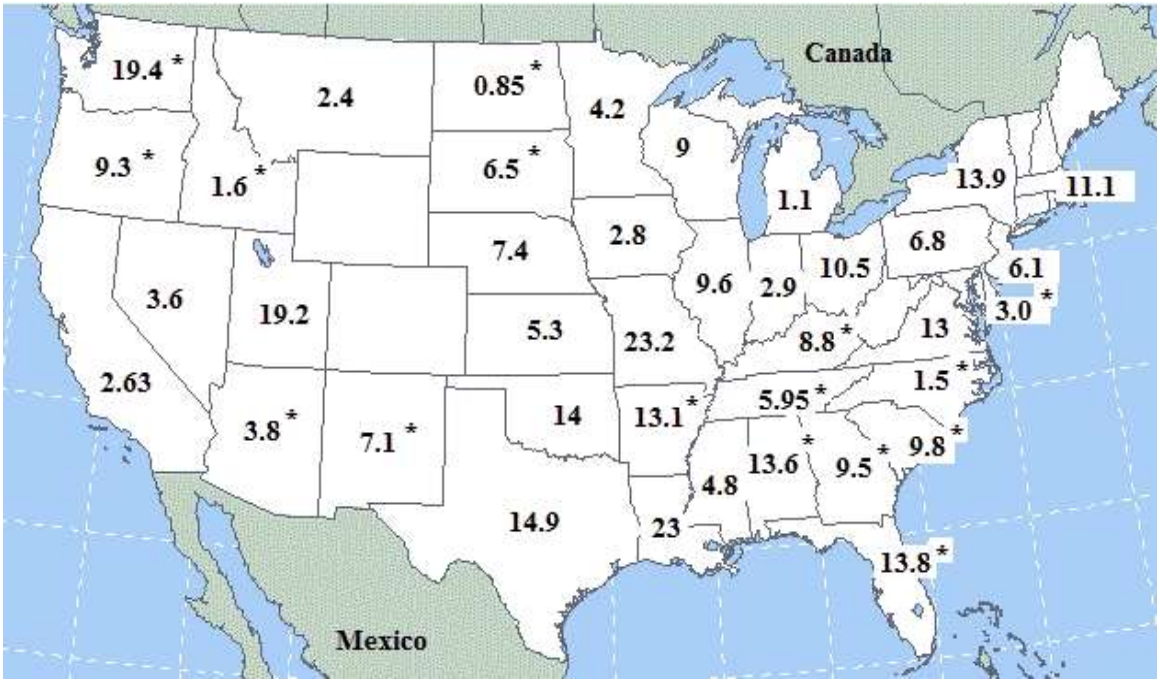

Figure 1.1- Percentage impairment of river reaches for different states calculated according to information from EPA website. (*) defines the percentage based on impaired reach length (mile) to the total length examined; otherwise, the number of DO-related impairments to the total number of impairments was used to calculate the percentage of impairment.

For example, Chapra (1997) introduced a comprehensive model for evaluation of oxygen cycle in aquatic environments. Chapra and Runkel (1999) considered the effect of storage zone (dead zone, hyporheic exchange) on dissolved oxygen variations below a point source to investigate the significance of such physical process. Graves et al. (2004) examined water quality characteristics of storm water runoff from major land uses in south Florida. They captured frequent low dissolved oxygen conditions as a consequence of runoff event from the watershed. They also defined a DO concentration for each land type. According to Welch et al. (1998) land cover change, especially removal of riparian vegetation, as well as land use alteration generally results in increased erosion, increased algal production, changes to temperature regimes, and reduced concentration of DO. Duan et al. (2008) collected land use/land cover data from two

different datasets to study water quality change in Saint Louis Bay watershed in Mississippi. In addition, various studies were undertaken to address DO-related water quality issues in different rivers (Cox, 2003) by means of modeling tools. While extensive efforts have been made in improving DO modeling, no existing model is generally perfect for instream DO estimation due to the diversity of factors controlling DO variations, such as hyporheic exchange, air-water interaction, and instream geochemical processes.

While billions of dollars in federal, state, and local funds have been spent on development and implementation of dissolved oxygen TMDLs plans the validity and usefulness of plans contingents on thorough identification and determination of various processes that affect dissolved oxygen changes in river systems. Furthermore, environmental changes like low flow condition, high flow condition, land use/cover have impact on dissolved oxygen changes in rivers.

1.2. Study Area

The Amite River watershed is selected for the present research. Amite River watershed is one of the fast growing areas in the southeast Louisiana (Figure 1.2). It includes the metropolitan area of Baton Rouge with the population of 227000 (Patil, 2009) and has major industrial areas in the region. The Amite River has the biggest watershed in the Lake Pontchartrian basin and has been impaired due to low dissolved oxygen. The Amite River watershed experiences a typical subtropical humid climate with mild winters (November through April) and hot summers (May through October), and abundant rainfall. Annual average temperature varies from 19 to 21^{o}C (66 to 69^{o}F) with July averaging 28^{o}C (82^{o}F) and January averaging 12^{o}C (53^{o}F).

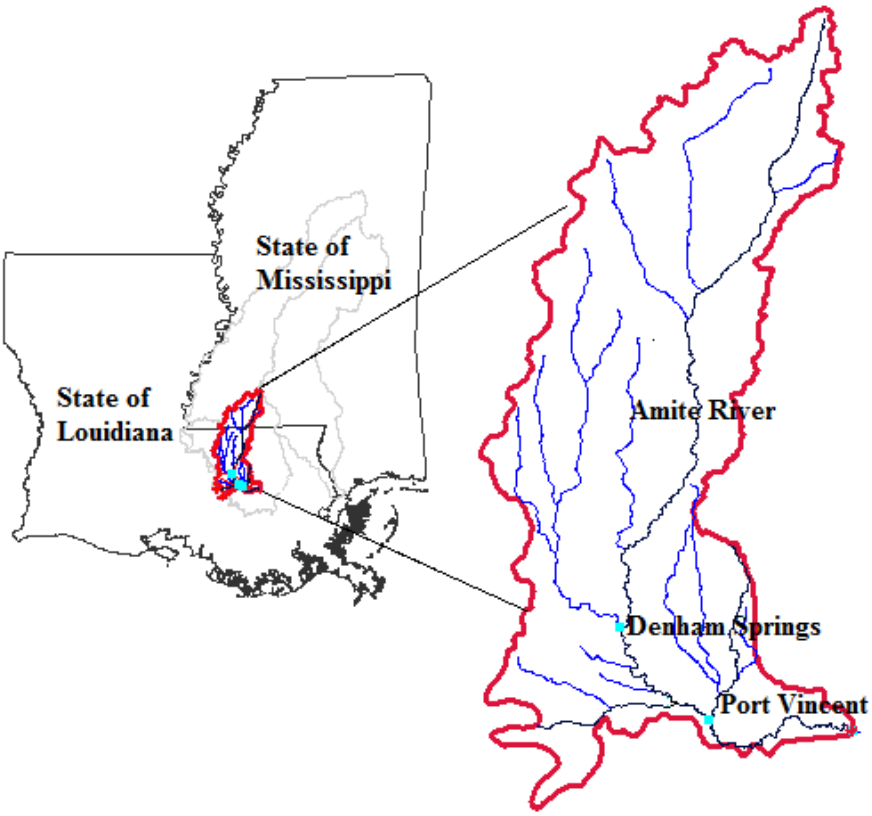

Figure 1.2-Amite River watershed location and monitoring stations

1.3. Goals and Objectives

The overall goal of this study is to improve our understanding of instream DO variations in response to environmental changes at temporal and various spatial scales ranging from catchment scale to river reach and further to station scales. As stated, aquatic life requires oxygen dissolved in the water column for survival. Accurate determination of DO in impaired rivers/streams would help us define best management practices more efficiently. Based on Figure 1.3, the specific objectives of this dissertation are:

(1) to improve and re-calculate the reaeration coefficient by incorporating hyporheic exchanges and dispersion process into governing equations;

(2) to determine temporal variation in dissolved oxygen in the Amite River with emphasis on the effect of sediment resuspension on DO, and

(3) to model and map spatial variation in dissolved oxygen along the Amite River, and

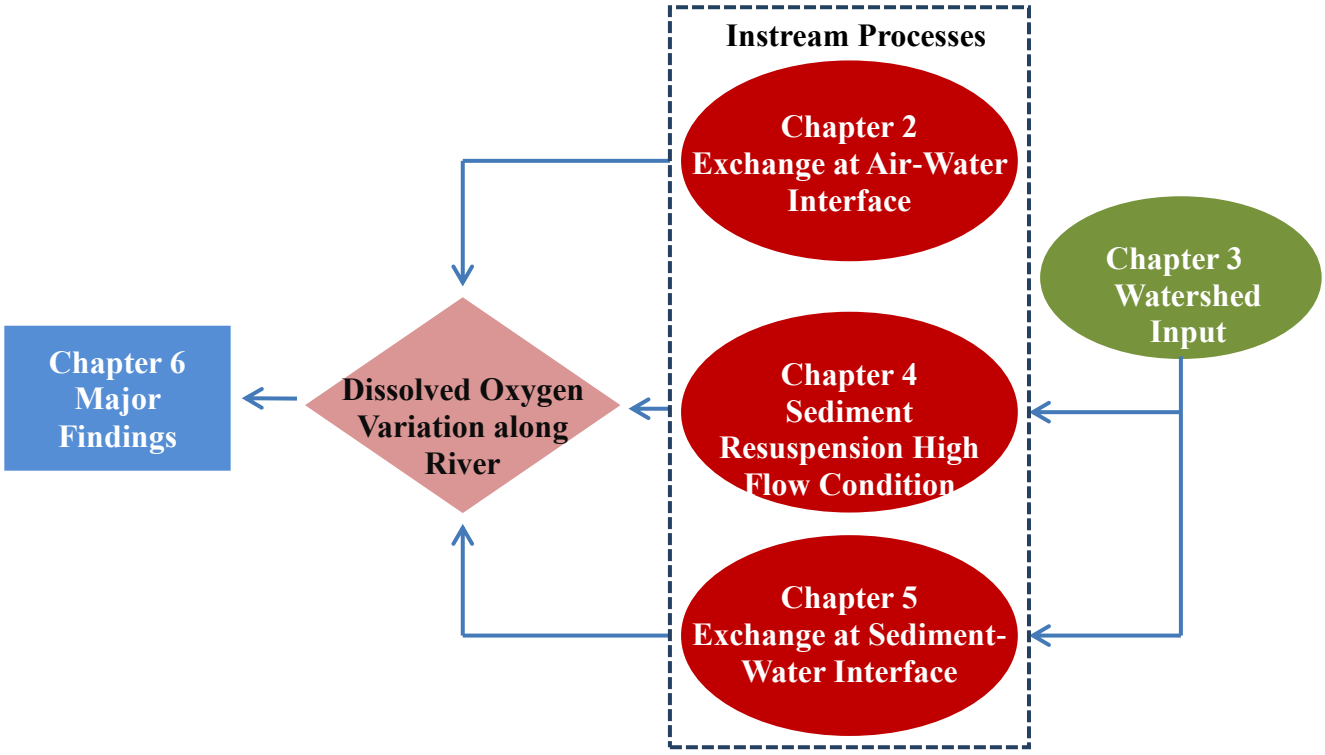

Figure 1.3- Flowchart showing relationship among dissertation chapters

1.4. Scope and Organization of Dissertation

There are numerous causal relationships between DO fluctuation and stressors in aquatic environment according to US EPA, as shown in Figure 1.4. Addressing all of these relationships in a single study is rather implausible. The incorporation of all processes into a single model makes parameterization and calibration of the model difficult, if not impossible, due to the requirement of large amounts of data which are not readily available. In addition, some of the causal links in Fig. 1.4 become unimportant under certain conditions. Therefore, widely used models are not usually suited (Vellidis et al., 2006). For instance, the simulation of DO by using

WASP model may require the evaluation of more than 70 parameters if all interacting processes are incorporated. While this dissertation intends to keep DO modeling as simple as possible, the focus is more on hydrologic and hydraulic processes responsible for DO changes along rivers/streams. Unlike conventional modeling of DO, the effect of storage zones (hyporheic exchange) on DO variation is considered in the present study. The hyporheic exchange process accounts for exchange of DO between the main river channel and surrounding environment. Thus, a river system is considered as an integrated system involving mass exchanges between surface and subsurface water and between main channel and side pockets along the main channel. In addition, the assumption of plug-flow was employed in previous studies which are mostly based on Streeter-Phelps model. The assumption of plug-flow ignores the actual mixing that takes place particularly in rivers. Mixing is important to the exchange of oxygen at atmosphere-water interface. Thus, mixing processes, including dispersion and hyporheic exchange processes, are included in the simulation of DO changes in this dissertation. In next chapter, such interactions are examined and evaluated.

Considering effects of watershed-scale land use/land cover changes and non-point source BOD loadings on instream DO variations is a new feature of the present dissertation. The main contribution of this dissertation is, however, to present modeling tools which are capable of capturing temporal and spatial variations in DO along rivers/streams. To this end, the effect of sediment resuspension on DO concentration in water column during high flow condition was incorporated into in the governing equations of DO changes. Furthermore, a new approach was introduced to computing primarily vertical DO changes at various spatial scales in low land river

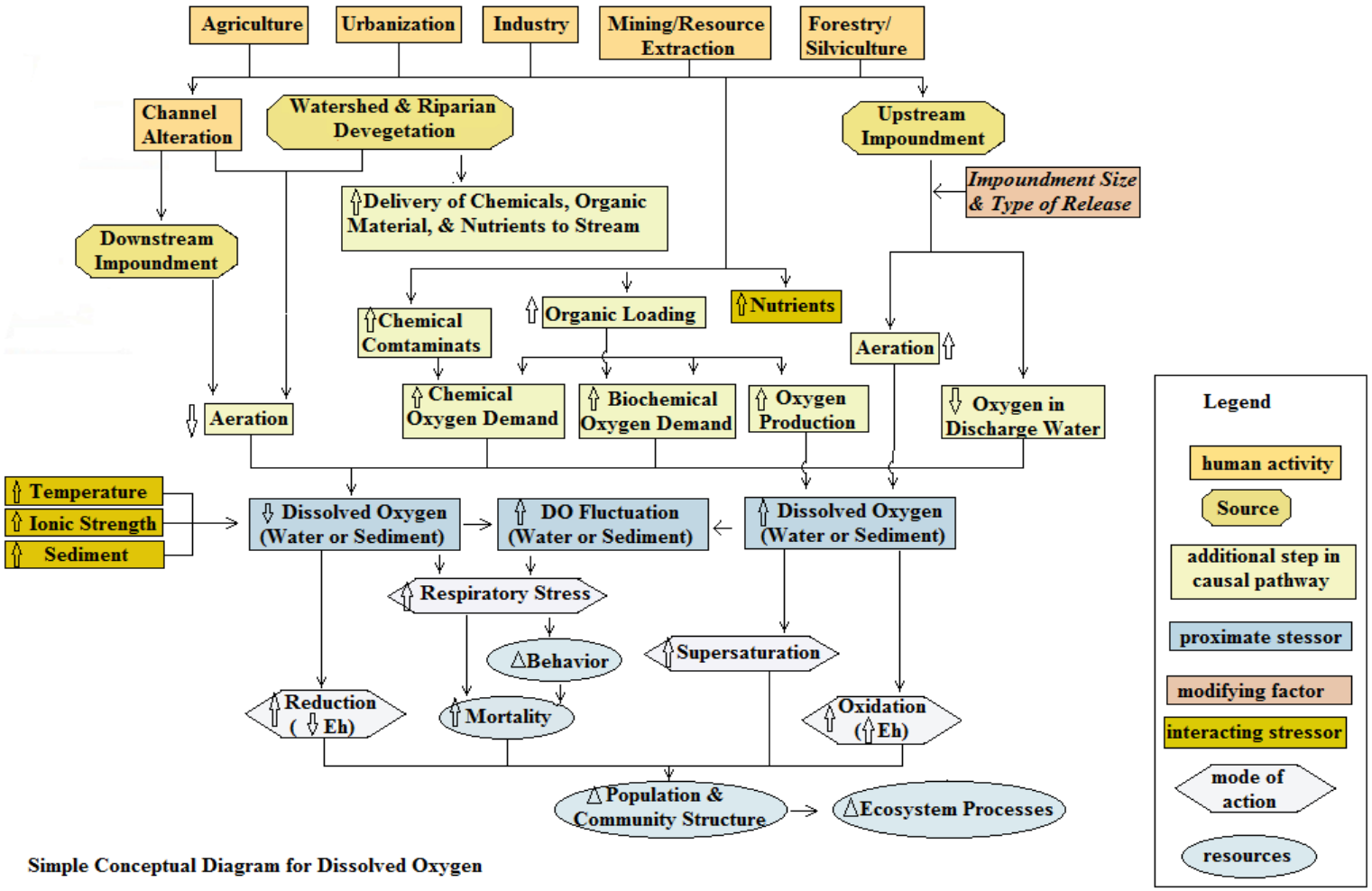

Simple Conceptual Diagram for Dissolved Oxygen

Figure 1.4- Causal relationship among DO changes and stressors with system response to changes

[Re-draw from original diagram; Source USEPA website, 2011]

or streams with organic-rich fine-grained bottom sediments during low flow condition. Although this dissertation considers the impact of anthropogenic practices through land-use and land cover change, it does not explicitly include biochemical reactions due to presence of organic materials, nutrients, chemical contaminants, and reduced metals. More specifically, oxidation and reduction capacities, algal bloom effect, and carbon fixation effect are not directly considered in this study. While lumped effects of these DO-consuming processes are considered in proposed models, the main focus of the dissertation will be on hydrologic and hydraulic processes such as dispersion, hyporheic exchange (transient storage), sediment resuspension during high flow conditions, oxygen exchange at the air-water interface and the water-sediment interface during low flow, and the effect of watershed-based non-point source BOD loading due to watershed-scale hydrologic processes. Based on aforementioned objectives and the scope, dissertation will be organized as follows:

- Chapter 1- Introduction
- Chapter 2- VART Model-Based Method for Estimation of Instream Dissolved Oxygen and Reaeration Coefficient: This chapter focuses on exchange of oxygen at air-water interface. The objective of this paper is to investigate the combined effect of transient storage and longitudinal dispersion on the reaeration coefficient and thereby on DO in streams. To that end, the VART model presented by Deng and Jung (2009) is modified in this paper to simulate the instream DO deficit. The VART model includes both the transient storage and longitudinal dispersion mechanisms. The longitudinal dispersion is estimated using the method presented by Deng et al. (2001). Since the reaeration coefficient is unknown, the VART model is solved inversely to estimate the reaeration coefficient. The inversely solved

reaeration coefficient is then compared with existing empirical equations to assess the effect of the transient storage and longitudinal dispersion on the reaeration coefficient.

- Chapter 3- Watershed Modeling of Amite River for Estimation of BOD Loading: In this chapter, watershed based modeling of Amite River will be performed by using Hydrological Simulation Program-Fortran (HSPF). Different types of data and parameters; meteorological, geographical, hydrological data as well as hydraulic data, should be provided for modeling Amite River watershed. The model will then be calibrated for flow, temperature, dissolved oxygen, and biological oxygen demand (BOD) from across the watershed.
- Chapter 4- Modeling Sediment Resuspension-Induced DO Variation in Fine-Grained Streams: The primary objective of this study is to present a simple yet effective model for simulation of DO transport and exchanges across water-sediment and water–air interfaces in rivers. While the emphasis of this paper is on the effect of sediment resuspension on DO, a novel feature of the current study is to simulate DO variations in both low flow without sediment resuspension and high flow with sediment resuspension with a single model, called VART–DOS model, greatly simplifying the DO modeling. The objective will be achieved by incorporating sediment resuspension effect into our instream VART–DO model from the second chapter.
- Chapter 5- Modeling Spatial Variations in Dissolved Oxygen in Fine-Grained Streams under Uncertainty: In previous chapter, while the VART-DOS model included the effect of diffusive mass exchange on instream DO, the diffusive layer was not explicitly included in the model. As a result, the VART-DOS model is unable to produce the vertical profile of DO in the bottom sediment. The overall goal of this part of study is to develop a new model

for simulation of vertical and longitudinal variations in DO in fine-grained streams at daily time-scale. Thus, diurnal variation in DO will not be considered in this paper. Due to diverse spatial scales involved in DO variations and associated variability and uncertainties in model input parameters, specific objectives of this paper are (1) to present a new model including various physical and biogeochemical processes responsible for DO variations in fine-grained streams, (2) to examine the sensitivity of model parameters to identify sensitive parameters, (3) to simulate and analyze various cases representing the variability and uncertainty in model parameters, and (4) to apply the model to the Lower Amite River in Louisiana, USA to test the performance and demonstrate a practical application of the new model.

- Chapter 6- Summary and Conclusions: This chapter will summarize major findings of this dissertation.

1.5. References

Ahearna, D. S., Sheibleya, R. W., Dahlgrena, R. A., Andersonb, M., Johnsonc, J., Tate, K. W., (2005). "Land use and land cover influence on water quality in the last free-flowing river draining the western Sierra Nevada, California." *J Hydro*., 313.

Allan, J.D., Erickson, D.L., Fay, J., (1997). "The influence of catchment land use on stream integrity across multiple spatial scales." *Freshwater Biol.* 37 (1), 149–161.

Chapra, S.C. (1997). *Surface Water-Quality Modeling*. McGraw-Hill, New York, N.Y.

Chapra, S.C. and Runkel, R.L. (1999). "Modeling impact of storage zones on stream dissolved oxygen." *J. Envir. Eng.*, 125(5), 415-419.

Cox, B.A., (2003). "A review of currently available in-stream water-quality models and their applicability for simulating dissolved oxygen in lowland rivers." *Sci. Total Environ.,* 314-316, 335-377.

Duan, Z., Diaz, J.N., Martin, J.L., and McAnally, W.H., (2008). "Effects of Land-Use Changes on Saint Louis Bay Watershed Modeling." *J Coastal Res*.,10052, 117-124.

Graves, A.G., Wan, Y., and Fike, D.L., (2004). "Water quality characteristics of storm water from major land uses in south Florida." *JAWRA*, 03194.

Jones, K.B., Neale, A.C., Nash, M.S., Van Remortel, R.D., Wickham, J.D., Riitters, K.H., and O'Neill, R.V., (2001). "Predicting nutrient and sediment loadings to streams from landscape metrics: A multiple watershed study from the United States mid-Atlantic region." *Landscape Ecol*., 16, 301-312.

Motta, D., Abad, J.D., Garcia, M.H., (2010). "Modeling Framework for organic sediment resuspension and oxygen demand: Case of Bubbly Creek in Chicago." *J. Environ. Eng*., 136(9), 952-964.

Streeter, H.W. and Phelps, E.B., (1925). "A study of the pollution and natural purification of Ohio River." *Public Health Bulletin*, U.S. Public Health Service, Washington, D.C., No. 146.

U.S. EPA website water.epa.gov/type/rsl/monitoring/vms52.cfm, 2010.

U.S. EPA website <http://www.epa.gov/caddis/ssr_do4s.html>, 2011.

Vellidis, G., Barnes, P., Bosch, D.D., Cathey, A.M., (2006). "Mathematical simulation tools for developing dissolved oxygen TMDLs." American Society of Agricultural and Biological Engineers, 49(4).

Welch, E.B., Jacoby, J.M., and May, C.W. (1998). "Stream quality." In R. J. Naiman and R. E. Bilby, editors. River ecology and management: lessons from the Pacific Coastal Ecoregion. *Springer-Verlag*, New York, New York, USA.

CHAPTER 2
VART MODEL-BASED METHOD FOR ESTIMATION OF INSTREAM DISSOLVED OXYGEN AND REAERATION COEFFICIENT

2.1. Introduction

Dissolved oxygen (DO) concentration is a key health indicator of stream ecosystems. Variation in DO may be caused by various physical, chemical, and biological processes and factors. Extensive efforts have been made to understand the processes and factors responsible for DO fluctuations (Streeter and Phelps 1925; O'Connor-Dobbins 1958; Churchill et al. 1962; Chapra and Runkel 1999; Gualtieri et al. 2002; Duan et al. 2010). An important physical process controlling instream DO is the air-water exchange. The air-water exchange flux is commonly described using the reaeration-rate coefficient (Covar 1976; Melching and Flores 1999; Gualtieri et al. 2002).

A wide spectrum of empirical formulas have been proposed to estimate reaeration coefficient for water quality modeling, including the empirical equations proposed by Streeter Phelps (1925), O'Connor-Dobbins (1958), Churchill-Elmore-Buckingham (1962), Owens-Edwards-Gibbs (1964), and Langbein-Durrum (1967). The equations were generally obtained under certain assumptions and distinct hydraulic conditions. Therefore, they may not be applicable to streams other than those from which the equations were originally derived (Melching and Flores 1999; Gualtieri et al. 2002; Duan et al. 2010). Gualtieri et al. (2002) reviewed 20 equations found in the literature for estimation of reaeration coefficient. Most of the empirical equations were derived based on field or laboratory data along with the pioneer equation of the Streeter-Phelps (1925). Additional factors such as sediment oxygen demand, photosynthesis oxygen consumption, and respiration of plankton and other species were added to the original equation of Streeter-Phelps to get more realistic results for DO deficit in streams by

Dobbins (1964). This type of equations is essentially an advection-dispersion equation (ADE) with additional sink/source terms and can be written as (Bansal 1973):

$$\frac{\partial D}{\partial t} + U\frac{\partial D}{\partial x} = \frac{\partial}{\partial x}\left(E\frac{\partial D}{\partial x}\right) - K_2 D + K_1 L - P + R \quad (1)$$

where D is the DO deficit [ML^{-3}], U [LT^{-1}] is the flow velocity along *x* direction, E is the longitudinal dispersion coefficient [L^2T^{-1}], t is the traveling time [T], L is the BOD concentration [ML^{-3}], K_1 is the rate of biochemical oxidation of carbonaceous materials, and K_2 [T^{-1}] is the reaeration coefficient. The constants P and R represent photosynthesis rate and respiration rate in the water column, respectively.

In addition to the air-water exchange and instream reactions, sediment-water exchange (hyporheic exchange) has been found to play an important role in solute (including DO) transport in streams (Bencala 1983, Runkel 1998, Deng et al. 2009). Chapra and Runkel (1999) investigated the impact of the transient storage on the DO sag and BOD curves using the transient storage model (Bencala 1983, Runkel 1998). They clearly identified the difference between the minimum DO concentration that obtained using conventional Streeter-Phelps equation and the equation that incorporates the transient storage effect. They concluded that incorporation of this effect is important to river water quality modeling. While the transient storage effect was included, Chapra and Runkel (1999) ignored the dispersion term. In fact, dispersion process is generally not taken into account in DO modeling (Dobbins 1964).

Deng et al. (2010) examined the influence of shear dispersion and hyporheic exchange on instream solute transport, and how these two transport processes prevail in larger and smaller streams, respectively, using the Variable Residence Time (VART) model. They found that the effect of dispersion on solute transport is negligible as compared to hyporheic exchange in small streams but the dispersion process is more important than hyporheic exchange process in large

rivers. Both the dispersion and hyporheic exchange processes are important in moderate-sized streams.

The objective of this paper is to investigate the combined effect of transient storage and longitudinal dispersion on reaeration coefficient and thereby on DO in streams. To that end, the VART model presented by Deng and Jung (2009) is modified in this paper to simulate instream DO deficit. The VART model includes both the transient storage and longitudinal dispersion mechanisms. The longitudinal dispersion is estimated using the method presented by Deng et al. (2001). Since the reaeration coefficient is unknown, the VART model is solved inversely to estimate the reaeration coefficient. The inversely solved reaeration coefficient is then compared with existing empirical equations to assess the effect of the transient storage and longitudinal dispersion on the reaeration coefficient.

2.2. Materials and Methods

2.2.1. VART Model for DO Simulation

Natural streams and especially small streams are characterized by the hyporheic exchange (Deng et al. 2010) that affects biogeochemical processes and DO levels in water column. Therefore, extensive efforts have been made to model the hyporheic exchange process. A number of numerical models, such as transient storage model (Chapra and Runkel 1999, Bencala and Walters 1983) and continuous time random walk model (Boano et al. 2007), have been proposed. One of the recent models, VART model presented by Deng and Jung (2009), is able to generate multiple types of solute residence time distributions observed in streams while no user-specified residence time distribution functions are required. This is a powerful and unique feature of the VART model. Physically, the VART model includes three zones: (1) water column

zone, (2) an advection-dominated transient storage zone, and (3) an effective diffusion-dominated storage zone, as shown in Figure 2.1.

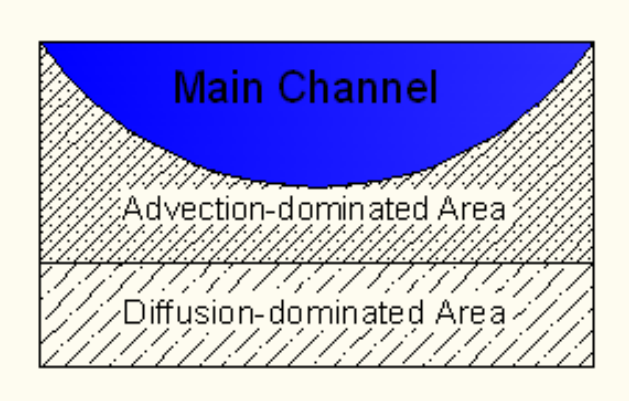

Figure 2.1- Typical Cross-Section of a Stream and its Storage Zones

Mathematically, the VART model, incorporating air-water exchange (reaeration) and other biogeochemical processes controlling DO, can be obtained by combining VART model (Deng and Jung 2009) and Eq. (1), leading to the VART-DO model:

$$\frac{\partial D}{\partial t} + U\frac{\partial D}{\partial x} = E\frac{\partial^2 D}{\partial x^2} + \frac{A_{adv} + A_{dif}}{A}\frac{1}{T_V}(D_S - D) - K_2 D + K_1 L - P + R \tag{2}$$

$$\frac{\partial D_S}{\partial t} = \frac{1}{T_V}(D - D_S) \tag{3}$$

$$A_{dif} = 4\pi D_E t_S \tag{4}$$

$$T_V = \begin{cases} T_{\min} & \text{for} \quad t \le T_{\min} \\ t & \text{for} \quad t \ge T_{\min} \end{cases} \quad (T_{min} > 0) \tag{5}$$

$$t_S = \begin{cases} 0 & \text{for} \quad t \le T_{\min} \\ t - T_{\min} & \text{for} \quad t \ge T_{\min} \end{cases} \tag{6}$$

where D_s is DO deficit in the storage zone, A_{adv}= advection-dominated area of storage zone, A_{diff}= diffusion-dominated area of storage zone, T_v = residence time in the storage zone, D_E =

effective diffusion coefficient in bottom sediment, T_{min} is the minimum residence time, t_s is the time since solute releases from storage zone to the mainstream. According to classic Streeter-Phelps model, the equation for DO changes along the rivers is usually coupled to the equation expressing BOD distribution. Thus, similar to VART-DO, VART-BOD can be considered with corresponding sources/sinks. VART-BOD and VART-DO are then solved jointly to get the concentration of BOD and DO along the rivers. As a result, besides DO observed data, BOD concentrations are also needed. More detailed descriptions about the VART model and its applications can be found in Deng and Jung (2009) and Deng et al. (2010). To discretize the VART-DO model and solve the equations efficiently, the split-operator method may be used. In the split-operator method, it is commonly assumed that the pure advection process and dispersion process occurs alternatively with time and the advection process occurs in the first half-time step and the dispersion along with transient storage and other reactions in the VART-DO model takes place in the second half for one time step. More details about the split-operator method can be found in Deng et al. (2006).

The last four terms in Eq. (2) are added to the original VART model to represent the oxygen exchange between air and water, BOD removal by oxidation, photosynthesis, and living species respiration, respectively. In order to identify the effect of reaeration (K_2 D) on DO, the last three terms in Eq. (2) is dropped in this study. In fact, the observed data used in this study were from river reaches that were free from BOD degradation and aquatic respiration and without the impact of diurnal photosynthesis. A solution of the VART model requires the estimation of several model parameters including E, D_E, A_s/A ($A_s = A_{adv} + A_{diff}$), and minimum residence time (T_{min}). For DO deficit, reaeration coefficient is an additional parameter that acts as a sink term in the model as it reduces DO deficit. In a forward problem, the model parameters are generally

assumed to be known from field tracer test data, typical values in the literature, or similar analysis. It is, however, not always possible to obtain suitable values for all of the parameters in advance. Field tracer tests are expensive and time-consuming. Values suggested in the literature often vary in a wide range. For instance, D_E value may range from 1.0×10^{-5} to 1.0×10^{-10} m^2/s (Elliott and Brooks 1997; Qian et al. 2008). One way to addressing this issue is to use an inverse modeling technique. If DO concentration data are available from field measurements, DO deficit can be calculated easily. Then, the problem becomes an inverse problem in which the model parameters can be estimated by means of an optimization algorithm.

2.2.2. Inverse Modeling

Inverse modeling (calibration) was widely used to estimate model parameters in groundwater-related problems (Sun 1994, Yeh 1986) while it was not employed frequently in surface water problems. It is possible to estimate the value of reaeration coefficient by changing the forward problem to an inverse one and making use of observation data. The inverse modeling technique generally involves two steps: (1) computation of objective function values based on observed data to obtain initial parameter estimations and (2) a more detailed parameter determination using an optimization scheme. Due to the uncertainties involved in field experiments and data collection, it is wise to utilize a random search technique to find reaeration coefficient that optimizes the calculated DO deficit values according to observed data.

The VART-DO model for calculating DO deficit may be formulated as:

$$D = f(MP, x, t) \tag{7}$$

where MP refers to the model parameters to be estimated and D, x, t are defined previously. Though the formulation was considered to calculate the DO deficit, it is possible to compute the

suitable values for MP by employing the field observation data for D. Therefore, the inverse problem can be formulated as:

$$\widetilde{MP} = g(\widetilde{D}, x, t) \tag{8}$$

in which $\widetilde{\mathrm{MP}}$ is the estimated parameter based on the observation data ($\widetilde{D}$). As discussed by Sun (1994), such inversed identification problem may be readily transferred to an optimization problem. In optimization problems, the objective function F_o(D) is commonly set as the output least square, i.e.,

$$F_O(\mathrm{D}) = \min_{K_2} \sum_{i=1}^{N} \frac{1}{N} \left(D_{obs.i} - D_{com_i}\right)^2 \tag{9}$$

where D_{obs} refers to the observed DO deficit value, D_{com} denotes the DO deficit value obtained from the numerical solution of VART model, and N is the number of observations.

In addition to parameter K_2, other VART model parameters may also be estimated using the inverse modeling technique. It is, however, advantageous to first conduct a sensitivity analysis to determine how sensitive the results are with respect to the change in individual model parameters. Those less sensitive parameters may be assigned the suggested value from references and therefore removed from the optimization procedure. Eq. (9) is then minimized for the remaining unknown parameters.

To solve the inverse problem of VART-DO model subject to the objective function in Eq. (9), the Simplex-Simulated Annealing (SIMPSA) (Cardoso et al., 1996) and the Genetic Algorithm (GA) (Matlab online help, 2009) are utilized. The advantage of SIMPSA is the employment of a simulated annealing technique through which solutions are generated stochastically and errors are minimized. The SIMPSA escapes the local optima to yield a global minimum. The main advantage of the GA is the improvement of results by ignoring the less

appropriate solutions. By the GA, appropriate values are calculated for the unknowns and then the SIMPSA uses these values as the initial guess to predict the final values by a random search. However, this procedure is soon recognized as being time-consuming and unnecessary. As a result, initial guesses are defined arbitrarily from the acceptable ranges for each of the unknowns. The returned values which minimize the objective function $F_O(D)$ in Eq. (9) are considered as the optimum value. The optimization process requires observed data for the DO deficit.

2.2.3. Observed Data

Churchill et al. (1962) gathered a large amount of DO data from Clinch, Holston, French Broad, Watonga, and Hiwassee Rivers and expressed reaeration coefficient as a function of flow characteristics such as flow depth and velocity. One outstanding feature of their work was that they selected the river reaches which were not polluted with decomposing organic materials. Oxygen demand of such materials could seriously affect the true reaeration coefficient. Furthermore, Churchill et al. in 1962 controlled the hydraulic conditions for their field experiments through hydraulic structures (e.g. dam) at the upstream of the selected reaches. This helped maintain a constant flow velocity during the field experiments. The steady state flow in their study obviated the need for hydrodynamic modeling for obtaining the velocity field. Additionally, the impoundment of water for a long time reduces the DO concentration and the reaeration can be obtained in a more realistic condition. Thus, Churchill et al. (1962) took reaches that were long enough to allow reaeration to take place to a measurable extent. They avoided the reaches that have major tributaries to prevent the different DO concentrations from disturbing the results.

To obtain the reaeration coefficient by applying the VART-DO model inversely, the observation data gathered by Churchill et al. (1962) were utilized. The DO deficit was directly

calculated from the data for DO concentration and measured temperature. DO concentrations in the saturation condition may be calculated as:

$$C_s = -6 \times 10^{-5} T^3 + 0.0071 T^2 - 0.3961 T + 14.6 \quad (10)$$

$$DO\ Deficit = C_s - C \quad (11)$$

in which Cs is the DO concentration in the saturated condition, and T is water temperature in degree Celsius. It should be pointed out that Eq. (10) is obtained by using the saturated DO concentration data for different temperatures collected by the Missouri Department of Natural Resources (2010). The coefficient of determination (R2) of Eq. (10) is 0.9999. A typical graph of the data was shown in Figure. 2.2. It is obvious from Figure 2.2 that the DO deficit decreases with distance from the upstream site to the downstream site due to the reaeration. Also, at both the upstream and downstream sites the DO deficit time series shows an increasing trend with time. According to Churchill et al (1962), the decrease in the DO concentration was due to the impoundment at upstream end of the reach.

2.2.4. Sensitivity Analysis

In order to evaluate the impact of the VART-DO model parameters on the DO deficit and corresponding K_2, a sensitivity analysis is performed for selected parameters. Three parameters (As/A, E, and K_2) involved in the VART-DO model for DO deficit were considered as unknown variables and estimated through inverse modeling. The procedure includes optimization of an objective function which is actually the root mean squared error (RMSE) between the calculated DO deficit and observed data. RMSE is the statistical criterion most commonly used in the literature to assess the performance of hydrologic models (Boyle et al., 2000; Moriasi et al., 2012), water quality models (Moriasi et al., 2012), and even watershed models (Moriasi et al., 2007).

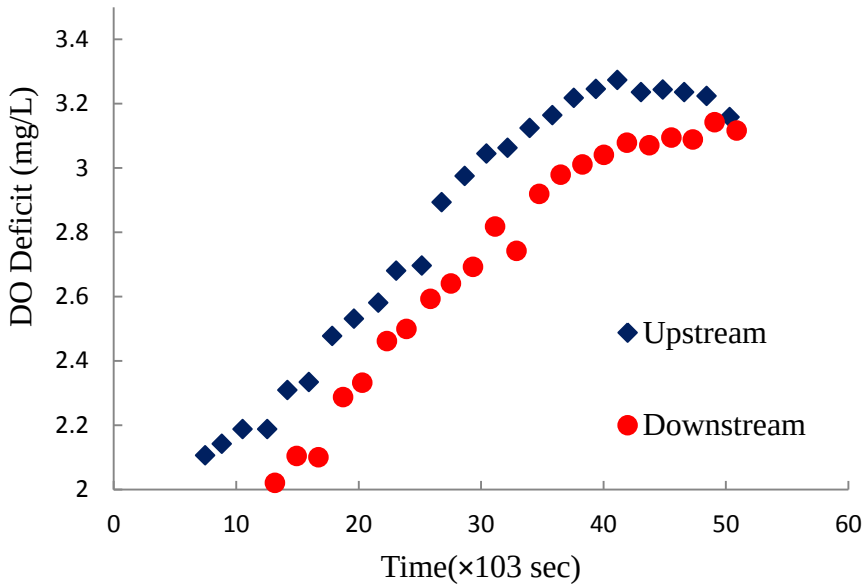

Figure 2.2- DO deficit data calculated for a reach along Clinch River using measured data by Churchill et al. (1996).

Different values were assigned to the modeling parameters and the Root Mean Squares Errors (RMSEs) between the calculated DO deficit and the observed data were determined (RMSE=$\frac{1}{N}\sqrt{\sum_{i=1}^{N}\left(D_{obs_i}-D_{com_i}\right)^2}$). To assess the effect of transient storage zone (As) on DO deficit, four differing values of 0, 0.2, 0.5, and 1 were assigned to the ratio As/A. These are typical values for As/A (Chapra and Runkel 1999). For effective diffusion coefficient, D_E, the recommended values between 1.0×10^{-5} to 1.0×10^{-10} m^2/s were considered. In fact, the effective diffusion coefficient was found to have very minor impact on DO deficit and was set to zero latter in the model. The main reason was that the relatively high flow velocity in the selected river reaches (Duan et al. 2009) significantly reduced the effective diffusion-induced DO exchange. Different values were also assigned to the dispersion coefficient (E). Initially, E value was set to zero to evaluate the results from previous studies. Then, E value was increased to

typical values (Deng et al. 2001). The flow velocity (U) and cross-sectional area (A) were determined using the data of Churchill et al. in 1962. The minimum residence time T_{min} is determined using the method presented by Deng et al. (2010).

The reaeration coefficient (K_2) was initially set to the value measured by Churchill et al. (1962) for the reaches along Clinch, Holston, French Broad, Watonga, and Hiwassee Rivers while dispersion coefficient and storage zone term were set to zero initially. The dispersion coefficient and As/A values were changed for different K_2 values to verify the changes in RMSE (mg/L). The results for Clinch River (experiment 3 in Churchill et al. (1962)) are summarized in Table 2.1. Therefore, the reference values for this river reach were: K_2= 2.26 (1/day), E=As/A=0 and RMSE= 0.092 (mg/L). In Table 2.1, the percentage change of RMSE was calculated using the reference value of RMSE.

It can be seen from Table 2.1 that increasing the As/A ratio and K_2 value increased the RMSE when E value is equal to zero. However, the minimum value for RMSE was obtained when E increased to values calculated from the formula of Deng et al. (2001). In this case, the As/A ratio was not zero, indicating the impact of storage zones on the reaeration coefficient K_2. Sensitivity analysis also demonstrated that for large changes in K_2, RMSE just underwent small changes. Table 2.2 shows that the K_2 value varies from 0.6 to 1.0 (1/day) while RMSE just changes from 0.043 to 0.051. Based on the sensitivity analysis, a combination of the values for dispersion coefficient, storage zone area ratio (As/A), and reaeration coefficient that returns the minimum RMSE for DO deficit is selected as the best result meeting Eq. (9).

Table 2-1- Results of sensitivity analysis in terms of RMSE/percent change of RMSE

As/A	K_2=0.676 (1/day)	K_2=1.710 (1/day)	K_2=2.260 (1/day)	K_2=3.380 (1/day)
		E= 0.0		
0.0	0.082/-11	0.057/-38	0.092/0.0*	0.182/ 98
0.2	0.066/-28	0.080/-13	0.119/ 29	0.209/127
0.5	0.113/ 23	0.148/ 61	0.182/ 98	0.263/186
1.0	0.222/141	0.262/185	0.292/217	0.361/292
		E= 50 (m^2/s)		
0.0	0.103/ 12	0.059/ -36	0.048/-48	0.069/-25
0.2	0.087/ -5	0.048/ -48	0.044/-52	0.080/-13
0.5	0.084/ -9	0.067/ -27	0.075/-18	0.112/ 22
1.0	0.126/ 37	0.132/ 43	0.143/ 55	0.178/ 93
		E=174 (m^2/s)		
0.0	0.114/ 24	0.082/-11	0.067/-27	0.048/-48
0.2	0.102/ 11	0.070/-24	0.056/-39	0.041/-55**
0.5	0.091/ -1	0.064/-30	0.053/-42	0.051/-45
1.0	0.096/ 4	0.082/-11	0.081/-12	0.091/ -1

*Corresponding to reference values **Corresponding to the minimum RMSE

Table 2-2- Results of sensitivity analysis for reaeration coefficient

K2	%K_2 change	RMSE	%RMSE change
0.6	0	0.043	0
0.8	33	0.044	2
0.9	50	0.047	8
1.0	67	0.051	18

2.3. Results

2.3.1. Scenario I: Reaeration Coefficient with E=0

According to Dobbins's (1964) verification cited by Esen and Rathbun (1976) the impact of the dispersion coefficient (E) on DO reaeration is negligible. Thus, for the first scenario E was set to zero. Additionally, due to the relatively high flow velocities in all the considered cases, D_E was also considered as zero. The rest of the modeling parameters are calculated through the optimization by minimizing Eq. (9) with respect to As/A, T_{min}, and K_2. The results are shown in Figure. 2.3 where the K_2 values calculated using the VART-DO model and existing empirical

methods fall along the 45 degree line. It means that the existing empirical methods are a special case of the VART-DO model when both the longitudinal dispersion and the transient storage effects are ignored.

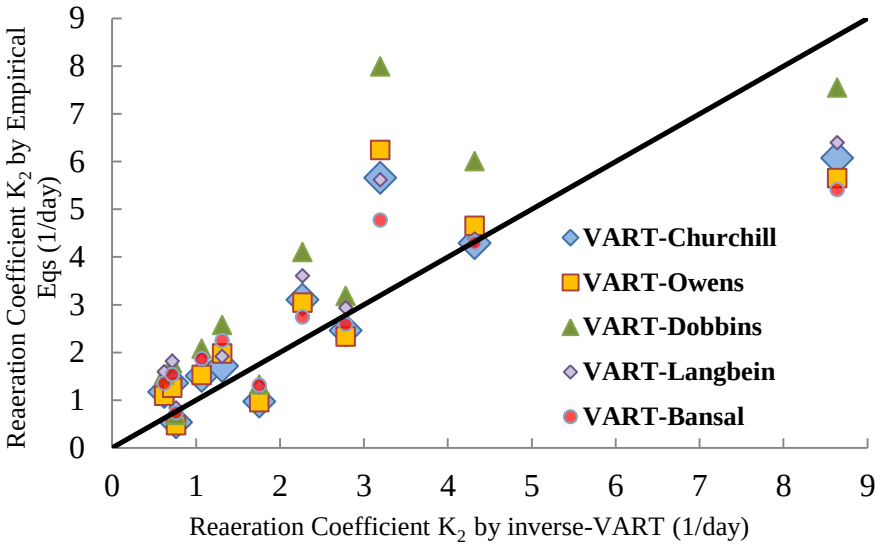

Figure 2.3- Comparison of reaeration coefficient of VART and empirical equations when dispersion is neglected; E=0.0.

However, a recent study by Deng et al (2010) showed that stream channel size affects the relative importance of the longitudinal dispersion and hyporheic exchange terms in a stream. Large rivers are dominated by instream advection and dispersion (large longitudinal dispersion coefficient) processes. The influence of hyporheic exchange on solute transport increases with decreasing channel size. Solute transport in small streams is affected more significantly by hyporheic exchange. Both the longitudinal dispersion and hyporheic exchange terms are important in moderate-sized rivers. It means that neither the longitudinal dispersion term nor the transient storage term should be dropped in solute transport modeling for moderate-sized rivers. It is also apparent from Table 2.1 that both the transient storage zone and the longitudinal dispersion affect K_2 values in most river reaches. For small streams, the transient storage term

should be included while for large rivers at least the longitudinal dispersion term should be taken into account. Due to the high uncertainty involved in the estimation of the longitudinal dispersion coefficient and the stream size effect. Two additional scenarios are considered for the dispersion coefficient.

2.3.2. Scenario II: Reaeration Coefficient with Strong Longitudinal Dispersion

Dispersion mechanism controls mixing of solute (including DO) in the water column. The longitudinal dispersion is calculated using the equation presented by Deng et al. (2001).

$$\frac{E}{HU_*} = \frac{0.01\psi}{8M_*}\left(\frac{B}{H}\right)^{5/3}\left(\frac{U}{U_*}\right)^2 \tag{12}$$

in which E is dispersion coefficient in the x direction, U_* is the shear velocity, H is the flow depth, B is the channel width, U is the average velocity, and ψ is a multiplier which is equal to 15 for the current scenario. M_* is defined as:

$$M_* = 0.145 + \frac{1}{3520}\left(\frac{U}{U_*}\right)\left(\frac{B}{H}\right)^{1.38} \tag{13}$$

The calculated K_2 values are plotted in Figure 2.4. It is clear that K_2 values for all river-reaches were shifted below the 45 degree line. In other words, all K_2 values estimated by the empirical equations are smaller than the values calculated from the inverse VART-DO model.

2.3.3. Scenario III: Reaeration Coefficient with Weak Longitudinal Dispersion

The value of parameter ψ in Eq. (15) is set as 1 in this scenario to represent the weak dispersion process in small streams. Calculated K_2 values for the selected river reaches are shown in Figure 2.5 A comparison between Figures 2.5 and 1.3 indicates that the results from the scenarios I and III are similar. The estimated parameter values meeting Eq. (9) for the selected river reaches are listed in Table 2.3.

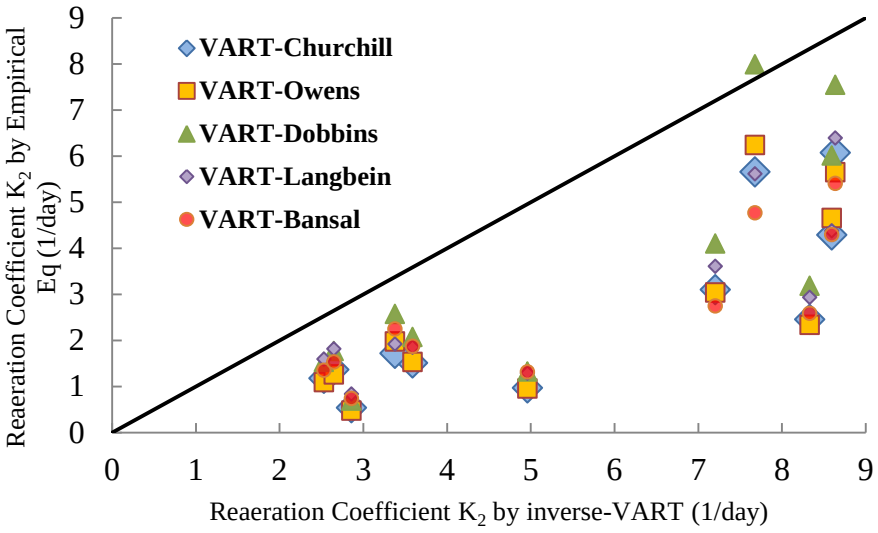

Figure 2.4- Comparison of reaeration coefficient of VART and empirical equations considering the dispersion coefficient with $\psi=15$ in the *Eq. 15.*

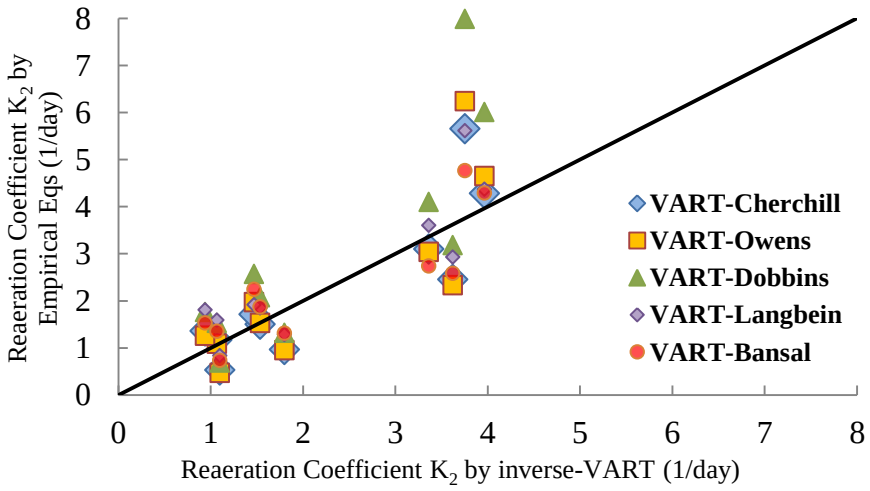

Figure 2.5- Comparison of reaeration coefficient of VART and empirical equations considering dispersion coefficient with $\psi=1$ *in the Eq. 15.*

2.4. Discussion

Based on the three designated scenarios and associated graphs (Figures 2.3-2.5), K_2 values are close to the predictions from existing empirical equations when the dispersion coefficient is

zero or very small. This implies that the existing empirical equations are a special case of the VART-DO model without the dispersion and transient storage effects. It is also true that increasing the dispersion coefficient enhances the mixing phenomena in the water column which subsequently increases the turbulence and transfer of mass from the very top layer to the bottom of the water column. As a result, the reaeration coefficient increases, as shown in Figures 2.3 and 2.4.

Table 2-3- Selected values for different river reaches based on optimization

River Reach	E (m^2/s)	As/A	T_{min} (hr)	K_2 (1/day)
Holston 1	359	0.000	0.402	2.862
Holston 2	403	0.001	0.590	2.399
Holston 3	408	0.000	0.357	2.652
Clinch 1	0.0	0.050	0.210	3.790
Clinch 2	0.0	0.023	0.241	2.527
Clinch 3	174	0.170	0.995	3.382
Clinch 4	280	0.002	0.330	.590
Clinch 5	262	0.061	0.548	4.963
French Broad	355	0.034	0.464	7.210
Watauga	0.0	1.000	1.000	8.640
Hiwassee	0.0	0.967	0.412	3.197

The effect of storage zones on the calculated DO deficit can be significant in some small streams like the Clinch River while the effect may become small or even negligible in some other rivers like the reaches along Holston River. It is also evident from sensitivity analysis that for a fixed K_2 value, different values of As/A can cause some noticeable changes in the results. The optimum K_2 values were selected from various combinations of parameter values for As/A, E, and reaeration coefficient according to Eq. (9) that minimizes the RMSE through an optimization procedure. The RMSE values calculated with the K_2 values from the existing empirical equations were not the minimum as compared with that from the VART-DO model. It

means that the K_2 values estimated using the existing empirical methods are not so accurate as compared with the K_2 values computed using the VART-DO model. Figures 2.6-2.10 show comparisons of the RMSEs between observed DO deficit and the calculated one by using the K_2 values of present study and those of empirical equations. In each graph, the x-axis is the RMSE of DO deficit with K_2 calculated using the VART-DO model while the y-axis is the RMSE of DO deficit with K_2 obtained from empirical equations. It can be seen from the figures that the RMSEs of the existing empirical methods are always higher than those of the VART-DO model. The smaller RMSE values or more accurate results from the VART-DO model were achieved by taking into account the transient storage and longitudinal dispersion effects. The impact of storage zones on DO may become more significant in some small urban streams where BOD is constantly present and flow velocity is generally small, as demonstrated by Chapra and Runkel (1999). The longitudinal dispersion increases the air-water DO exchange. The effective diffusion becomes important in natural streams with small flow velocity.

The optimization procedure used in this paper is able to produce the optimum K_2 value for observed DO data. In some cases like the Clinch River 5, K_2 values from present study is about 5 times greater than the values predicted by the empirical equations. Consequently, the inverse modeling of VART-DO model in combination of the optimization procedure seems to yield a more realistic estimation of reaeration coefficient (K_2) and thereby the DO concentration in streams.

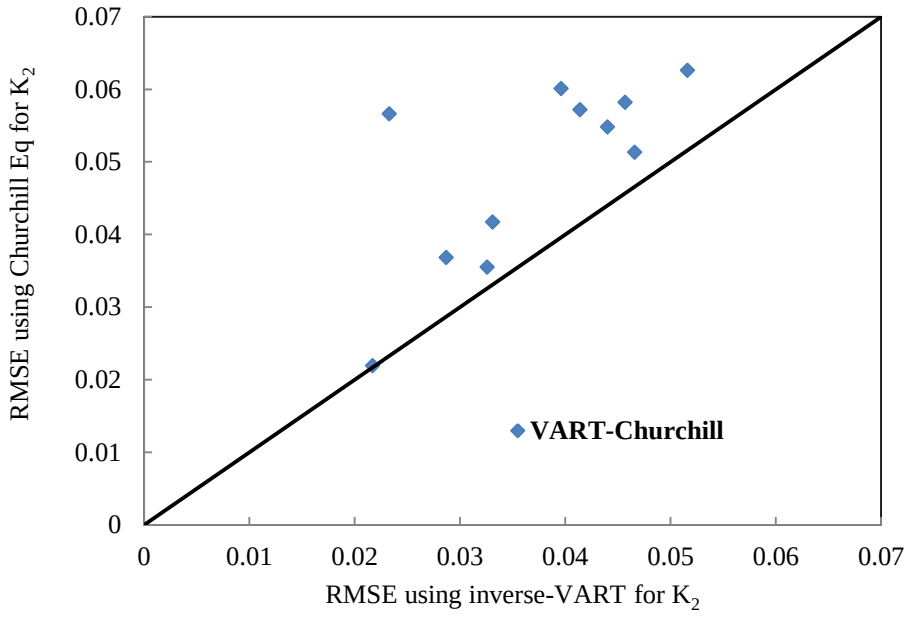

Figure 2.6- Comparison of RMSEs corresponding to K_2 from Churchill equation and inverse-VART

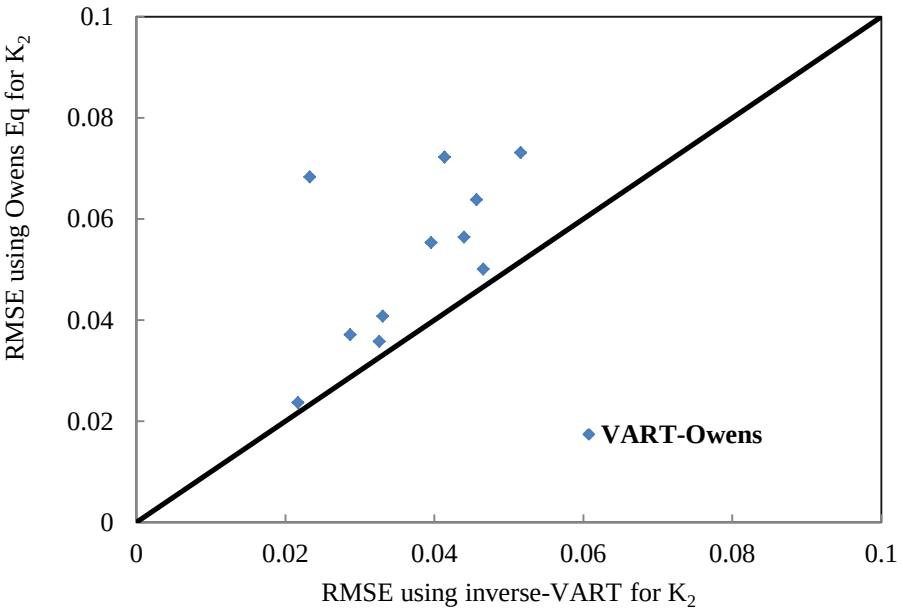

Figure 2.7-Comparison of RMSEs corresponding to the K_2 of Owens equation and inverse VART calculation

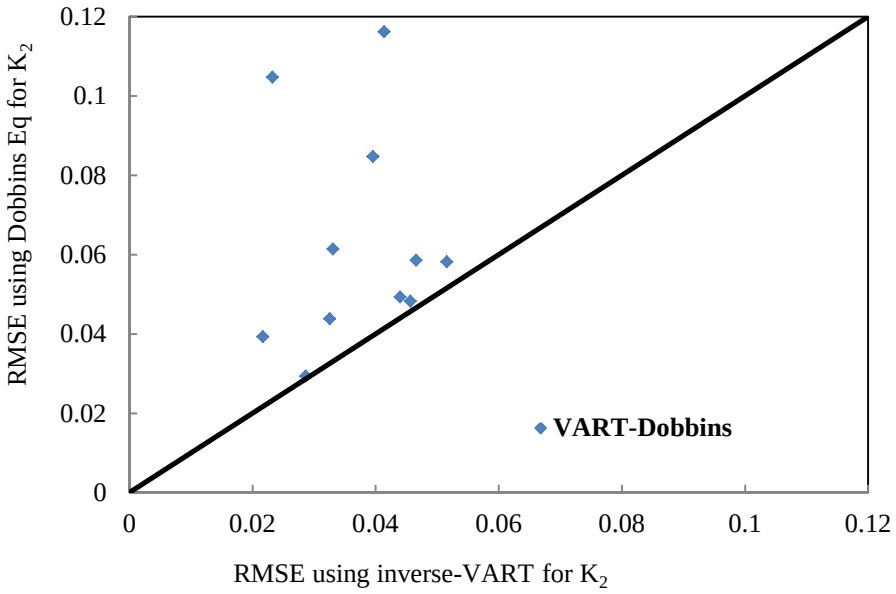

Figure 2.8- Comparison of RMSEs corresponding to the K_2 of Dobbins equation and inverse VART calculation

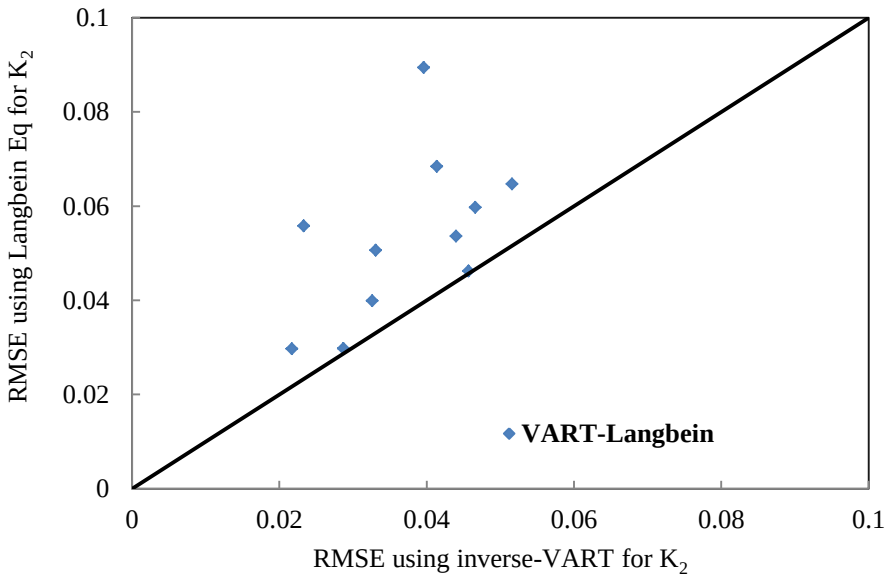

Figure 2.9- Comparison of RMSEs corresponding to the K_2 of Langbein equation and inverse VART calculation

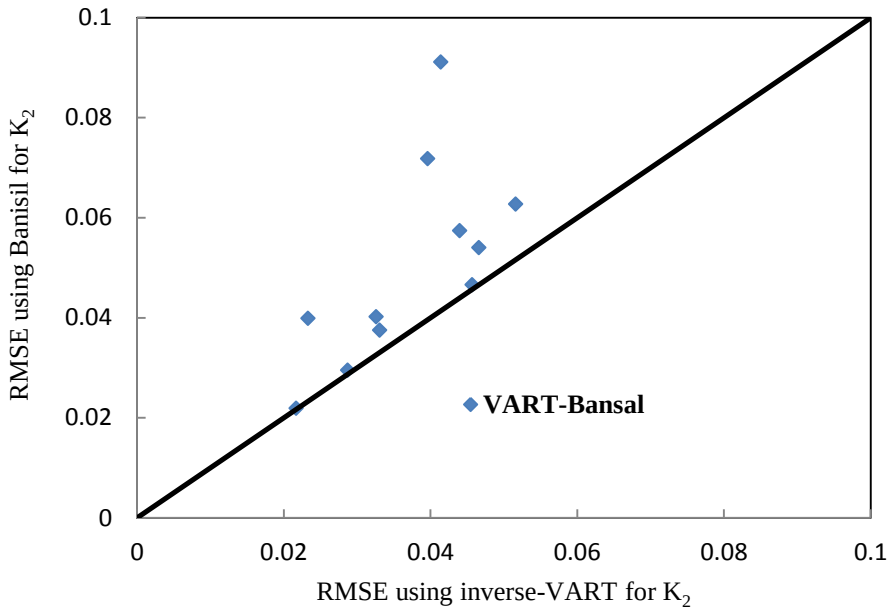

Figure 2.10- Comparison of RMSEs corresponding to the K_2 of Bansal equation and inverse VART calculation

2.5. Comparison of VART-DO with other models and main contributions of this chapter

In order to understand new contributions from this chapter, it is important to understand the difference between the VART-DO model and other widely used dissolved oxygen models such as Streeter-Phelps and water quality analysis simulation program (WASP).

(1) VART-DO model presented in this chapter is a simplified version of the general model VART-DO-3L (in Chapter 5) that includes major processes responsible for exchanges of DO at the air-water interface and water-sediment interface, mixing in water column through dispersion, and reactions such as BOD degradation. To understand the fundamental implications of transient storage zone (hyporheic exchanges) and dispersion processes on reaeration, in VART-DO model emphasis is on DO changes as the result interactions among these mechanisms. Furthermore, the impacts of diurnal processes of photosynthesis and respiration are ignored since available observed data are daily average DO

concentrations. This simplification and assumption is usually made in TMDL development for DO.

(2) VART-DO model is a relatively simple yet effective model for estimation of the reaeration coefficient and the DO concentration in streams in terms of major processes responsible for DO variations. The simple Streeter-Phelps model is usually unable to determine which process dominates the DO concentration in rivers, because it does not include a sufficient number of processes and thus does not meet the demand of simulating DO (Cox, 2003). In Streeter-Phelps model (Eq. 14), DO deficit (shortage of oxygen from saturation level) changes is related to the effects of reaeration (source term) and BOD degradation (sink term). It is also assumed in Streeter-Phelps model that DO distributed evenly at cross section and moves as plug flow with no mixing (Lin, 2001; http://en.wikipedia.org/wiki/Streeter-Phelps_equation) which limits the application of the model to small streams and short reaches.

$$\frac{\partial D}{\partial t} = k_1 L - k_2 D \tag{14}$$

In contrast, the WASP model (Wool et al., 2001; Vellidis et al., 2006), includes several other kinetic processes such as CBOD deoxygenation, NBOD deoxygenation, reaeration, sediment oxygen demand, nitrification/de-nitrification, mineralization of dissolved organic nitrogen, growth of phytoplankton and photosynthesis process, and respiration in addition to the time-varying processes of advection, dispersion, point and diffuse mass loading, and boundary exchange. These kinetic processes (Eq. 15) require identification of at least 70 modeling parameters, constants, and data sets (i.e. concentration of nitrate, CBOD, etc.).

$$\frac{\partial C}{\partial t} = k_2(C_{sat} - C) - k_D\theta_D^{(T-20)}\left(\frac{C}{k_{BOD}+C}\right)L - \frac{64}{14}k_{12}\theta_{12}^{(T-20)}\left(\frac{C}{k_{NIT}+C}\right)C_1 - \frac{SOD}{D}\theta_s^{(T-20)} + G\left(\frac{32}{12} + \frac{48}{14}\frac{14}{12}(1 - P_{NH_3})\right)C_4 - \frac{32}{12}k_{1R}\theta_{1R}^{(T-20)}C_4 \quad (15)$$

In which dimensionless P_{NH_3} is calculated as:

$$P_{NH_3} = NH_3\frac{NO_3^-}{(k_{mN}+NH_3)(k_{mN}+NO_3^-)} + \frac{k_{mN}}{(NO_3^-+NH_3)(k_{mN}+NO_3^-)} \quad (16)$$

C1, C4 are concentration of Ammonia-Nitrogen and Phytoplankton Carbon, respectively. In Eq. (15), the terms in the RHS are reaeration, BOD oxidation, nitrification, sediment oxygen demand, phytoplankton growth, respiration, respectively. In fact, the data needed to parameterize widely used WASP model is generally prohibitive. Thus, VART-DO model with 13 modeling parameters provides a simpler modeling framework that includes more important processes.

(3) VART-DO model is unique in terms of incorporation of dispersion and transient storage Effect. Hyporheic exchanges in VART-DO account for the interaction of main channel flow with surrounding dead zone water and subsurface flow (Bencala, 1983a, 1983b, 1993, 2000; Gooseff et. al., 2002; Runkel, 1998, 2002; Chapra and Runkel, 1999). From biochemical perspective, subsurface flows and storage zones are generally low in dissolved oxygen compared to stream water. Therefore, biogeochemical gradient is included in VART-DO. Unlike OTIS model used by Chapra and Runkel (1999), VART-DO considers dynamic changes of DO and variable residence time. In addition, dispersion process in VART-DO represents mixing and as showed induces more exchange of DO at water surface. Chapra and Runkel (1999) considered plug-flow (no mixing) in their studies. Table 2.4 presents the processes considered by VART-DO and comparison with Streeter-Phelps and WASP model in terms of level of complexity.

Table 2-4- Processes considered by different models

Process	Streeter-Phelps Model	VART-DO Model	WASP Model
Advection		×	×
Dispersion		×	×
Hyporheic Exchange		×	
Reaeration	×	×	×
CBOD Oxidation	×	×	×
NBOD Oxidation			×
Sediment Oxygen Demand			×
Nitrification			×
Phytoplankton Growth			×
Respiration			×

2.6. Conclusion

The study may be concluded with the following major findings:

1) This chapter presents an effective approach for estimation of the reaeration coefficient and the DO concentration in streams. The new approach is characterized by the VART-DO model and an optimization procedure for inverse modeling. VART-DO includes major processes affect DO concentration. To keep the VART-DO model relatively simple as compared to widely used WASP model, BOD degradation, diurnal DO changes (i.e. photosynthesis and respiration), and nitrification are ignored (as also induced by available observed data). This particularly helpful in understanding the effect of hyporheic exchange and dispersion processes on reaeration and DO changes.

2) Storage zones are indispensable parts of streams. In some river reaches like those along Hiwassee, Watauga, Clinch reach 3, and French Broad, the transient storage significantly affect the determination of optimum K_2 values. The storage zone effect may become more important in streams where biologically degraded materials impacts the DO concentration while the river reaches in the present study were selected such that the effect of biodegradable materials was negligible and the velocities were high. Storage zones can

reduce K_2 and RMSE values for about 30 percent. Therefore, it is more realistic to consider their effect in the DO modeling.

3) Dispersion mechanism is important to DO exchange. The study showed that strong longitudinal dispersion can increase K_2 values. According to the sensitivity analysis, dispersion coefficient may increase K_2 value by about 50 percent and decreases RMSE by about 48 percent.

4) The K_2 value computed using the VART-DO model may be up to 6 times greater than those obtained from existing empirical equations. The combined effects of storage zones and dispersion coefficient should be considered in estimation of K_2.

2.7. References

Bansal, M.K. (1973). "Atmospheric reaeration in natural Streams." *Water Research Pergamon Press*, Vol. 7, 769-782.

Bencala, K.E., (1983a). "Simulation of solute transport in a mountain pool-and-riffle stream with a kinetic mass transfer model for sorption." *Water Resour. Res.*, 19(3), 732-738.

Bencala, K.E. and Walters, R.A. (1983b). "Simulation of solute transport in a mountain pool-and-riffle stream: a transient storage model." *Water Resour. Res.*, 19(3), 718-724.

Bencala, K.E. (1993) A perspective on stream-catchment connections. Journal of the North American Benthological Society, 12, 44

Bencala, K.E., (2000) "Hyporheic zone hydrological processes." Hydrological Processes, 14, 2797.

Boano, F., Packman, A.I., Cortis, A., Revelli, R., and Ridolfi, L. (2007). A continuous time random walk approach to the stream transport of solutes, Water Resour. Res., 43, W10425, doi:10.1029/2007WR006062.

Boyle, D.P., Gupta, H.V., Sorooshian, S. (2000). "Toward improved calibration of hydrologic models: combining the strengths of manual and automatic methods." *Water Resources Research*, 36(12), 3663-3674.

Cardoso, M.F., Salcedo, R.L, and Azevedo, F.D. (1996). "The SIMPLEX-Simulated Annealing Approach to continuous non-linear optimization." *Computers Chem. Engng.*, 20(9), 1065-1080.

Chapra, S.C. and Runkel, R.L. (1999). "Modeling impact of storage zones on stream dissolved oxygen." *J. Envir. Eng.*, 125(5), 415-419.

Churchill, M.A., Elmore, H.L., and Buckinghum, R.A. (1962). "The prediction of stream reaeration rates." *J. sanit. Engng. Div. Am. Soc. Civ. Engrs* 88, SA-4.

Covar, A.P. (1976). "Selecting the proper reaeration coefficient for use in the water quality models." *Proc., Environmental Modeling and Simulation*." U.S. EPA, Washington D.C., 340-343.

Deng, Z.-Q., Jung, H.-S., and Ghimire, B. (2010). "Effect of channel size on solute residence time distributions in rivers." *Advances in Water Resources*, 33 (9), 1118–1127.

Deng, Z-Q. and Jung, H-S. (2009). "Variable residence time-based model solute transport in streams." *Water Resources Research*, Vol. 45, W03415.

Deng, Z-Q., Bengtsson, L., Singh, V. P. (2006). "Parameter estimation for fractional dispersion model for rivers." *Environ Fluid Mech*, No. 6, 451-475.

Deng, Z.-Q., Singh, V. P., and Bengtsson, L. (2001), "Longitudinal dispersion coefficient in straight rivers." *Journal of Hydraulic Engineering*, 127(11), 919-927.

Dobbins, W.E. (1964). "BOD and oxygen relationships in streams." *Am. Soc. Civil Engineers Jour.*, Vol. 90, No. SA-3, 53-78.

Duan, Z., Martin, J.L., Stockstill, R.L., McAnally, W.H., and Bridges, D.H. (2009). "Modeling streamflow-driven gas-liquid transfer rate." *environmental engineering sciences*, 26(1), 155-161.

Duan, Z., James, M., Tang, Y. (2010). "Modeling oxygen mass transfer rate through the air-water surface in stratified flows." *Proc., World Environmental and Water Resources Congress*, ASCE, Providence, RI, 371-408.

Elliott, A.H., and Brooks, N.H. (1997). "Transfer of nonsorbing solutes to a streambed with bed forms: Laboratory experiments ." *Water Resour. Res.*, 33(1), 137-151.

Esen, I.I. and Rathbun, R.E. (1976). "A stochastic model for predicting the probability distribution of the dissolved-oxygen deficit in streams." U.S Geological Survey, Washington, D. C., No.913.

Gooseff M.N., McKnight D.M., Lyons W.B. and Blum A.E., (2002). " Weathering reactions and hyporheic exchange controls on stream water chemistry in a glacial meltwater stream in the McMurdo Dry Valleys." Water Resources Research, 38, 1279.

Gualtieri, C., Gualtieri, P., and Doria, G.P. (2002). "Dimensional analysis of reaeration rate in streams." *Journal of Environmental Engineering*, 128(1), 12-18.

Langbein, W.B. and Durrum, W.H., (1967). "The reaeration capacity of streams." U.S. Geological Survey, Washington D.C, Circular 542.

Lin S., 2001, Water and Wastewater Calculations manual, McGraw Hill, ISBN 0-07-137195-8
Matlab Online help manual Ver. 7.8.0.347 (R2009a).

Melching, C., and Flores, H.E., (1999). "Reaeration equations derived from U.S. Geological Survey database." *Journal of Environmental Engineering*, 125(5), 407-414.

Missouri Department of Natural Resources. "Maximum Dissolved Oxygen Concentration Saturation Table." <http://www.dnr.mo.gov/env/esp/wqm/DOSaturationTable.htm> (Nov. 12, 2010)

Moriasi, D.N., Arnold, J.G., Van Liew, M.W., Bingner, R.L., Harmel, R.D., Veith, T.L. (2007). "Model evaluation guidelines for systematic quantification of accuracy in watershed simulations." *American Society of Agricultural and Biological Engineering*, 50(3), 885-900.

Moriasi, D.N., Wilson, B.N., Douglas-Mankin, K.R., Arnold, J.G., Gowda, P.H. (2012). "Hydrology and water quality models: use, calibration, and validation." *American Society of Agricultural and Biological Engineering*, 55(4), 1241-1247.

O'Connor, D.J. and Dobbins, W.E., (1958). "Mechanism of reaeration in natural streams." *Trans. Am. Soc. Civ. Engrs*, 123 (2934), 641-684.

Owens, M., Edward, R.W., and Gibbs, J.W. (1964). "Some reaeration studies in streams." Int. J. Air and Wat. Pollut. 8, 469.

Qian, Q., Voller, V.R., and Stefan, H.G. (2008). "A vertical dispersion model for solute exchange induced by underflow and periodic hyporheic flow in stream gravel bed." *Water Resour. Res.*, 44, W07422.

Runkel R.L. (1998) One-Dimensional Transport with Inflow and Storage (OTIS): A Solute Transport Model for Streams and Rivers, USGS WRIR 98 – 4018

Runkel R.L. (2002) A new metric for determining the importance of transient storage. Journal of the North American Benthological Society, 21, 529

Streeter, H.W. and Phelps, E.B., (1925). "A study of the pollution and natural purification of Ohio River." *Public Health Bulletin*, U.S. Public Health Service, Washington, D.C., No. 146.
Sun, N.Z., (1994). "Inverse Problem in Groundwater Modeling." Kluwer Academic Publishers, Dordrecht, The Netherlands.

Vellidis, G., Barnes, P., Bosch, D.D., Cathey, A.M., (2006). "Mathematical simulation tools for developing dissolved oxygen TMDLs." American Society of Agricultural and Biological Engineers, 49(4).

Wool, T.A., Ambrose, R.B., Martin, J.L., and Comer, E.A., (2001). "Water quality analysis simulation program (WASP) version 6.0: User's manual. Atlanta, GA.: U.S. Environmental Protection Agency, Region 4.

Yeh, W. W-G. (1986). "Review of Parameter identification procedures in groundwater hydrology: The inverse problem." *Water Resources Research,* 22(2), 95-108.

CHAPTER 3
WATERSHED MODELING OF AMITE RIVER FOR ESTIMATION OF BOD LOADING

3.1. Introduction

Water quality modeling is commonly conducted to estimate the impact of various changes such as agricultural practices, urbanization, and land cover changes, on surface and subsurface water and assist in decision making processes (Laroche et al., 1996). These processes usually consist of (1) defining the priority for watersheds with higher intervention (Phillps, 1989), (2) determining critical zones within watershed (Maas et al., 1985), (3) considering best management practices, and (4) evaluating achievable surface water quality (Larsen et al., 1988). Among many computer models, watershed models are essential and effective tools for investigating complex nature of mechanisms that are influential to water quality conditions of water bodies. Hydrological Simulation Program- FORTRAN (HSPF) is a continuous simulation model (Bicknell et al., 2001) that is widely used for watershed modeling and management. HSPF was developed by the U.S. Environmental Protection Agency (USEPA) and supported by U.S. Geological Survey (USGS). As part of the present study, the main objectives in this chapter are (1) simulating and calibrating flow discharge, (2) simulating and calibration of temperature, (3) modeling and calibration dissolved oxygen (DO), and (4) obtaining biological oxygen demand (BOD) concentration in Amite River between Denham Springs and Port Vincent using HSPF model. The modeling results are used to supplement the observation data we had from USGS stations along the Lower Amite River.

3.2. Materials and Methods

3.2.1. Better Assessment Science Integrating point and Non-point Sources (BASINS)

The US Environmental Protection Agency (USEPA) developed the Better Assessment Science Integrating point and Non-point Sources (BASINS) that encompasses multiple modeling powers with a geographical information system (GIS; ArcGIS®) (Brun and Band, 2000). In fact, BASINS modeling framework employs the national watershed data and the state-of-the-art environmental assessment for a multi-purpose environmental analysis. BASINS provides three broad sets of metadata: (1) spatially distributed data, (2) environmental monitoring data, and (3) other data which are accessible externally through download. Land use/land cover, urbanized areas, populated place locations, reach file version 1 (RF1), soils (STATSGO), elevation (DEM), national elevation dataset (NED), major roads, USGS hydrologic unit boundaries (accounting unit, cataloging unit), EPA regional boundaries, state boundaries, county boundaries, federal and Indian lands, and eco-regions are all included in BASINS as spatially distributed data. Environmental monitoring data such as water quality station summaries, water quality observation data, bacteria monitoring station summaries, weather station sites, USGS gaging stations, and permit compliance system sites and loadings are usually provided by USEPA and are embedded into BASINS. Data such as national hydrography dataset (NHD), national land cover data (NLCD), population data, and list of impaired waters can be downloaded and used in BASINS framework. Figure 3.1 shows a snapshot of the data layers in BASINS platform. These layers will be shown in the following paragraphs in detail. The GIS-based hydrologic modeling tool in BASINS allows the user to modify, for example, the land use attributes and define different scenarios for identification of a watershed behavior. Therefore, BASINS is a useful

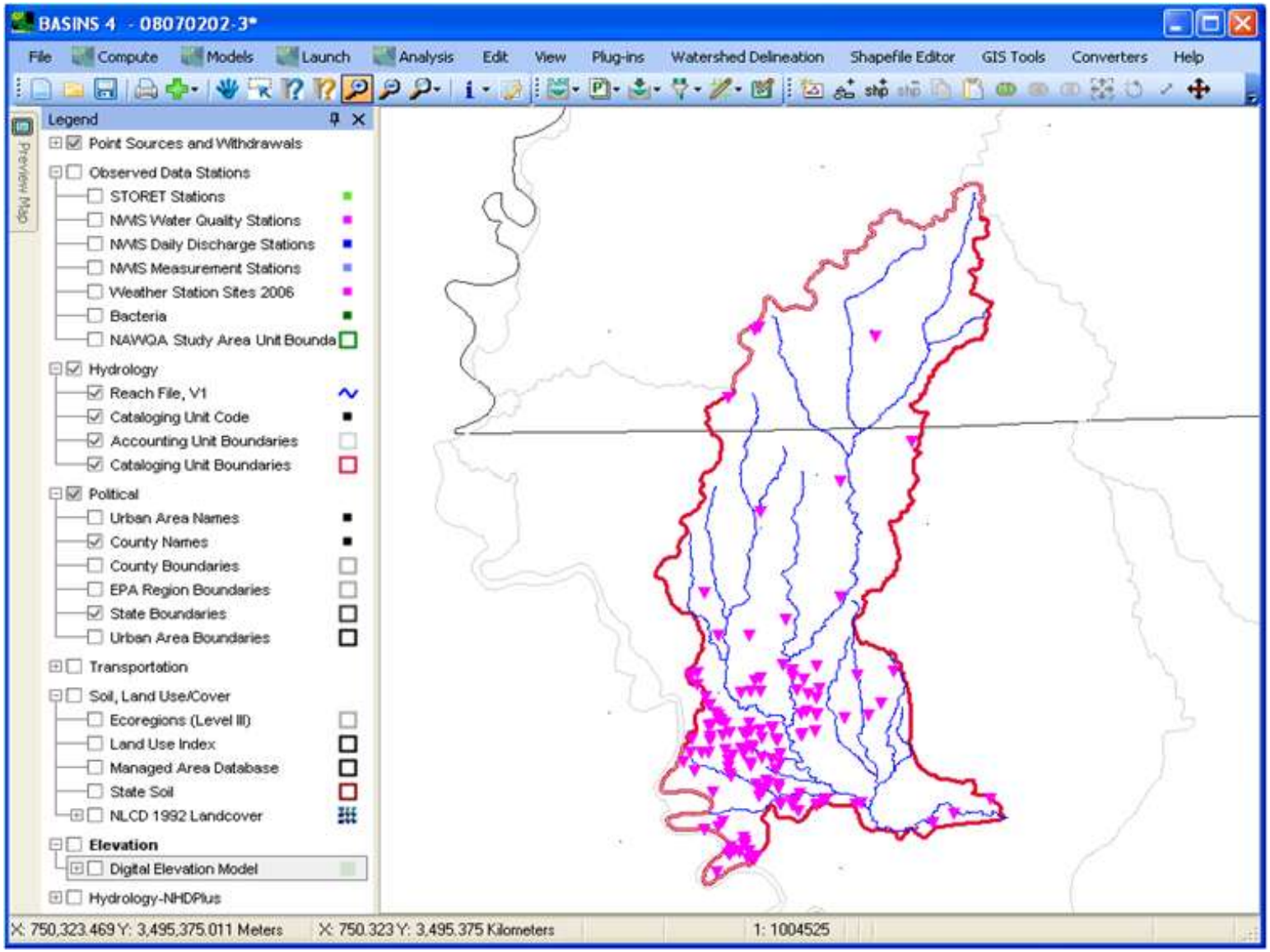

Figure 3.1- Right: Amite River model in BASINS; Left: various data layers

framework for analysis and development of TMDL standards and guidelines nationwide (Borah and Bera, 2004) and design of Best Management Practices.

GIS interface of BASINS enables retrieving pre-digitalized Amite River watershed and download the data from various databases to be used in watershed modeling. In Figure 3.2 Amite River watershed, flow networks, main streams, and tributaries are depicted. A digitalized soil information layer (NRCS-STATSGO soil database) and land use /land cover data layer (US Geological Survey (USGS)-GIRAS database) (Figure 3.3) are usually used in further classification of areas in the watershed (Singh et al., 2005). Based on the topology and existing stream network, the watershed is divided into five smaller and hydrologically connected subwatersheds. Since the focus of present study in on dissolved oxygen changes in the Amite River between Denham Springs and Port Vincent, watershed was delineated so that the outlets of subwatersheds are aligned with the observatory stations at these two stations which is also helpful for calibration practices. A USGS elevation data (digital elevation model, DEM) (Figure 3.4) layer along with a pre-digitalized stream network data layer (National Hydrography Dataset, NHD) (Figure 3.2) were used for watershed delineation (Singh et al., 2005). Figure 3.5 shows the sub-watersheds and their corresponding outlets across the Amite River watershed. For hydrological simulation, time series of climate data such as precipitation, potential ET, air temperature, dew point, solar radiation are required. BASINS can access to the meteorological stations in the study area to retrieve climate data for the period of simulation. In Figure 3.6, the stations in the Amite River watershed are shown. The data from Baton Rouge station was used in the present studies. The latest version of BASINS 4 was utilized in characterizing flow condition and determination of water quality indicator (DO and BOD) in this study.

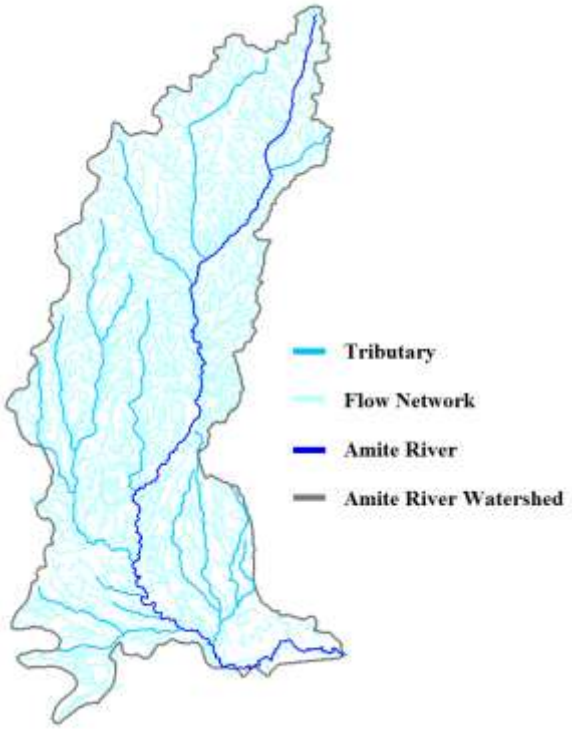

Figure 3.2- Amite River watershed and river systems in BASINS4

3.2.2. Hydrological Simulation Program- FORTRAN (HSPF)

One of the modeling tools integrated in BASINS is Hydrological Simulation Program-FORTRAN (HSPF). HSPF model is a comprehensive, continuous watershed-scale simulation model, which has a modular structure and is a lumped parameter model (Singh et al., 2007; Albek et al., 2004) with great complexity (Al Abed and Al Sharif, 2008). The model is capable of considering both point and non-point pollution sources and performs flow and water quality routing in river reaches. The main challenge about HSPF model is that a large number of parameter values should be defined. These values cannot be obtained from field data. Instead, calibration practice is needed (Singh et al., 2007). HSPF model has three main modules, including PERLND, IMPLND, and RCHRES for simulating pervious and impervious land segments and river reaches/reservoir, respectively (Singh et al., 2007; HSPF manual, Bicknel et

al. 2001). HSPF estimates surface runoff using hourly time step as a function of infiltration that is computed using Philip's equation (Philip, 1957). A storage routing technique is used to rout water from one reach to the next during stream processes. The hydraulic characteristics of the reaches in the model are defined by parameters in the function table (FTABLEs). These FTABLEs define the volume-discharge relationships in the reaches.

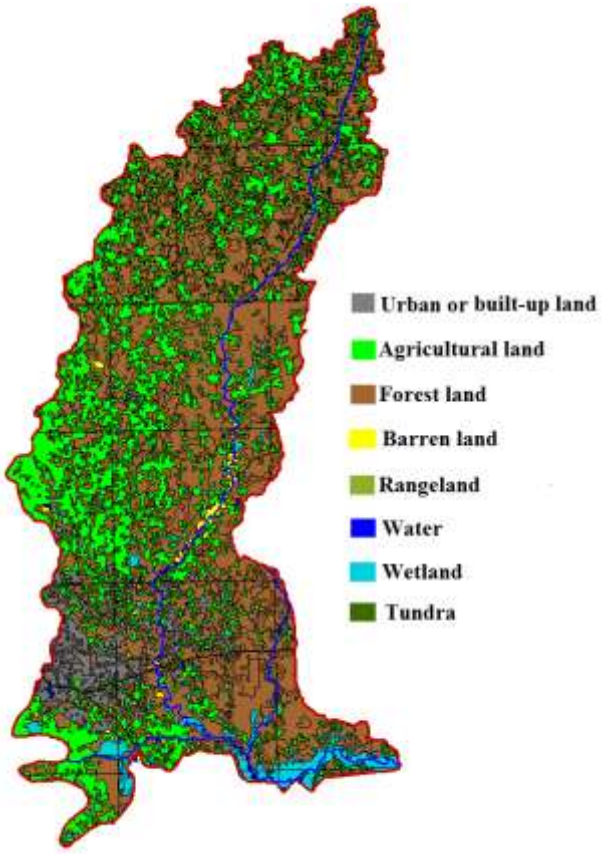

Figure 3.3- Soil, land use/cover across Amite River watershed in BASINS4

Derived from the Stanford Watershed Model (SWM), HSPF accounts for all stream flow components: base-flow, interflow, and runoff. HSPF is a comprehensive package for water quality modeling for both conventional and toxic organic pollutants. HSPF allows integrated simulation of land and soil contaminant runoff process with instream hydraulic, water

temperature, sediment transport, nutrients, and sediment-chemical interactions (Donigian and Huber, 1991). The result of HSPF simulations based on precipitation is producing time history of the runoff flow rate, sediment load, chemicals, nutrients, and pesticides at any points in the watershed. Therefore, it is a suitable model for simulation of runoff, erosion, and fate and transport of pollutants.

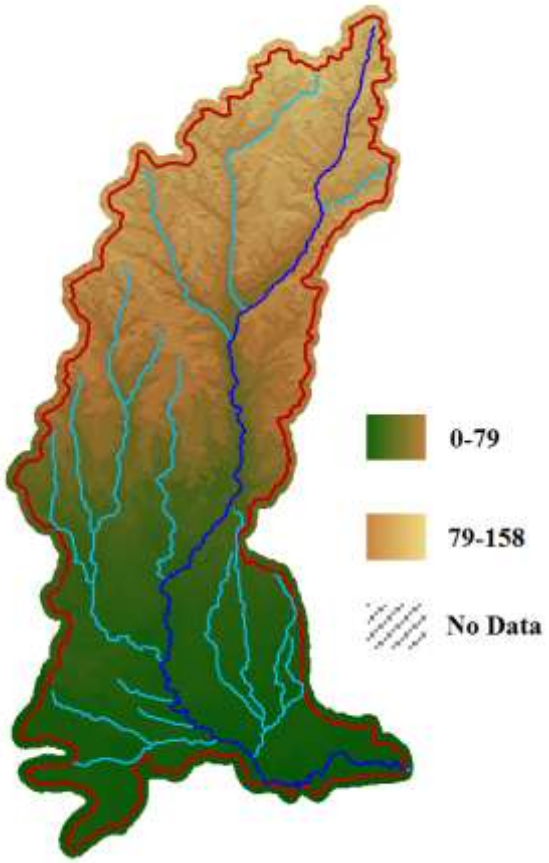

Figure 3.4- Digital elevation map of Amite River watershed in BASINS4

Since HSPF model uses continuous records of rainfall, evapotranspiration, temperature, and solar intensity for simulation, only those watersheds which are in a reasonable vicinity of meteorological stations with reliable long-term climate data can be modeled properly. Moreover, for the calibration purposes, the watershed has to have USGS gauge stations that have historical

discharge flow and water quality information. For present study, these conditions are satisfied since the data from Baton Rouge meteorological station; close to the river reach from Denham Springs to Port Vincent, for the simulation period (year 1990) is available. In addition, at both Denham Springs station at upstream and Port Vincent station at downstream USGS observatory data for flow and DO are available.

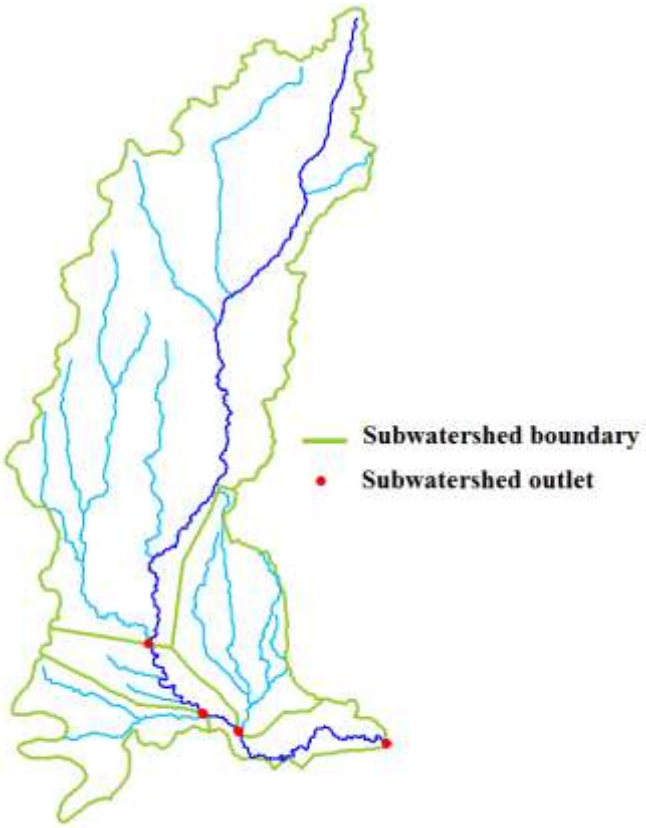

Figure 3.5- Sub-watersheds delineated across Amite River watershed and outlets in BASINS4

In the HSPF model, several subroutines are called to simulate flow runoff, sediment loads, and water quality. The subroutine OXRX includes the longitudinal advection of DO (defined as DOX in HSPF) and BOD, sinking of BOD materials, benthic oxygen demand, release of BOD materials from bottom sediment, reaeration, and oxygen depletion due to decay of BOD materials in determining oxygen balance. The HSPF model uses an empirical nonlinear equation

to relate dissolved oxygen at saturation to water temperature (Bicknell et al., 1996). The instream DO model involves the biochemical oxygen demand and dissolved oxygen balance to determine the in-stream dissolved oxygen concentration. The balance of biochemical oxygen demand and dissolved oxygen mainly accounts for reaeration, sediment oxygen demand (SOD), biochemical oxygen demand (BOD) and benthic and phytoplankton activities. Dissolved oxygen is consumed by organic materials (denoted as CBOD) and by nitrogenous BOD (denoted as NBOD) through nitrification process are considered in the HSPF simulation. The reaeration coefficient is calculated as a power function of hydraulic depth and velocity (Covar, 1976).

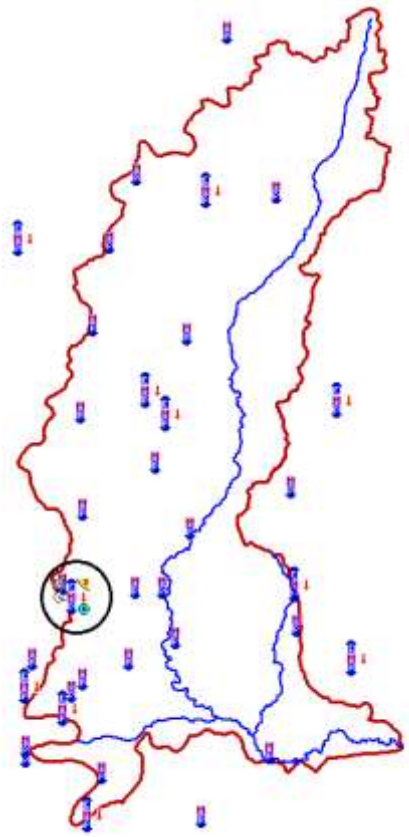

Figure 3.6- Meteorological stations across Amite River watershed and Baton Rouge station encircled in BASINS4

3.3. Results

3.3.1. Simulation of flow discharge in the Amite River

Flow discharge along the Amite River at Port Vincent was simulated and the results are shown in Figure 3.7. Several hydrological parameters affect the simulation results and should be adjusted to calibrate the model. The sensitive parameters are lower zone nominal storage (LZSN), upper zone nominal storage (UZSN), infiltration (INFILT), interflow inflow parameter (INTFW), inflow recession parameter (IRC), groundwater recession parameter (KVARY) and basic groundwater recession rate (AGWRC). To assure the simulation results, observation data from USGS station at Denham Springs was also shown for comparison. Further evaluation of flow duration curves (Figure 3.7) revealed that for a large portion, particularly during high flow condition, both simulated and observed data match well. For low flow condition, however, the two curves deviated. Since the flow condition in Amite River at Port Vincent is usually high due to flow from different tributaries, the simulated flow discharge is used for the further studies in following chapters.

3.3.2. Simulation of dissolved oxygen and biochemical oxygen demand in the Amite River

The DO and BOD are simulated with the water quality module after satisfactory flow discharge simulation and calibration. The contribution of land uses in producing BOD and nitrogenous contaminant has great impact on the results for DO and instream BOD concentration. Since sparse DO data from Denham Springs and Port Vincent are available, they are used to check the simulation results. Figures 3.8 and 3.9 show the simulation results for DO change at Denham Springs and instream BOD concentration along Amite River. These results will be used in the next chapter for simulation of sediment resuspension effect on DO variation along Amite River.

3.3.3. Land use and land cover changes across the Amite River watershed

The primary land use in the Amite River watershed was forest with 60% in early 1990's. However, urbanization and agricultural practices during past decades caused significant changes of land uses/land cover across the Amite River. Figure 3.10 depicts the land use changes of the Amite River watershed based on National Land Cover Database (NLCD) for years 1992, 2001, and 2006. Based on these land use data, from 1992 to 2006 urban area doubled and cropland increased by 70% while forests reduced by 60% (Figure 3.11). Such changes in land use/land cover should be accounted for properly in any TMDL development. Since these land use/land cover changes affect the watershed BOD loads into the Amite River.

3.4. Discussion and Conclusion

HSPF model was used to simulate flow discharge, DO, and BOD concentration at Denham Springs station in the Amite River. However, HSPF had a huge number of modeling parameters which need to be well defined. In this study, the general procedures suggested by USEPA were followed to first calibrate the flow discharge. To that end, a trial and error approach was used to define the best value for each of the modeling parameters within their defined ranges. These ranges are defined by USEPA based on results from studies on various rivers across the country. Following the calibration of flow discharge, DO and BOD were calibrated according to the suggestion provided in HSPF manual. Available observed flow and data were used in calibration and BOD concentration was obtained once model was calibrated. The BOD concentration results showed that flow discharge is substantial in magnitude of BOD that discharged from watershed into the Amite River. Thus, the maximum concentration of BOD during January was five times the concentration of BOD in July 1990.

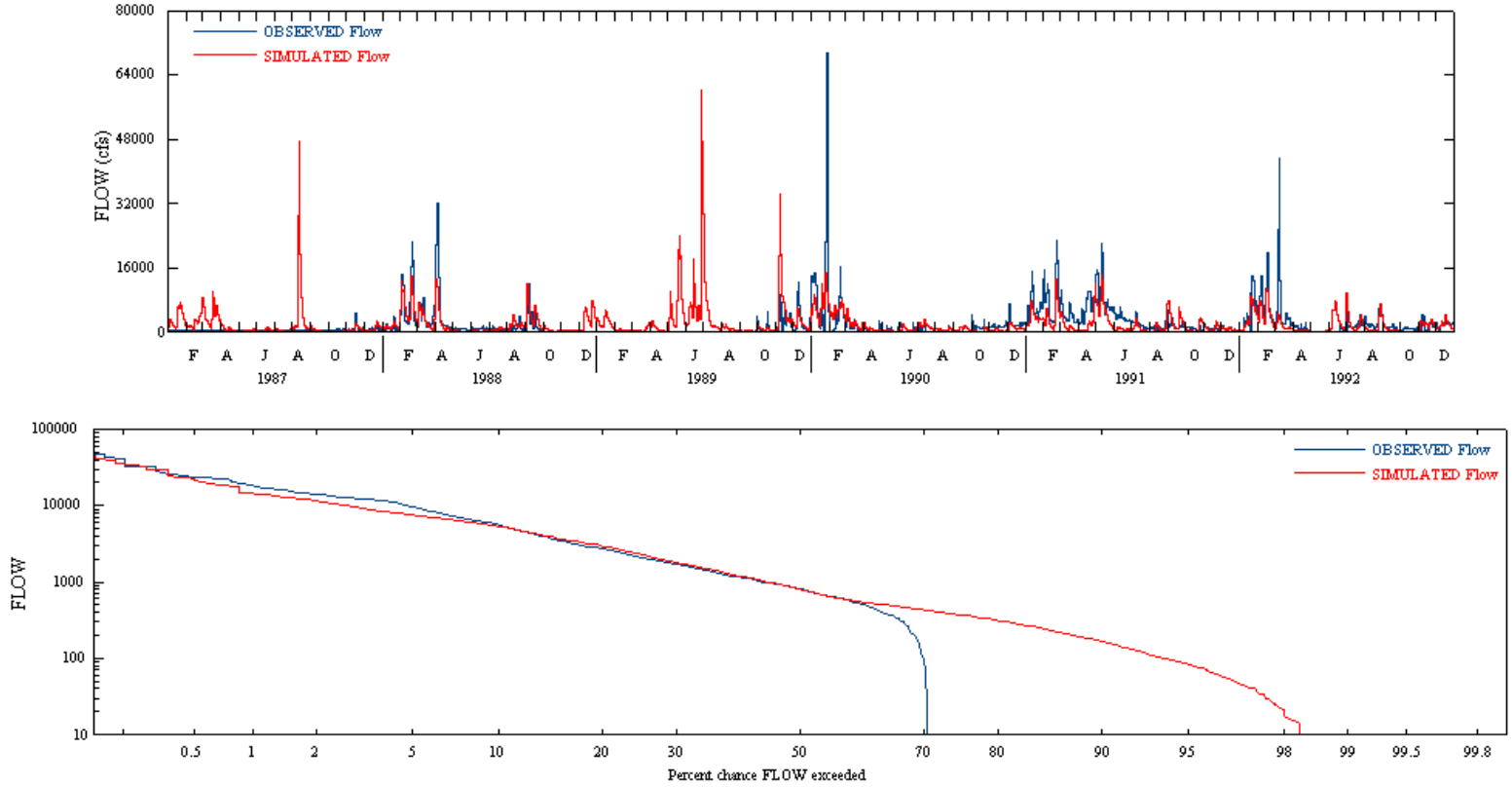

Figure 3.7- Upper panel: simulated and observed flow in Amite River. Lower panel: flow duration curves after calibration

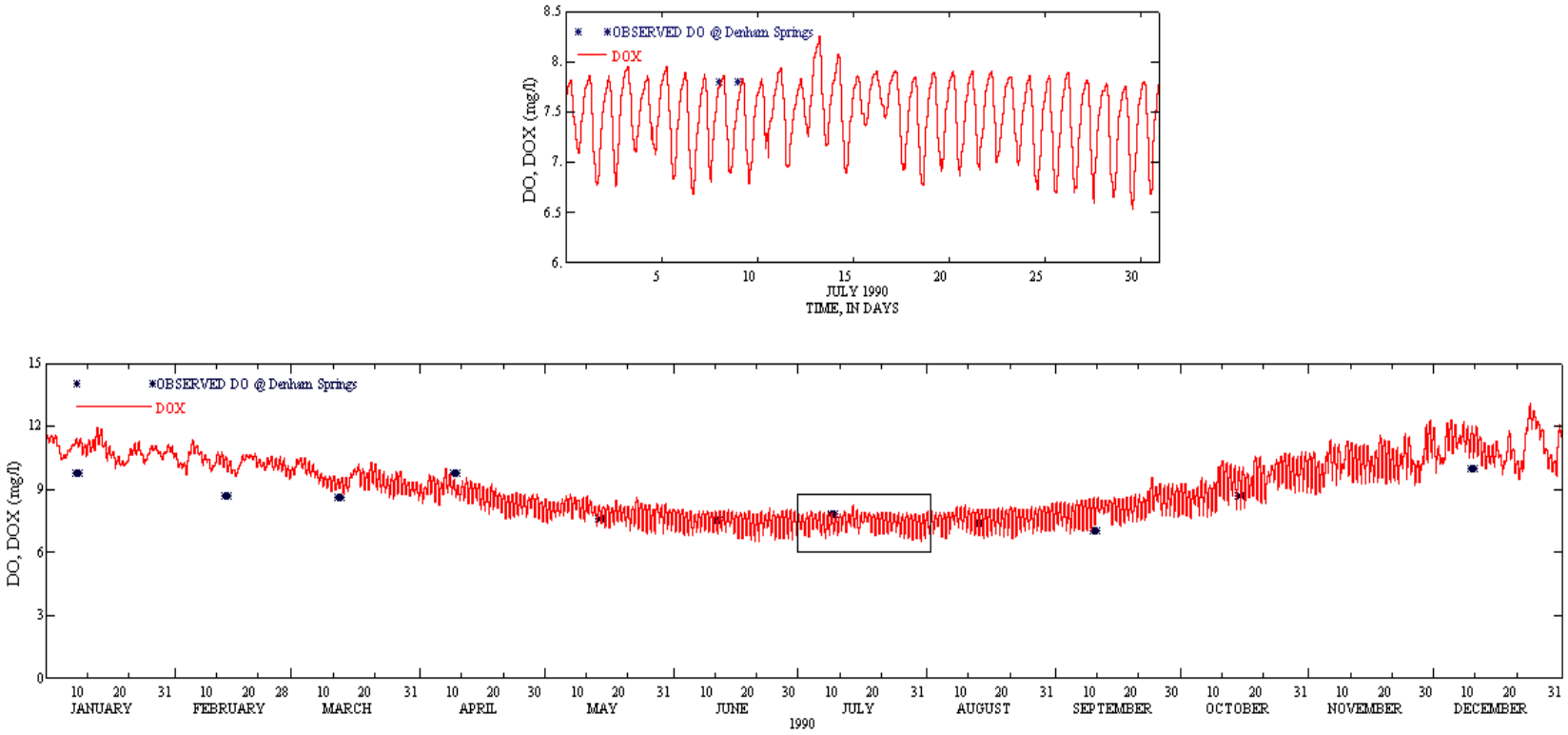

Figure 3.8- Simulated DO concentration at Denham Springs; up: for July 1990 and down: for the year 1990

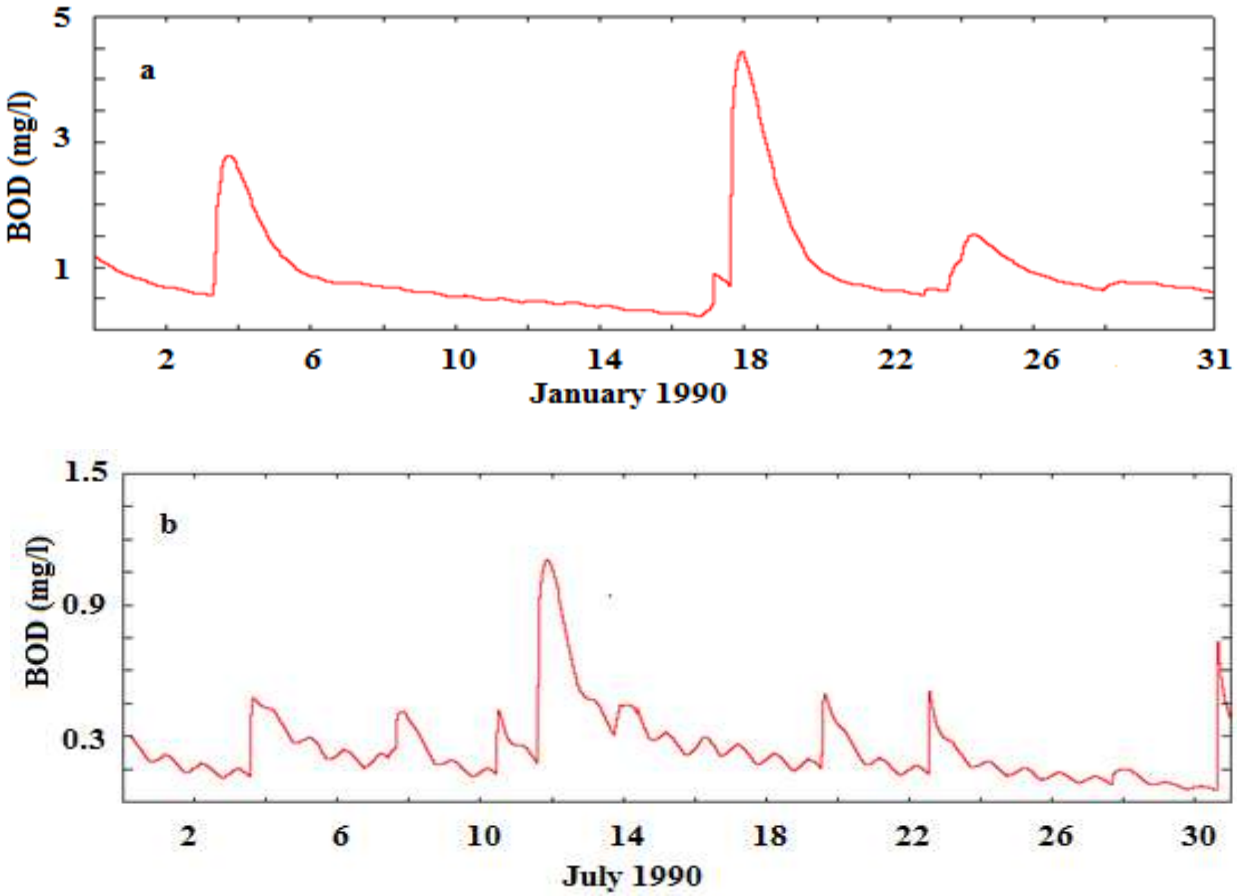

Figure 3.9- BOD input from Amite River watershed: a) for January 1990; b) for July 1990

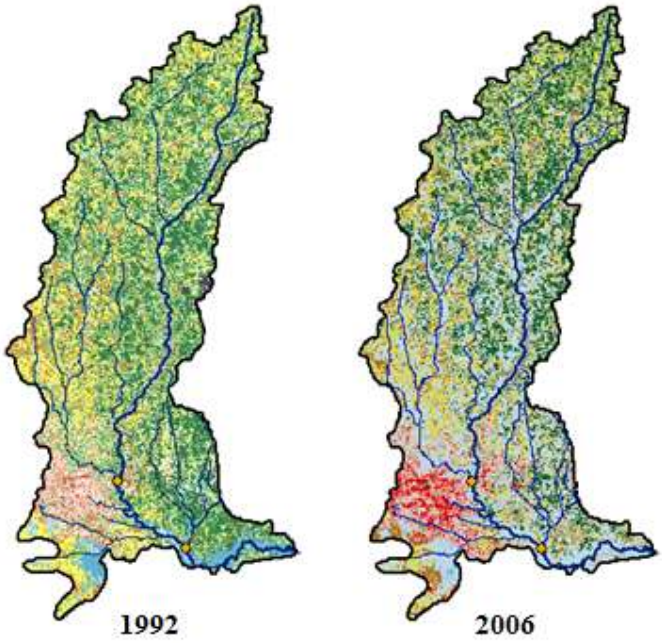

Figure 3.10- Comparison of land use/land covers across the Amite River watershed

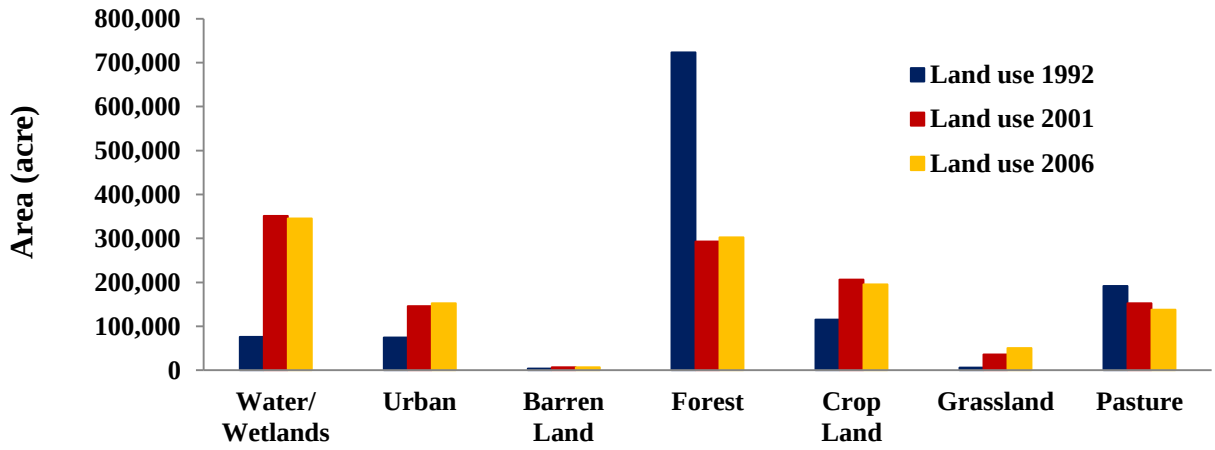

Figure 3.11- Land use/land cover changes in the Amite River watershed

3.5. References

Al-Abed, N., Al-Sharif, M. (2008). "Hydrological modeling of Zarqa River Basin-Jordan using the hydrological simulation program-FORTRAN (HSPF) model." Water Resour. Manag., 22 (9), 1203-1220.

Albek, M., Ülker, B.Ö., Albek, E. (2004). "Hydrological modeling of Seydi Suyu watershed (Turkey) with HSPF." J. Hydro., 285, 260-275.

Bicknell, B.R., Imhoff, J.C., Kittle, J.L., Donigian, A.S., Johanson, R.C. (2001). "Hydrological Simulation Program–Fortran (HSPF): User's Manual Release 12." US *Environmental Protection Agency*: Athens, GA.

Borah, D.K., Bera, M., (2004). "Watersehd-scale hydrologic and non-point source pollution models: Review of applications." Transaction of ASAE, 47(3), 789-803.

Brun, S.E., Band, L.E. (2000). "Simulating runoff behavior in an urbanizing watershed." Comput. Environ. Urban., 24, 5-22.

Covar, A.P. (1976). "Selecting the proper reaeration coefficient for use in water quality models." US EPA conference on Environmental Simulation Modeling, April 19-22.

Donigian, Jr., A.S., Huber, W.C. (1991). "Modeling of nonpoint source water quality in urban and non-urban areas." US Environmental Protection Agency, EPA/600/3-91/039,Athens, GA

Laroche, A.M., Gallichand, J., Lagace, R., Pesant, A., (1996). "Simulating atrazine transport with hspf in an agricultural watershed." J. Environ. Eng., 122 (7).

Larsen, D.P., Dudley, D.R., and Hughes, R.M. (1988). "A regional approach for assessing attainable surface water quality." J. Soil and Water Conservation, 43(1), 171-176.

Maas, R.P., Smolem, M.D. and, Dressing, S.A. (1985). "Selecting critical areas of nonpoint-source pollution control." J. Soil and Water Conservation, 40(1), 68-71.

Patil, A., (2009). "An uncertainty-based approach to the total maximum daily load development." PhD Dissertation, Louisiana State University.

Phillip, J.R. (1957a). "The theory of infiltration: Sorptivity and algebraic infiltration equations." Soil Science, 84, 257-264.

Phillips, J. D. (1989). "Nonpoint source pollution risk assessment in a watershed context." Envir. Mgmt., 13(4), 493-502.

Singh, J., Knapp, H.V., Arnold, J.G., and Demissie, M., (2007). "Hydrological modeling of the iroquois river watershed using hspf and swat." J. Ame. water Resour. Ass., 41(2).

CHAPTER 4
MODELING SEDIMENT RESUSPENSION-INDUCED DO VARIATION IN FINE-GRAINED STREAMS

4.1. Introduction

Dissolved Oxygen (DO) is by far the most important water quality indicator for aquatic life (Williams and Boorman, 2012; Patil and Deng, 2012). The instream DO variation may be caused by various environmental factors. The DO becomes low in summer and high in winter following seasonal temperature variation trend. In general, the DO also experiences diurnal variations especially in small streams. During sunny days, the DO level commonly rises due to photosynthesis oxygen production. DO drops to a low level at night due to the respiration of aquatic plants. Decreased DO levels may also be indicative of water pollution due to discharges of oxygen-consuming contaminants such as COD (chemical oxygen demand) and BOD (biochemical oxygen demand) that are abundant in untreated sewage, partially treated sewage, organic discharges, and anoxic discharges.

In addition to the widely documented natural and pollution-induced variations (Chapra 1997), it is also found that the DO level in streams with organic-rich fine-grained sediment exhibits significant fluctuations during flood events due to sediment resuspension, as shown in Figure 4.1. The peak flow of 35.11 m^3/s on July 13, 1990 produced maximum sediment erosion (calculated in the following section) with the minimum DO of 2 mg/l in the Amite River, Louisiana, USA. Similar results of DO reduction as the result of sediment resuspension were also observed in other studies (Waterman et al. 2011, Hwang et al. 2011, Motta et al. 2010).

The reduction in DO concentration due to sediment resuspension is generally attributed to the sediment resuspension-enhanced decomposition of labile organic matter by aerobic microorganisms in water column (Hopkinson 1985, 1987, and 1996; Lopez and Garcia, 2001). It

was reported that the concentration of organic materials in fine-grained bottom sediment is much higher (orders of magnitude) than that in the water column (Wainright and Hopkinson, 1996). Sediment resuspension may cause the release of labile organic matter from bottom sediment to the water column and rapid decomposition of the released organic matter, leading to acceleration of oxygen consumption in water column and subsequent DO drawdown.

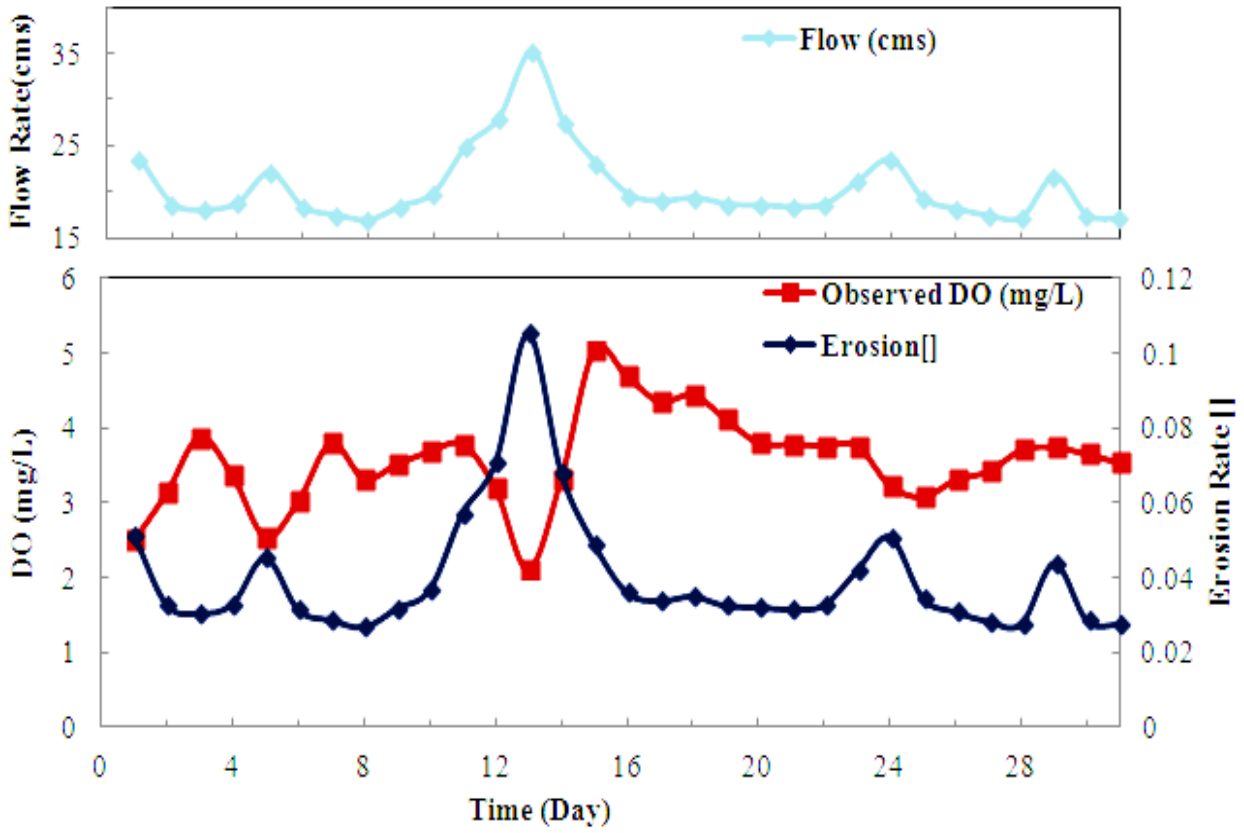

Figure 4.1- Flow, erosion rate, and DO concentration at Port Vincent Station during July 1990 in Amite River

The focus of previous studies was more on measurement and quantification of sediment oxygen demand (SOD) rather than effect of sediment resuspension on DO variation (Berg et al., 2003; Arega and Lee, 2005). Motta et al. (2010) presented a modeling framework for studying

the effect of organic sediment resuspension on dissolved oxygen concentration in rivers. The model made it possible to capture the additional oxygen demand from sediment resuspension. Waterman et al. (2011) made in situ measurement of suspended sediment oxygen demand. They presented a mathematical equation relating sediment resuspension oxygen demand to concentration of total suspended solids and oxygen concentration with site-specific constant parameters. Waterman et al. (2011) found that during the early phase of sediment resuspension, oxygen demand increased twice as high as the background sediment oxygen demand (SOD). Finally, they concluded that oxygen demand is one order of magnitude higher during sediment resuspension than sediment without resuspension.

In the studies of Motta et al. (2010), the modeling framework needs several parameters from bottom sediment and water column which are not usually available; i.e. BOD concentration attached to particles in bottom sediment or to particles in water column. As a result, their modeling framework cannot easily be implemented for other rivers. The equation of Waterman et al. (2011) requires concentration of total suspended solids. Unless calculated from erosion rate of bottom sediment, total suspended solids' observed data may not be readily available as in the case of the Amite River.

With VART-DO, it was previously shown in chapter two that hyporheic exchange and dispersion mechanism have effects on fate and transport of dissolved oxygen in rivers. The primary objective of this study is to present a simple yet effective model for simulation of DO transport and exchanges across water-sediment and water-air interfaces in rivers with emphasis on effect of sediment resuspension on DO variation. The objective will be achieved by incorporating sediment resuspension effect into our instream VART-DO model obtained in chapter two.

4.2. Materials and Methods

4.2.1. Conceptual Model for In-Stream Dissolved Oxygen

Major mechanisms and processes responsible for instream DO variations are conceptually described in Figure 4.2. It is generally recognized that DO variation in a stream can be affected by mass fluxes across the air-water and water-sediment interfaces in addition to longitudinal transport and reactions. Sediment resuspension and respiration of living species and photosynthesis can also influence DO concentration. BOD degradation, nitrification, existence of reduced metals and other chemical/biological reactions often result in DO consumption in benthic sediment. As mentioned in chapter two the DO exchange between the overlying water column and the benthic sediment can be affected by the transient storage and the Sediment Oxygen Demand (SOD).

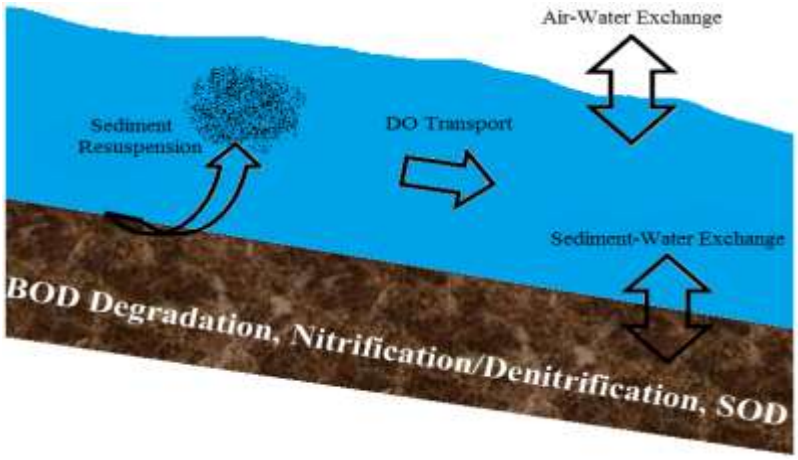

Figure 4.2- Mechanisms that affect DO changes along a river

4.2.2. Numerical Model for In-Stream Dissolved Oxygen

By extending the **VA**riable **R**esidence **T**ime (VART) model (Deng and June 2009, Deng et al. 2010), in chapter two a new model was presented, called VART-DO model, for simulation of

instream dissolved oxygen (DO) transport and exchanges across both air-water and water-sediment interfaces. The VART-DO model consists of the following equations:

$$\frac{\partial D}{\partial t} + U\frac{\partial D}{\partial x} = E\frac{\partial^2 D}{\partial x^2} + \frac{A_{adv.} + A_{diff}}{A}\frac{1}{T_V}(D_S - D) - K_2 D + K_D L - P + R \qquad (1)$$

$$\frac{\partial D_S}{\partial t} = \frac{1}{T_V}(D - D_S) \qquad (2)$$

$$T_V = \begin{cases} T_{min} & for\ t \le T_{min} \\ t & for\ t \ge T_{min} \end{cases} \quad (T_{min} > 0) \qquad (3a)$$

$$A_{diff} = 4\pi D_E t_S \quad with \quad t_S = \begin{cases} 0 & for\ t \le T_{min} \\ t - T_{min} & for\ t \ge T_{min} \end{cases} \qquad (3b)$$

where in above equations D is the DO deficit [ML^{-3}] (the difference between saturation DO concentration and actual DO level) in water column, D_S is the DO deficit [ML^{-3}] in the storage zone, U is the flow velocity [LT^{-1}] along x direction, E is the longitudinal dispersion coefficient [L^2T^{-1}], t is the traveling time [T], K_D is the rate [T^{-1}] of biochemical oxidation of carbonaceous materials, K_2 is the reaeration coefficient [T^{-1}], A_{adv} = advection-dominated storage zone area [L^2], A_{diff} = diffusion-dominated storage zone area [L^2], T_V = residence time [T] in the storage zone, D_E = effective diffusion coefficient [L^2T^{-1}] in bottom sediment, T_{min} = minimum residence time [T], and t_s = the time [T] since solute release from the storage zone to the mainstream. Parameters P, R, and L are photosynthesis oxygen production [$ML^{-3}T^{-1}$], oxygen consumption during aerobic respiration [$ML^{-3}T^{-1}$], and BOD concentration [ML^{-3}] in the water column, respectively. The VART-DO model along with many existing empirical DO models is applicable to streams without sediment resuspension.

The resuspension of bottom sediment containing labile organic matter during flood events may cause rapid decomposition of the released organic matter and accelerate oxygen consumption and subsequent DO drawdown in water column. In order to develop a general

model that is applicable to both low flow without sediment resuspension and high flow with sediment resuspension, the VART-DO model is further extended to incorporate the sediment resuspension process and other DO consumption mechanisms such as SOD described in Figure 4.2. The extended DO model is called VART-DOS and the extended Eq. (1) can be rewritten as:

$$\frac{\partial C}{\partial t} + U\frac{\partial C}{\partial x} = \frac{\partial}{\partial x}\left(E\frac{\partial C}{\partial x}\right) + \frac{A_{adv.} + A_{diff.}}{A}\frac{1}{T_V}(C_s - C) + K_2\,\Theta_a^{(T-20)}(C_{sat} - C)$$

$$- K_D\Theta_D^{(T-20)}\left(\frac{C}{K_{BOD} + C}\right)L - \frac{SOD}{H} - \Lambda C \qquad (4)$$

in which C = DO concentration [ML^{-3}], Θ_a = temperature coefficient for reaeration (-), K_D = oxidation coefficient [T^{-1}], Θ_D = temperature coefficient for deoxygenation (-), K_{BOD} = half saturation constant for BOD oxidation (mgO_2/L), SOD = oxygen uptake by bottom sediment [$ML^{-2}T^{-1}$], Θ_s = temperature coefficient for SOD correction (-), and Λ = DO consumption rate [T^{-1}] due to sediment resuspension. The terms on right-hand side in Eq. (4) include longitudinal dispersion, transient storage zone effect, reaeration, deoxygenation of input BOD from watershed, sediment oxygen demand, and sediment resuspension-induced DO consumption, respectively. The DO concentration in the storage zone can be written as:

$$\frac{\partial C_s}{\partial t} = \frac{1}{T_V}(C - C_s) \qquad (5)$$

In Eq. (4), the DO consumption rate Λ is defined as:

$$\Lambda = \alpha\beta^m\,\frac{E_s w_s}{H_b(1-\lambda)} \qquad (6)$$

where w_s [L/T] is sediment settling velocity and can be determined using the method proposed by Cheng (1997); λ[-] is the porosity of sediment; H_b [m] is the depth of sediment erosion; Parameters α and m are empirical coefficients. Parameter β takes into account the effect of temperature on DO consumption and it is defined as the ratio of daily average temperature to

summer average temperature of water. Parameter E_s is a dimensionless rate of erosion and can be determined using the following formula introduced by Smith and McLean (1977):

$$E_s = \frac{0.65\gamma_o(\frac{\tau^*}{\tau_c^*} - 1)}{1 + \gamma_o(\frac{\tau^*}{\tau_c^*} - 1)} \tag{7}$$

Eq. (7) was widely mentioned in literature to calculate the erosion rate (Garcia, 2008) especially for the present Amite River where detailed concentration of suspended sediment is not available. It was previously used by Motta et al. (2010) in the case of Bubbly Creek in Chicago, IL. Bottom sediments in Bubbly Creek are made of silt/fine sand with median size (D_{50}) of 82μm. For Amite River, based on limited available data, a D_{50} value of 50μm was used (the lower range of the sediment size). In Eq. (7), γ_o is a dimensionless constant with a value 2.4e-3; τ^* and τ^*_c are dimensionless shear stress and critical shear stress, respectively, and τ^* is defined as:

$$\tau^* = \frac{(U^*)^2}{Sgd} \tag{8}$$

$$Shear\ velocity\ (U^*) = \sqrt{R_H g s_o} \tag{9}$$

in which R_H[L] is hydraulic radius; g [L/T^2] is gravitational acceleration; d [L] is particle size; S [-] is specific gravity of submerged sediment; s_o refers to bottom slope that may be approximated using Manning's equation when flow rate, cross sectional area, Manning's coefficient are known. Settling velocity in Eq. (6) is calculated as:

$$w_s = \frac{\nu}{d}(\sqrt{25 + 1.2d_*^2} - 5)^{1.5} \tag{10}$$

$$d_* = (\frac{(G-1)}{\nu^2})^{\frac{1}{3}} d \tag{11}$$

in which G [-] is specific gravity of sediment; ν [L^2/T] is kinematic viscosity of water. In Eq. (4), Reaeration coefficient (K_2) is obtained using O'Connor and Dobbins (1958) formulation:

$$K_2\left(1/_{day}\right) = \frac{3.93\,U^{0.5}}{H^{1.5}} \tag{12}$$

The dispersion coefficient (E) is calculated using the formula proposed by Deng et al. (2001):

$$\frac{E}{HU_*} = \frac{0.01\psi}{8M_*}\left(\frac{B}{H}\right)^{5/3}\left(\frac{U}{U_*}\right)^2 \tag{13}$$

in which U_* is the bottom shear velocity, H is the depth of water, B is the width of river, U is the velocity, and ψ is a multiplier. M_* is defined as:

$$M_* = 0.145 + \frac{1}{3520}\left(\frac{U}{U_*}\right)\left(\frac{B}{H}\right)^{1.38} \tag{14}$$

In Eq. (4), K_D is considered as $0.2d^{-1}$, Θ_a is 1.024 (Chapra, 1997), Θ_D is 1.040 (Alp and Melching, 2006), and Θ_s equals 1.065 (Zison et al., 1978).

According to the abovementioned equations, VART-DOS is formulated to capture sediment resuspension-induced DO reduction (last term on right hand side of Eq. 4) as well as the effect of storage zone and hyporheic exchange along rivers (2^{nd} term on right hand side of Eq. 4, and Eq. 5). Thus, VART-DOS makes it possible to consider the interaction between hyporheic exchange and sediment resuspension effect in consuming DO. Such interactions are probably dependent on hydraulic conditions and morphology of bottom sediment.

4.2.3. Study Area

The Amite River is located in southeastern Louisiana, USA and it has a drainage area of approximately 3435 km^2, as shown in Figure 4.3. The Amite River watershed has experienced significant changes in land use and climate since 1950s. The forest land has dropped from 60% in 1954 to current 27% while urban areas have increased by 10% and agricultural areas by over 20%. The drastic change in land use and land cover has significantly increased nonpoint source

discharges of pollutants and nutrients to streams, causing organic enrichment of the Amite River and particularly bed sediment (Deng and Patil, 2011). As a result, the Lower Amite River is impaired for dissolved oxygen, nitrate/nitrite, chlorides and total phosphorus (Patil and Deng, 2011; Jung and Deng, 2010; and Mishra and Deng, 2009). The Amite River flows generally southwestward to the Lake Pontchartrain estuary that is connected to the Gulf of Mexico. Therefore, the Amite River (especially the Lower Reach of the Amite River) is a coastal river characterized with organic-enriched fine-grained sediment (Deng and Patil, 2011).

4.2.4. Data Collection

The hydrologic data used in this paper were collected from various sources. According to Mishra and Deng (2009), the sediment concentration in the Amite River before Denham Springs station is in the range of 3-114 mg/L. In the Lower Amite River, based on recent survey conducted by USGS, the bottom sediment is composed of primarily fine grained of clay, silt, fine sand. For this study, it was assumed that sediment particles had median size of 50μm in the Lower Amite River which is especially representative of sediment particles in Port Vincent. The observed flow and DO data were obtained from USGS (2011) and simulations by Patil and Deng (2010). The geometry and sediment parameters of Lower Amite River are presented in Table 4.1. Mays (2001) mentioned that Manning's coefficient in major natural streams (with width > 100 ft) with no boulders varies in the range 0.025-0.06. Thus, Manning's coefficient is set as 0.04 for the Amite River. The parameters $A_{adv.}/A$, D_E, α, and m in the VART-DOS model are obtained through calibrations.

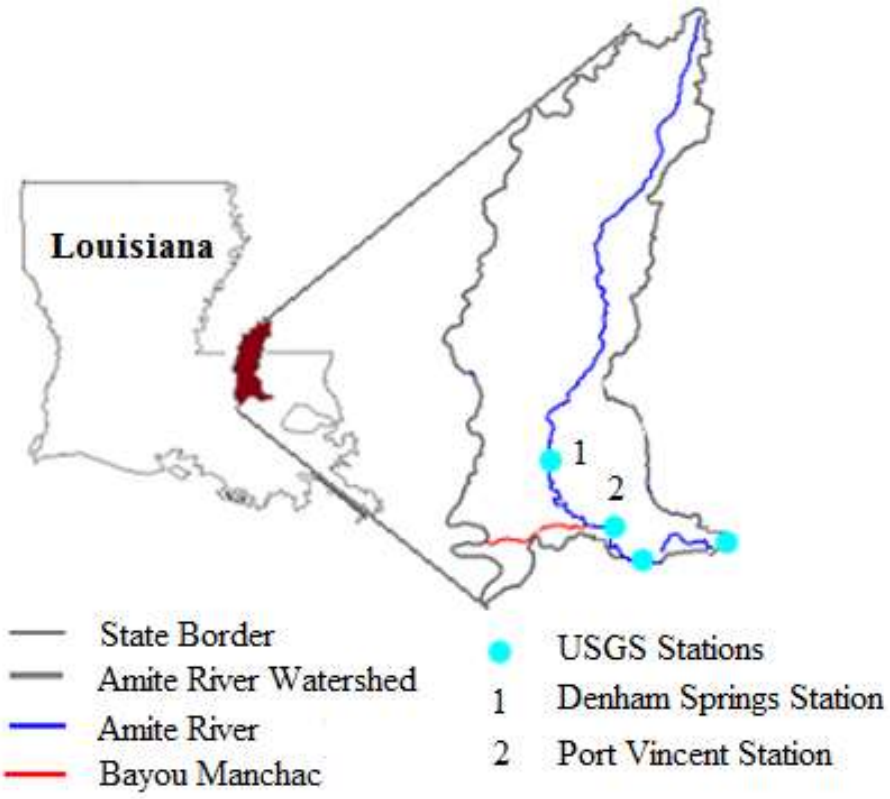

Figure 4.3- Map of Amite River watershed showing the study reach from Denham Springs to Port Vincent

Table 4-1- Geometry and sediment parameters of Amite River

Date	$A(m^2)^{(a)}$	$H(m)^{(a)}$	$E(m^2/s)^{(b)}$	$Ws\ (m/s)^{(b)}$	$Porosity(\lambda)^{(c)}$	$G^{(d)}$	d (μm)
Jan-90	222	2.82	45	1.85E-04	0.45	2.6	50
Jul-90	56	1.2	4.5	1.85E-04	0.45	2.6	50

(a) From USGS (1974); (b) Calculated; (c) According to McWhorter and Sunada (1977); (d) For silt and clay particles (Das, 2008)

4.2.5. Determination of model parameters

There are no point source discharges of BOD along the Amite River. Therefore, the elevated BOD level in the Amite River is attributed to nonpoint source discharges of BOD from the watershed during rainfall events. Nonpoint source BOD loading was obtained in chapter three by using HSPF watershed modeling for the Amite River watershed. As mentioned earlier in chapter three, the HSPF model is a spatially distributed and temporally continuous watershed model and

it can simulate the daily time-series of hydrologic and water quality processes. Observation data collected by the USGS from the Amite River at Denham Springs and Port Vincent are used to calculate and calibrate flow discharge, instream temperature, and instream DO concentration in chapter three. The BOD concentration corresponding to the calibrated model is considered as watershed loading of BOD to the Amite River. Figure 4.4 (a repetition of Figure 3.9) shows time series of simulated BOD concentration for January 1990 and July 1990, respectively.

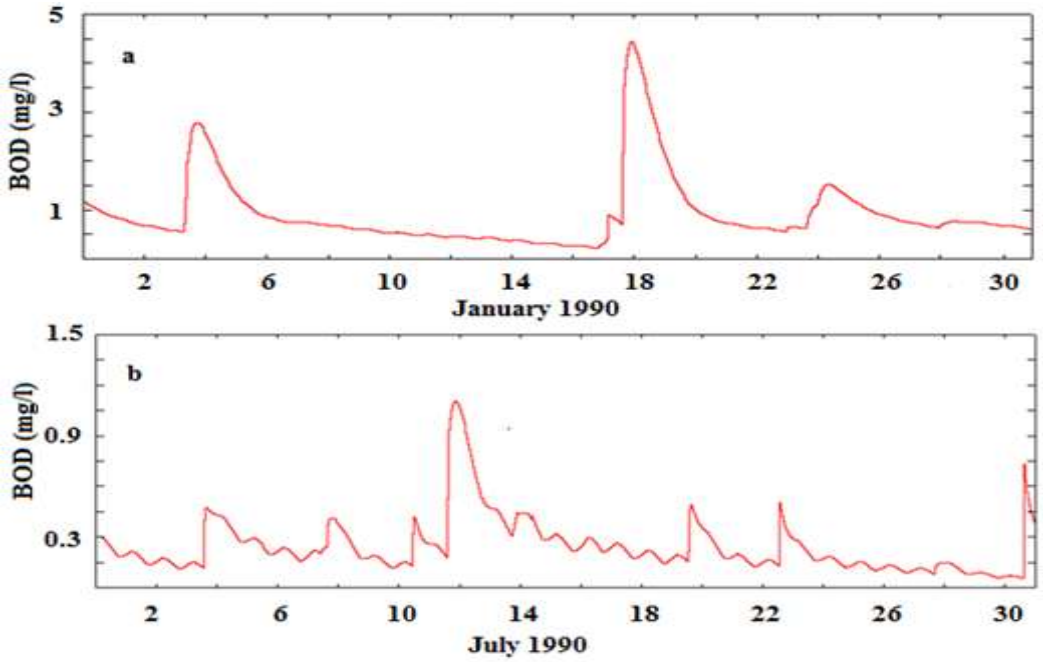

Figure 4.4- BOD Input from Amite River watershed: a) for January 1990; b) for July 1990

A recent report issued by Louisiana Department of Environmental Quality (LDEQ) on total maximum daily load (TMDL) for the Bayou Manchac (a tributary of the Amite River, as shown in Figure 4) used a BOD concentration of 11.3 mg/l (BOD1 and BOD2) for the Bayou Manchac according to 3 days (June 5, 6, and 7 in 2007) of BOD data collected from the Bayou Manchac in 2007 (LDEQ 2010). Obviously, the observed BOD level in the Bayou Manchac was much higher than the simulated BOD level in 1990 in the Amite River. The difference between the BOD

levels in the Bayou Manchac and the Amite River may be attributed to the change in land use and land cover during the period of 1990 - 2007. In order to understand the effect of uncertain BOD loading on simulated DO concentration, a sensitivity analysis is conducted for various BOD loading rates to the Amite River. A SOD value of 0.16 $g/m^2/day$ was recommended for the Amite River system by LDEQ (2010). This value is also used in the VART-DOS model for simulation of DO concentration along the Amite River in January and July of 1990. In addition, a high SOD value of 3.5 $g/m^2/day$ is also employed in the sensitivity analysis to examine the impact of high SOD, which is typically associated with combined sewer overflow (Chapra, 1997; Motta et al., 2010), on DO simulation results. The parameters α and m in Eq. (6) are determined through model calibration. More specifically, the parameters α and m are calibrated by using the Amite River data in January 1990 and the calibrated values for α and m are 5.5 and 9, respectively. The calibrated constant values for parameters α, β, and m are then used for DO simulations for July 1990.

4.2.6. Sensitivity Analysis of VART-DOS Model

Since this study focuses on the effect of sediment resuspension on instream DO reduction, a sensitivity analysis is performed primarily for VART-DOS model parameters related to sediment resuspension terms under two scenarios: with and without sediment resuspension. The sensitivity of simulated DO to other model parameters was presented in the second chapter. Results of sensitivity analysis for sediment-related parameters, including sediment settling velocity, sediment porosity, depth of bottom sediment, and flow discharge are presented in Table 4.2. It is clear from Table 4.2 that DO is sensitive to flow discharge. Sediment resuspension increases with increase in flow discharge. Consequently, effect of storage zone and hyporheic exchange becomes minimal in such environments. The sensitivity of simulated DO to settling velocity,

porosity, and bottom sediment depth depends on the variation range of parameter value. The DO is not sensitive to the variation of the parameters in some ranges. Beyond the ranges, the parameters may considerably affect the DO concentration. A 20% increase in β (effect of temperature in Eq. (4)) value can significantly affect instream DO with up to 4 times of variation due to proposed power equation.

Table 4-2- Sensitivity analysis of sediment resuspension parameters

Parameters	With 20 % increase of parameter change	With 20% decrease of parameter change
	Percent change in DO	
Settling Velocity (W_s)*	-1%	32%
Sediment Porosity (λ)	-1%	20%
Depth of Bottom Sediment (H_b)	24%	-2%
Flow Discharge (Q)	-17%	79%

* Change in settling velocity is due to change in particle size.

The sensitivity of simulated DO to BOD and SOD terms is summarized in Table 4.3. It can be seen from Table 4.3 that while the simulated DO is not sensitive to BOD and SOD variations, the incorporation of sediment resuspension in the VART-DOS model can markedly reduce the root mean square error of the model. Without incorporating sediment resuspension effect ($\Lambda=0$), all nRMSEs of simulations are high and vary in a relatively wide range of 0.76 – 1.36. A ten-time increment in watershed BOD input only reduces the nRMSE by maximum14% when SOD is 3.5 g/m^2/day. Increasing SOD from 0.16 g/m^2/day to 3.5 g/m^2/day reduces instream DO by 36%. When sediment resuspension effect is incorporated into the VART-DOS model ($\Lambda\neq0$), the nRMSEs for different BOD and SOD combinations become relatively low and vary in a narrow range of 0.19 – 0.23, indicating the importance of sediment resuspension to instream DO fluctuations. This means that sediment resuspension is a dominant mechanism responsible for DO variations in the Amite River. In fact, 83% of DO reduction can be attributed to sediment

resuspension when SOD= 0.16 g/m^2/day while 75% of DO reduction is due to sediment resuspension when SOD = 3.5 g/m^2/day.

Table 4-3- Effects of BOD and SOD on DO change along the Amite River

Watershed BOD (mg/L)	SOD g/m^2/day	Without sediment resuspension	With sediment resuspension
		Normalized Root-Mean-Square error	
Time series in Figure 4b	0.16	1.36	0.23
10×Time series in Figure 4b	0.16	1.23	0.21
Time series in Figure 4b	3.5	0.89	0.21
10×Time series in Figure 4b	3.5	0.76	0.19

4.3. Applications of VART-DOS model to Amite River

The Lower Amite River (sub-segment 040303) was on US EPA's 2006 Impaired Water 303(d) list because it was "not supporting" its designated use of Fish and Wildlife Propagation (Deng and Patil, 2011). The Lower Amite River was impaired for dissolved oxygen, nitrate/nitrite, chlorides, and total phosphorus. Suspected causes of impairment were organic enrichment/oxygen depletion and nutrients. The Amite River was subsequently scheduled for the development of TMDL for several water quality parameters including DO. The proposed VART-DOS model was applied to the Lower Amite River between Denham Spring and Port Vincent. To understand the effect of sediment resuspension on DO concentration, the model was run for the winter month January and the summer month July of 1990, respectively. The DO data observed monthly at Denham Springs was used as the upper boundary condition. USGS flow data were used to run and calibrate HSPF model. The calibrated HSPF model was employed to

generate daily data for DO at Denham Springs. Patil and Deng (2010) used HSPF model to obtain daily DO data for Port Vincent station (Figure 4.3).

By using equation (7), the erosion rate in the Amite River was defined to have the maximum value of 0.11 on July 13 of 1990. According to Fig. 4.1, there were also other occasions that erosion rate increased as flow discharge increased showing direct correlation between erosion rate and flow discharge. However, the erosion rate did not reach the maximum of 0.11 on July 13 in 1990. For the rest of the time during July 1990, the erosion rate had the minimum value of 0.03. As mentioned, the high erosion rate of July 13, 1990 caused organic-rich materials of river bed to suspend in water column and consume DO according to equation 6. Figures 4.5 and 4.6 shows a comparison of DO concentrations simulated using the VART-DOS model and observed at the Port Vincent in January and July 1990. It can be seen from Figure 4.5 that in the January the simulated DO concentration matches the observed one reasonably well with an nRMSE value of 0.42. In addition, there is no significant longitudinal variation in DO level from the Denham Springs to the Port Vincent. Figure 4.6 indicates that the DO level simulated using the VART-DOS model is able to capture the overall variation trend in the observed one with a relatively small nRMSE value of 0.23. The DO variation is highly affected by high flow-induced sediment resuspension. Figure 4.6 also shows that the DO level drops significantly from the Denham Springs to the Port Vincent on July 13, 1990, illustrating the cumulative effect of DO consumption along the Amite River due to sediment resuspension. However, there are a couple of points in Figure 4.6, where simulated DO concentrations do not fit observed ones well. For instance, the simulated DO level was dropping while observed DO level was rising around July 29, 1990. Such contradictory variation can be attributed to effects of some other factors, which

were not considered in the model, such as non-uniform particle size and thus non-uniform erosion.

The simulation results shown in Figure 4.6 confirm that the low summer DO level in the Port Vincent is caused by sediment resuspension. When sediment resuspension term is incorporated into numerical modeling ($\Lambda \neq 0$), the simulated DO concentration in the Amite River generally follows the variation trend in the observed data with fairly small nRMSE. Obviously, the effect of sediment resuspension on DO is significantly enhanced by high temperature in summer. High temperature in combination with sediment resuspension exaggerates the decomposition of the organic matter in sediment and thereby accelerates oxygen consumption in water column and subsequent DO drawdown.

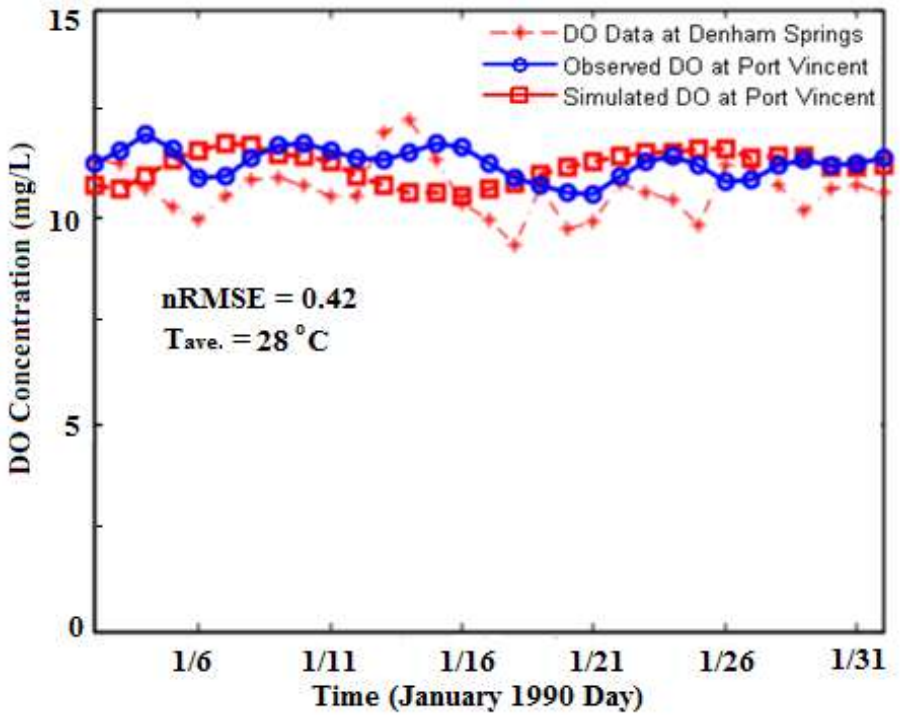

Figure 4.5- DO change at Port Vincent for January 1990

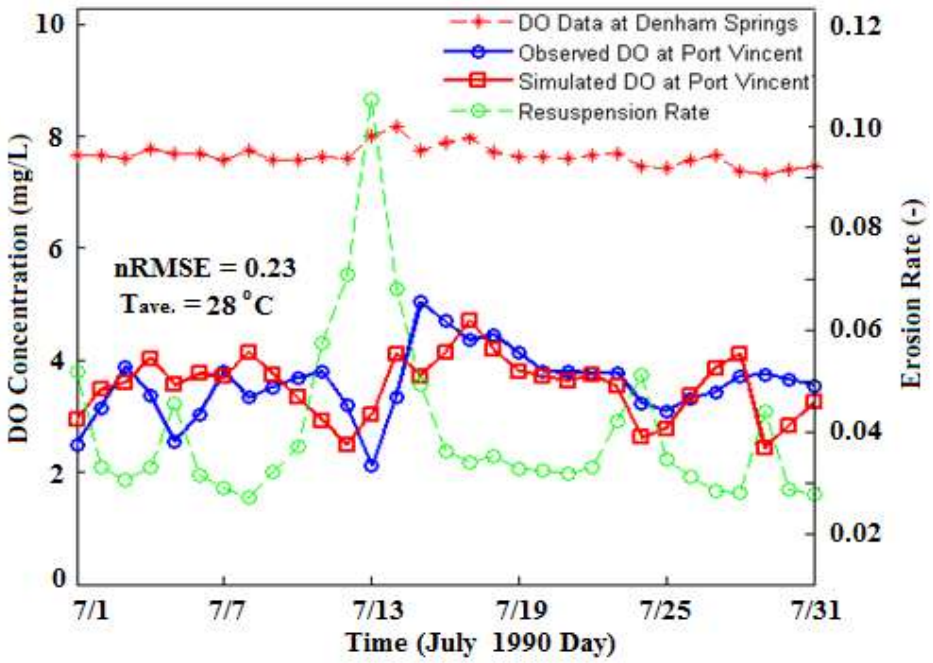

Figure 4.6- DO change at Port Vincent for July 1990

4.4. Comparison of VART-DOS with other DO models and main contributions of this chapter

In order to understand new contributions from this chapter, it is important to understand the difference between the VART-DOS model and other widely used dissolved oxygen models such as Streeter-Phelps and water quality analysis simulation program (WASP).

(1) VART-DOS model presented in this chapter is a simplified version of the general model VART-DO-3L (presented in Chapter 5) that includes major processes responsible for exchanges of DO at the air-water interface and water-sediment interface, mixing in water column through dispersion, and reactions such as BOD degradation. Unlike VART-DO-3L, in VART-DOS exchange of DO at water sediment interface is considered by the lumped term SOD. However, VART-DOS has an additional term that represents sediment

resuspension effect on DO variation. In fact, this sediment resuspension term relates the reduction of DO in water column to the erosion rate of solids/particles in river bed and includes the lumped effect of processes and reactions that consume DO in bottom sediment (i.e. carbonaceous and nitrogenous BOD accumulation, existence of reduced metal ions). Such simplification/idealization is unavoidable, because detailed data of all affecting processes are rarely available.

(2) VART-DOS is an intermediate model that is capable of modeling DO by accounting for sediment resuspension. Based on simple pioneer Streeter-Phelps model, when velocity increases as the result of flood event, reaeration intensifies leading to higher dissolved oxygen concentration. In favor of simplicity, Streeter-Phelps model does not consider all important processes and thus is unable to capture the dominant processes correctly. On the other hand, widely used water quality analysis simulation program (WASP) model requires determination of 29 parameter data and identification of 90 coefficients for defining sediments/solids' impact on DO variations. For other processes like nitrification, BOD degradation, and algae effects, WASP still needs additional data to parameterize which is not readily available. Besides, WASP model requires time series settling velocity to calculate suspension of bottom particles. In most of the cases, detailed data for defining theses modeling parameters and additional variables are rarely available. Thus, VART-DOS model with 24 modeling parameters is a relatively simple model. In addition, it lumps the adverse DO consuming processes in the coefficient (Λ) which is a function of erosion rate of bottom solids/particles, settling velocity of particles, porosity of particles, depth of accumulated particles, and temperature.

4.5. Conclusions

This chapter presents a simple yet effective model, called VART-DOS model, for simulation of instream DO transport, DO exchanges across water-sediment and water-air interfaces, and DO variation in response to sediment resuspension. The objectives and originality of present study can be summarized as:

1) For many rivers like the Amite River in this study, frequent flood events can have significant effect on reducing DO concentration due to sediment resuspension. Thus, quantifying the amount of oxygen that consumes as a result of sediment resuspension should be included in mathematical modeling beside the usual mechanisms such as SOD and BOD degradation.

2) The dependency of DO changes to temperature was considered in the additional term that represents sediment resuspension-induced DO reduction. It is an important feature and enables VART-DOS to be used for both hot and cold weather condition.

3) For simulation of DO by VART-DOS, flow discharge, DO concentration, and daily temperature were the only observation data that needed. Modeling parameters of VART-DOS are less than the parameter of widely used model WASP or modeling framework introduced by Motta et al. (2010) for studying sediment resuspension effect on DO. VART-DOS parameters can be determined using appropriate equations in the text (i.e., Eq. (13) is used for obtaining dispersion coefficient), using reference values from literature (i.e., K_D is 0.2 d^{-1} (Rosman, 2006)), or by calibrating VART-DOS (i.e., $A_{adv.}$, α, and m). So, VART-DOS can be implemented for any river.

4) VART-DOS was employed for DO simulation along the Amite River. Results show that simulated DO and observed data match satisfactorily; nRMSE was 0.42 for January 1990 and

0.23 for July 1990. The results also confirmed that sediment resuspension can cause up to 83% reduction in DO concentration.

5) When sediment resuspension effect develops, storage zone effect and hyporheic exchange (like other processes) becomes negligible. However, for small flow discharge and before sediments become fully suspended, DO change is affected by hyporheic exchange as examined by VART-DO. Thus, VART-DOS accommodates different processes in simulation of DO.

4.6. References

Alp, E., and Melching, C.S. (2006). Calibration of a model for simulation of water quality during unsteady flow in the Chicago Waterway System and application to evaluate use attainability analysis remedial actions. Technical Rep. No. 18, Institute for Urban Environmental Risk Management, Marquette Univ., Milwaukee, Wis.

Arega, F., Lee, JHW. (2005). Diffusional mass transfer at sediment-water interface of cylindrical sediment oxygen demand chamber. J. Environ. Eng.; 131(5): 755-767.

Berg, P., Røy, H., Jannsen, F., Meyer, V., Jørgensen, B.B., Huettel, M., de Beer, D. (2003). Oxygen uptake by aquatic sediments measured with a novel-invasive eddy-correlation technique. Mar. Ecol. Prog. Ser.; 261: 75-83.

Chapra, S.C. (1997). Surface Water-Quality Modeling. New York, N.Y, USA: McGraw-Hill.

Cheng, N.S. (1997). Simplified settling velocity formula for sediment particle. J. Hydraul. Eng.; 123(2): 149-152.

Das, B. (2008). Fundamentals of geotechnical engineering. Third edition, United States of America.

Deng, Z-Q., Singh, V.P., Bengtsson L. (2001). Longitudinal dispersion coefficient in straight rivers. J. Hydraul. Eng.; 127(11): 919-927.

Deng, Z-Q., Jung, H-S. (2009). Variable residence time-based model solute transport in streams. Water Resour. Res.; 45: W03415, doi:10.1029/2008WR007000.

Deng, Z-Q., Jung, H-S., Ghimire, B. (2010). Effect of channel size on solute residence time distributions in rivers. Adv. Water Resour.; 33 (9): 1118–1127, doi: 10.1016/j.advwatres.2010.06.016.

Deng, Z-Q., Patil, A. (2011). Assessment of water quality variation in Amite River watershed under changing climate and land use. Water Quality: Current Trends and Expected Climate Change Impacts, IAHS Publ.; 348

Garcia, M.H. (2008). "Sediment transport and morphodynamics." Sedimentation engineering: Processes, measurements, modeling and practice, ASCE manual of practice 110, M. H. Garcia, ed., ASCE, Reston, Va., Chap. 2, 21–163.

Hopkinson, C.S., Jr. (1985). Shallow-water benthic and pelagic metabolism: evidence of heterotrophy in the near shore Georgia Bight. Mar. Biol.; 87: 19-32.

Hopkinson, C.S., Jr. (1987). Nutrient regeneration in shallow-water sediments of the estuarine plume region of the near-shore Georgia Bight, USA. Mar. Biol.; 94:127-142.

Hwang, K.Y., Kim, H.S., Hwang, I. (2011). Effect of Resuspension on the Release of Heavy Metals and Water Chemistry in Anoxic and Oxic Sediments. Clean – Soil, Air, Water; 39 (10), 908–915

Lopez, F., García, M.H. (2001). Risk of Sediment Erosion and Suspension in Turbulent Flows. J. Hydraul. Eng.; 127(3), 231-235.

Louisiana Department of Environmental Quality (LDEQ) (2010). Bayou Manchac watershed TMDL for biochemical oxygen-demand substances (Phase I)- final report, Baton Rouge, LA, USA.

Mays, L. (2001). "Water resources engineering." John Wiley & Sons, New York, NY.

McWhorter, D.B., Sunada, D.K. (1977). Groundwater hydrology and hydraulics. Fort Collins, CO, USA: Water Resour. Publication.

Mishra, P.K., Deng, Z-Q. (2009). Sediment TMDL Development for the Amite River. J. Water Resour. Manag.; 23(5): 839-852.

Motta, D., Abad, J.D., Garcia, M.H. (2010). Modeling Framework for organic sediment resuspension and oxygen demand: Case of Bubbly Creek in Chicago. J. Environ. Eng.; 136(9): 952-964.

Nordin, C.F., Sabol, G.V. (1974). Empirical data on longitudinal dispersion in rivers. Water-Resources Investigations; 20-74, US Geological Survey, Denver, CO.

O'Connor, D.J., and Dobbins, W.E. (1958). Mechanisms of reaeration in natural streams. Transactions, ASCE, 123(2934), 641–684.

Patil, A., Deng, Z-Q. (2010). Analysis of uncertainty propagation through model parameters and structure. Water Sci. Tech.; 62(6): 1230-1239.

Patil, A., Deng, Z-Q. (2011). Bayesian approach to estimating margin of safety for total maximum daily load development. J. Environ. Manage.; 92: 910-918.

Patil, A., Deng, Z-Q., Malone, R.F. (2011). Input-data resolution induced uncertainty in watershed modeling. Hydrological Processes; 25(14): 2302-2312.

Patil, A., Deng, Z-Q. (2012). Input-data measurement induced uncertainty in watershed modeling. Hydrolog. Sci. J.; 57(1): 118-133.

Rosman, P. C. (2006). Referencia tecnica do Sisbahia—Sistema base de hidrodinâmica ambiental Programa COPPE: Engenharia oceânica, Área de Engenharia Costeira e Oceanográfica, Rio de Janeiro, Brasil

Smith, J., McLean, S. (1977). Spatially averaged flow over a wavy surface. J. Geophys. Res.; 82: 1735–1746.

U.S. Geological Survey website: <http://waterdata.usgs.gov/usa/nwis/uv?site_no=07378500>, (Feb.15, 2011)

Wainright, S.C., Hopkinson, C.S., Jr. (1996). Effects of resuspension on organic matter processing in coastal environments: a simulation model. J. Mar. Syst.; 11: 353-368

Waterman, D.M., Waratuke, A.R., Motta, D., Catano-Lopera, Y.A., Zhang, H., Garcia, M.H. (2011). In situ characterization of resuspended-sediment oxygen demand in Bubbly Creek, Chicago, Illinois. J. Environ. Eng.; 137(8): 717-730, doi:10.1061/(ASCE)EE.1943-7870.0000382

Williams, R.J., Boorman, D.B. (2012). Modelling in-stream temperature and dissolved oxygen at sub-daily time steps: An application to the River Kennet, UK. Sci Total Environ; 423:104–110.

Zahraeifard, V., Deng, Z-Q. (2012). VART Model-Based Method for Estimation of Instream Dissolved Oxygen and Reaeration Coefficient. J. Environ. Eng.; 138(4) DOI: 10.1061/(ASCE)EE.1943-7870.0000494.

Zison, S.W., Mills, W.B., Diemer, D., and Chen, C.W. (1978). Rates, constants and kinetic formulations in surface water quality modeling. Rep. No. EPA/600/3-78-105, U.S. Environmental Protection Agency *ERL ORD,* Athens, Ga.

CHAPTER 5
MODELING SPATIAL VARIATIONS IN DISSOLVED OXYGEN IN FINE-GRAINED STREAMS UNDER UNCERTAINTY

5.1. Introduction

Urbanization and agricultural development have produced increasing discharges of nutrients and oxygen-consuming pollutants, such as Biochemical Oxygen Demand (BOD), to streams (Cox, 2003; Corsi et al., 2011), causing nutrient enrichment in streams and particularly lowland streams with fine-grained sediment (primarily clay and silt < 63 μm) (Zahraeifard and Deng, 2012a; Deng and Patil, 2011; Todd et al. 2009; Parr and Mason, 2004; Owens and Walling, 2002) as discussed in chapter four. The fine-grained streams are generally characterized by a fluid mud (fluff or flocculent) layer or surficial fine-grained sediment lamina as the interface between relatively consolidated stream bed-sediment and overlying stream water (Droppo and Stone, 1994; McAnally et al., 2007; Kleeberg et al., 2008; Garcia 2008). The flocculent layer has been found to serve as a reactor especially in nutrient enriched streams (Westrich and Förstner 2007), causing significant exchange of solutes (nutrients, contaminants, dissolved oxygen, and temperature) across the sediment-water interface. The exchange controls nutrient uptake and retention (Jung and Deng, 2011; O'Connor and Hondzo, 2008) and dissolved oxygen distribution (Hondzo et al., 2005; Taylor et al., 2003; Sweerts et al., 1991) in streams. Extensive efforts have been made to understand mass exchange across the sediment-water interface in nutrient enriched, fine-grained streams (Westrich and Förstner, 2007).

Stone and Droppo (1994) investigated chemical characteristics and formation of surficial fine-grained laminae (SFGL) in three south-western Ontario rivers in Canada. They found that the formation of SFGL is a complex process resulting from a range of physical, chemical and biological variables interacting at a variety of spatial and temporal scales within and out of the

river channel. Westrich and Förstner (2007) presented an overview of the state-of-the-art on the formation and stability of sediment-water interface and mass fluxes across the interface in fine-grained streams. Despite the importance of the flocculent layer to the transport, transformation, and fate of nutrients and pollutants in nutrient-enriched streams, very few models are available for simulation of mass fluxes across the flocculent layer.

The transient storage model has been widely used for simulation of hyporheic exchange in rivers (Bencala and Walters, 1983; Runkel, 1998). Basically, the transient storage model is only applicable to gravel and sandy rivers where mass fluxes across the sediment-water interface are primarily driven by advective transport. The mass exchange across the sediment-water interface in fine-grained streams is highly affected by diffusive fluxes. Higashino et al. (2004) presented a boundary layer-based model for simulation of unsteady diffusive mass transfer across the sediment-water interface. While the model was novel, it is only applicable to stagnant water bodies without the flocculent layer. In chapter four, a new model was proposed, called VART–DOS model, for simulation of instream DO transport, DO exchanges across water–sediment and water–air interfaces, and DO variation in response to sediment resuspension based on the VART model (Deng and Jung, 2009) and an early version of VART–DO model proposed in chapter two. While the VART-DOS model included the effect of diffusive mass exchange on instream DO, the diffusive layer was not explicitly included in the model. As a result, the VART-DOS model is unable to produce the vertical profile of DO in the bottom sediment. In fact, most existing models are incapable of simulating both vertical and longitudinal variations in DO in fine-grained streams while understanding of the spatial variations in DO is essential to the management and restoration of impaired streams.

The overall goal of this paper is to develop a new model for simulation of vertical and longitudinal variations in DO in fine-grained streams at daily time-scale. It means that diurnal variation in DO will not be considered in this paper. Due to diverse spatial scales involved in DO variations and associated variability and uncertainties in model input parameters, specific objectives of this paper are (1) to present a new model including various physical and biogeochemical processes responsible for DO variations in fine-grained streams, (2) to examine the sensitivity of model parameters to identify sensitive parameters, (3) to simulate and analyze various cases representing the variability and uncertainty in model parameters, and (4) to apply the model to the Lower Amite River in Louisiana, USA to test the performance and demonstrate a practical application of the new model.

5.2. Materials and Methods

5.2.1. Study River Reach – Lower Amite River

The Amite River watershed is located in southeastern Louisiana, USA and it encompasses a drainage area of approximately 3435 km^2 (Deng and Patil, 2011), as shown in Figure 6.1. The Amite River flows generally southwestward to Lake Pontchartrain estuary that is connected to the Gulf of Mexico. The Lower Amite River downstream of the Denham Springs station and particularly the Port Vincent station is affected by tides. Therefore, the Lower Amite River is a typical fine-grained coastal river with 81.9% of bed sediment being finer than 62 μm and 100% of bed sediment being finer than 1 mm at the Port Vincent station. While no sediment data are available for the Denham Springs station, the sediment composition for the Denham Springs station should lie between the Port Vincent and the Magnolia stations. It was observed in September 2008 at the Magnolia station (Figure 6.1) that 88.2% of bed sediment being finer than 0.5 mm and 100% of bed sediment being finer than 1 mm. The fine sediment accounts for 96% –

100% and 62% – 93% of suspended sediment at the Port Vincent and Magnolia stations, respectively. The maximum suspended sediment concentration observed in the Lower Amite River exceeded 2200 mg/L, creating favorite environment for the formation of flocculent layer or surficial fine-grained sediment lamina during the recession period of flood event and following low flow period.

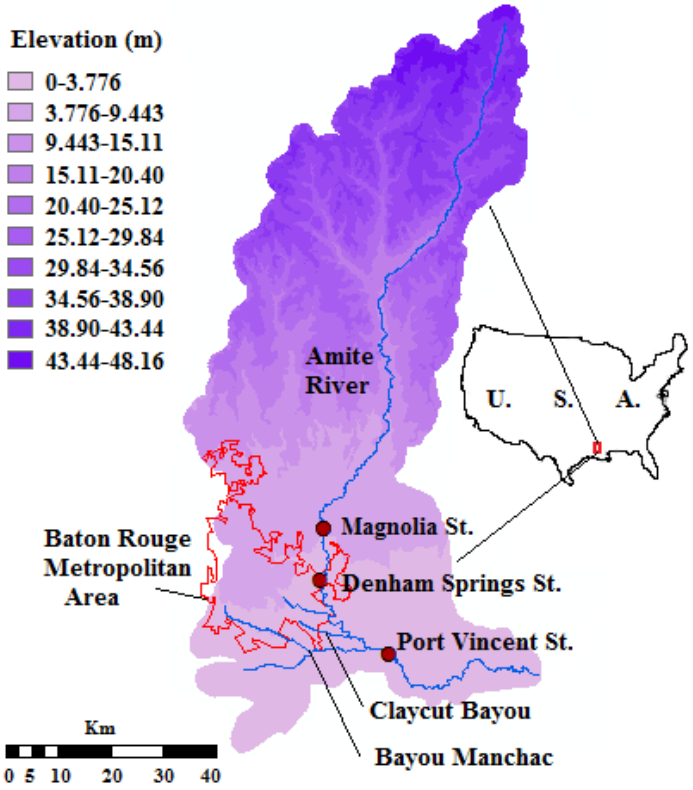

Figure 5.1- Map of Amite River watershed showing the study reach from Denham Springs to Port Vincent

Current land use in the Amite River watershed is characterized by hardwood forest in the north and agriculture (60%), forest (26%) and urban (12%) in the south (Figure 5.2). The southern part of the Amite River watershed has experienced significant changes in land use/land cover and water quality over the past six decades. As a result, the Lower Amite River (Subsegment 040303) is on US EPA's 2006 Impaired Water 303(d) List because it was "not

supporting" its designated use of Fish and Wildlife Propagation. The Lower Amite River is impaired for DO and nutrients due to organic enrichment. The Lower Amite River was subsequently scheduled for the development of a Total Maximum Daily Load (TMDL) for DO. The development and implementation of the TMDL requires understanding of spatial variations in DO. The requirement initiated this study.

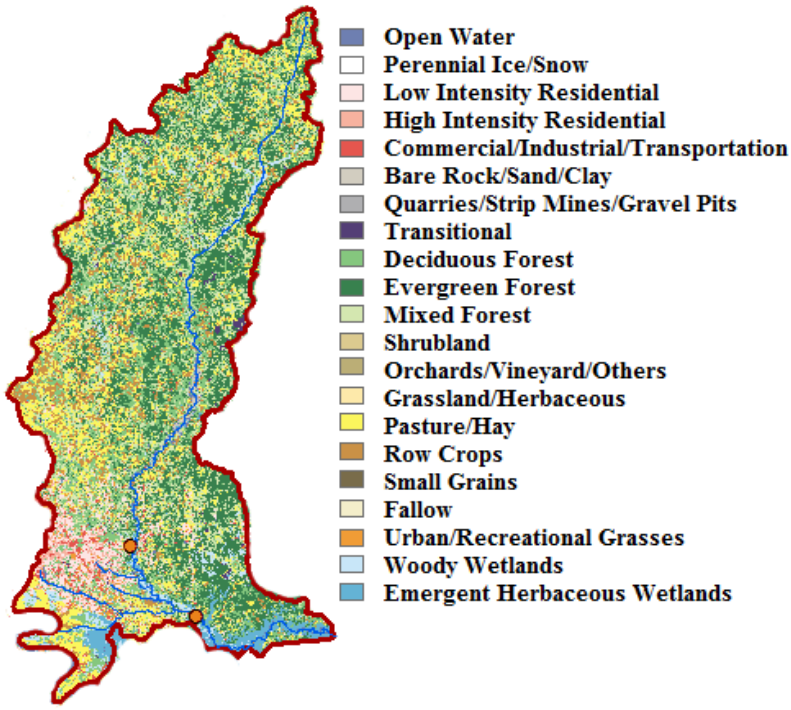

Figure 5.2- Land use and land cover in the Amite River watershed

5.2.2. Triple-Layer Conceptual Model for Instream DO Fluxes and Processes

Various physical and biogeochemical processes responsible for DO fluxes involved in fine-grained streams can be conceptually described using the following triple-layer model, as shown in Figure 5.3. A stream with fine-grained sediment is vertically divided into three layers, including overlying water column, an advection-dominated storage zone (flocculent layer), and a diffusion-dominated storage zone in relatively consolidated stream bed-sediment. Processes

responsible for daily DO variations in water column layer include the reaeration at the air-water interface, the exchange at the overlying water-sediment (flocculent layer) interface (transient storage), BOD degradation, and longitudinal advection and dispersion. It is assumed that DO level in the water column is uniform. It means that depth-averaged DO concentration is employed for water column.

A novel feature of the triple-layer model is the incorporation of flocculent layer into DO exchange and reaction processes. Observations have demonstrated that suspended fine-grained sediment particles often adhere to each other because of their charged behavior and transport commonly in the form of flocs/aggregates in streams and especially coastal rivers with suspended sediment concentration being higher than 500 mg/L (Ganaoui et al., 2007; Hulbert et al., 2002). Settling of the flocs generally produces a fluid mud (flocculent) layer or surficial fine-grained (muddy) sediment lamina as the interface between relatively consolidated stream bed-sediment and overlying stream water. Therefore, the flocculent layer represents the most recently deposited material with a thickness of up to 8 mm (Droppo and Amos, 2001) and is often manifested as a stationary fluid undergoing primary consolidation. It is often transient, forming a temporary, low-density, high organic and water content blanket over the existing streambed between flood/erosion events. Much of the sediment forming the flocculent layer is deposited in a flocculated state with relatively uniform concentrations of DO, nutrients, and contaminants. The porosity and vertical thickness of flocculent layer may decrease with time and bulk density increases accordingly, causing high uncertainty in the structure and thereby modeling of flocculent layer. Since the flocculent layer is formed due to floc settling (advection) of suspended sediment in water column, it is assumed that the DO exchange between the overlying water column and the flocculent layer is dominated by advective transport (transient storage-

release). The DO exchange between the flocculent layer and the relatively consolidated stream bed-sediment is assumed to be controlled by diffusive transport. In addition to the physical processes, reactions may also take place in the flocculent layer. In fact, the flocculent layer has been found to be biogeochemically active in nutrient enriched streams (Westrich and Förstner, 2007).

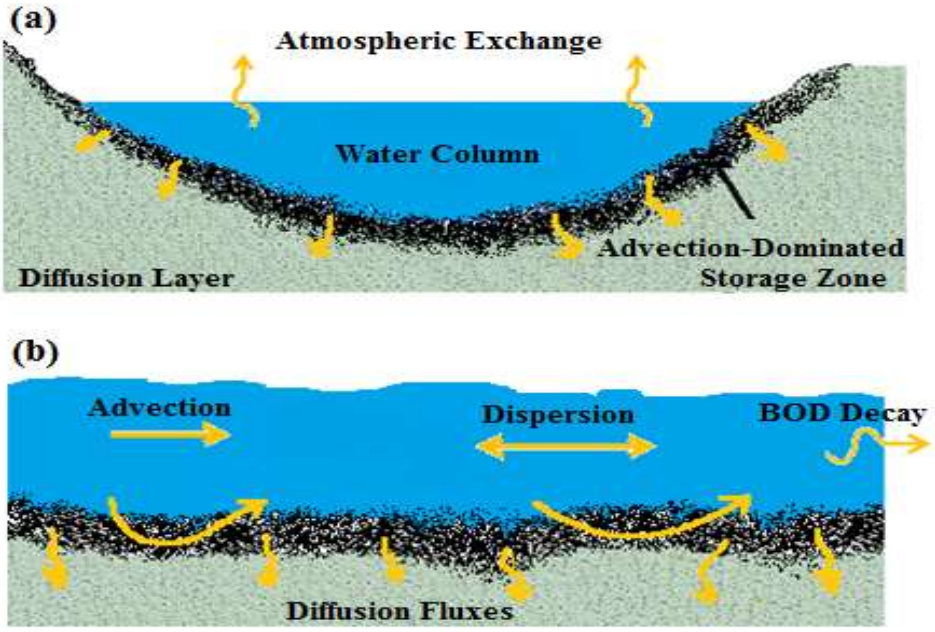

Figure 5.3- (a) Vertical profile of a typical streams including water column, advection-dominate storage zone and diffusion-layer and (b) Longitudinal profiles and the processes that affect DO changes

While the flocculent layer behaves like noncohesive sediment, the stream bed-sediment layer is relatively consolidated and characterized by much higher critical shear stress than that of the flocculent layer (Ganaoui et al. 2007). Therefore, DO variations in the bed-sediment are affected primarily by the diffusive DO exchange between the flocculent layer and the bed-sediment, and Sediment Oxygen Demand (SOD). Previous studies and models on instream DO generally focused on this layer and its interaction with the water column layer (Higashino, 2011;

Higashino and Stefan, 2011; Arega and Lee, 2005; Steinberger and Hondzo, 1999). Therefore, a mathematical model describing DO exchange across the three layers is needed for simulation of DO variations in fine-grained streams.

5.2.3. Mathematical Model for Spatial Variations in DO: VART DO-3L Model

The triple-layer conceptual model can be described mathematically with the following three equations:

$$\frac{\partial C}{\partial t} + U\frac{\partial C}{\partial x} = \frac{\partial}{\partial x}(E_x \frac{\partial C}{\partial x}) + (\frac{A_{adv} + A_{dif}}{A})(\frac{1}{T_V})(C_F - C) + K_2(C_{sat} - C) - K_1 L \quad (1)$$

$$\frac{\partial C_F}{\partial t} = \frac{1}{T_V}(C - C_F) - D_e \frac{\partial C_s}{\partial y}\bigg|_{y=0} \frac{P_{ws}}{(\frac{A_s}{A}).A} - R \quad (2)$$

$$\frac{\partial C_s}{\partial t} = D_e \frac{\partial^2 C_s}{\partial y^2} - \mu_o \quad (3)$$

where C = DO concentration in water column [ML^{-3}], C_F = DO concentration [ML^{-3}] in the flocculent layer, C_{sat} = saturation concentration of DO, U = average flow velocity [LT^{-1}] along x direction, E_x = longitudinal dispersion coefficient [L^2T^{-1}], t = traveling time [T], K_1 = biochemical oxidation rate of carbonaceous materials [T^{-1}], L = BOD concentration [ML^{-3}] in the water column, K_2 = reaeration coefficient [T^{-1}], A = cross-sectional area of stream channel [L^2], A_{adv} = advection-dominated storage zone (flocculent layer) area [L^2] with the thickness of δ_{adv} [L], A_{dif} = diffusion-dominated storage zone (stream-bed sediment) area [L^2] with the thickness of δ_{dif}, $A_s = A_{adv} + A_{dif}$, T_V = residence time [T] in the storage zone, D_e = effective diffusion coefficient in the bottom sediment layer, P_{ws} = wetted perimeter of stream channel, R = lumped reaction term representing SOD in the flocculent layer, and μ_o = lumped reaction term denoting SOD in the bottom sediment. Eqs. (1) - (3) are derived following the similar procedure presented

in Deng and Jung (2009). The second term on the right hand side of Eq. (2) is essentially a boundary condition. Eqs. (1) – (3) are the mathematical description of the conceptual triple-layer model, called VART DO-3L, for simulation of spatial and temporal variations in DO in fine-grained streams. The VART DO-3L model is a new development of VART series of models (Zahraeifard and Deng, 2012a and 2012b; Ghimire and Deng, 2012; Deng et al., 2010; Deng and Jung, 2009).

To solve Eq. (3), the boundary condition of C_s (1,t) = C_F(i) is considered at the interface between the flocculent layer and the bottom sediment, where i refers to numerical node number along the river reach. Another boundary condition is $\partial C_s / \partial y\big|_{y=\infty} = 0$. Practically, the lower boundary or the DO penetration depth (δ_{dif}) can be determined following the method presented by Deng and Jung (2009), who defined the diffusion dominated storage zone area as:

$$A_{diff} = 4\pi D_e t_s \tag{4}$$

in which π = 3.14 and t_s = the time [T] since solute (including DO) release from the storage zone to the mainstream. The time t_s can be substituted with the minimum residence time (T_V) for the DO simulation. Eq. (4) can be rewritten as:

$$\delta_{dif} = 4\pi(\frac{D_e}{A})HT_V \tag{5}$$

where H = stream water depth. Eq. (5) can be utilized to provide a reference value for DO penetration depth, depending on the effective diffusion coefficient and T_V. Based on the value of δ_{dif}, the lower boundary for the diffusive bottom sediment layer can be defined for the numerical solution of Eqs. (1) – (3). Eq. (2) can be discretized in the finite difference form as:

$$\frac{C_F{}^{n+1}(i) - C_F{}^{n}(i)}{\Delta t} = \frac{1}{T_V}(\frac{C^{n+1}(i) + C^{n}(i)}{2} - \frac{C_F{}^{n+1}(i) + C_F{}^{n}(i)}{2}) - D_e \frac{C_F^{n+1}(i) - C_s^{n+1}(2)}{\Delta y} \frac{P_{ws}}{(\frac{A_s}{A}).A} - R \tag{6}$$

where $C_s^{n+1}(2)$ is DO concentration at a grid point in the diffusion dominated bottom sediment layer and is calculated using the following discretized form of Eq. (3):

$$\frac{C_s^{n+1}(2)-C_s^n(2)}{\Delta t}=D_e\frac{C_s^n(3)-2C_s^n(2)+C_s^n(1)}{\Delta y^2}-\mu_o \tag{7}$$

Since $(C_s^n(1))_i=C_F^n(i)$, $C_s^{n+1}(2)$ can be calculated from Eq. (7) as:

$$C_s^{n+1}(2)=C_s^n(2)+D_e(\frac{\Delta t}{\Delta y^2})(C_s^n(3)-2C_s^n(2)+C_F^n(i))-\mu_o\Delta t \tag{8}$$

Eq. (8) can be solved for $C_S^{n+1}(2)$ at any node in the longitudinal flow direction. Eq. (6) is then solved to obtain the DO concentration C_F in the flocculent layer. To determine the DO concentration in the water column, Eq. (1) is discretized following the split-operator method present in Deng et al. (2010).

5.2.4. Estimation of VART DO-3L Model Parameters

The VART DO-3L model involves multiple parameters and requires values for each parameter. The average flow velocity U can be determined using tracer test data or flow discharge and channel cross-section area A. The longitudinal dispersion coefficient E_x can be estimated using the method presented by Deng et al. (2001). The area ratio (A_s/A) and the residence time T_V for gravel or sandy rivers are usually determined using tracer test data (Chapra and Runkel, 1999; Deng and Jung, 2009; Deng et al., 2010; O'Connor et al., 2010) or the published A_s/A value for a similar river in the literature. However, tracer test data were rarely available for streams with fine-grained sediment. As a result, the parameters, A_s/A and T_V, are highly uncertain and the uncertainty should be taken into account in simulating DO using the VART DO-3L model. The parameter μ_o may also vary in a wide range from 50 to 2000 $mgl^{-1}d^{-1}$, as used by Higashino et al. (2004). Rosman (2006) reported the value of 3.55×10^{-6} (1/s) for K_1 at

20°C. O'Connor and Harvey (2008) introduced the following scaling relationship in Eq. (9) for calculation of D_e, based on molecular diffusion and fluid-flow and sediment conditions:

$$\frac{D_e}{D'_m} = \begin{cases} 5\times10^{-4}\,\mathrm{Re}_*\,Pe_k^{6/5} & for \quad \mathrm{Re}_*\,Pe_k^{6/5} \geq 2000 \\ 1 & for \quad \mathrm{Re}_*\,Pe_k^{6/5} < 2000 \end{cases} \tag{9}$$

where Pe_k is permeability Péclet number; Re_* is the shear Reynolds number; and D'_m is a generalized molecular diffusion coefficient in bottom sediment by considering porosity and tortuosity. Péclet number and shear Reynolds number are calculated as:

$$Pe_k = \frac{u_*\sqrt{K}}{D'_m} \tag{10}$$

$$\mathrm{Re}_* = \frac{u_* k_s}{\nu} \tag{11}$$

in which u_* is shear velocity [L/T]; ν is kinematic viscosity [L^2/T]; k_s is roughness height of sediment; and K is permeability of sediment and defined as:

$$K = 5.6\times10^{-3}\,\frac{\theta^3}{(1-\theta)^2}\,d_g^2 \tag{12}$$

where θ is porosity of sediment and d_g is geometric mean particle size of bottom sediment. The parameter D'_m is defined as $D'_m = \beta D_m$ in which D_m is molecular diffusion coefficient. The parameter β is calculated as:

$$\beta = \frac{1}{1+3(1+\theta)} \tag{13}$$

Molecular diffusion coefficient for DO has been reported as 2.29×10^{-9} (m^2/s) at 25°C (Boudreau, 1996 and DiToro, 2001). The roughness height k_s was found to vary from 1 - 65 mm for silt and 20 - 400 mm for clayey sediment (Hosia, 1980). Due to uncertainties involved in the parameters in Eqs. (9) – (13), the effective diffusion coefficient D_e also varies in a wide range (Deng et al.,

2010). Based on sediment characteristics of θ = 0.4, and k_s= 8.4 mm for the Amite River at Denham Springs station, D_e is calculated to be 2.5×10^{-6} (m^2/s). The effective diffusion coefficient D_e for the Amite River at the Port Vincent station is found to be 7.4×10^{-8} (m^2/s) according to sediment characteristics of d_g = 0.009 mm, θ = 0.8, and k_s= 25.5 mm.

There are three reaction terms/parameters in Eqs. (1) – (3), including K_1L, R, and μ_o. The BOD concentration L in Eq. (1) was the BOD loading from the Amite River watershed obtained in chapter three. The parameter L is a time-dependent variable ranging from 0.15 mg/L to 1.05 mg/L with the average of 0.6 mg/L based on the simulation results (L_{HSPF}) from the HSPF model. Rosman (2006) suggested K_1 = 0.2 d^{-1} at 20°C. With temperature correction factor θ_D =1.040 (Alp and Melching, 2006), it was assumed that K_1 changes uniformly from 0.27 d^{-1} (at 25°C) to 0.36 d^{-1} (at 40°C) in the Amite River. The parameter R in Eq. 2 is a lumped sink term, representing various reactions that consume DO, such as BOD degradation in the flocculent layer. Detailed data for quantification of R are hardly available due to the dynamic nature of the flocculent layer. Therefore, the parameter R is highly uncertain and may vary in a wide range. To address the uncertainty, the parameter R is varied in the range of 0 - 275 $mgl^{-1}d^{-1}$ for several cases. The reaction term, μ_o, denotes sediment oxygen demand (SOD) due to biological activity and may vary from 100 $mgl^{-1}d^{-1}$ to 2000 $mgl^{-1}d^{-1}$ (Higashino et al., 2004). Due to uncertainties involved in the model input parameters, it is important to conduct a sensitivity analysis and identify sensitive parameters so that more efforts could be put into the determination of the sensitive parameters.

5.2.5. Sensitivity Analysis of Model Input Parameters

There are two types of sensitivity analysis: local sensitivity analysis and global sensitivity analysis (Sobol, 1993; van Griensven et al., 2006). The global sensitivity analysis, more

specifically Sobol global sensitivity analysis, is utilized in this paper. The global sensitivity analysis focuses on the pattern of change in model output due to change in model input parameters over a potential variation range of parameter value rather than a single parameter value. As a result, the global sensitivity analysis is able to show the relative importance of individual model input parameters more reasonably as compared with the local sensitivity analysis (van Griensven et al., 2006).

Sobol global sensitivity analysis is a variance-based Monte Carlo technique (Sobol, 1993; Fesanghary et al., 2009; van Griensven et al., 2006). If $Y= f(x_1, x_2, x_3, \ldots, x_k)$ is the model equation with $x_1, x_2, x_3, \ldots, x_k$ being the input parameters or variables and Y being the model output, the total variance of Y can be formulated as follows:

$$V(Y) = \sum_{i=1}^{k} V_i + \sum_{1 \le i < j \le k} V_{ij} + \ldots + V_{1,2,\ldots,k} \tag{14}$$

where $V(Y)$ is the total variance of the output variable Y; V_i measures the effect of parameter x_i; and other terms describe effects of mutual interaction. Decomposition of Eq. (14) yields two types of sensitivity indices defined as:

$$S_i = \frac{V_i}{V(Y)} \tag{15}$$

$$S_{Ti} = 1 - \frac{V_{-i}}{V(Y)} \tag{16}$$

where S_i is the first-order sensitivity index for the i-th parameter and S_{Ti} refers to total sensitivity index for the i-th parameter. The index S_i includes the main effect of parameter x_i on the output variable (Y). It shows the variance reduction that would be achieved by fixing that parameter. The magnitude of S_i indicates the importance of the i-th parameter. This is called Factor Prioritization (FP) setting (Saltelli et al. 2004). The parameter V_{-i} depicts the sum of all variance terms that do not include the index i. The index S_{Ti} is the sum of all effects due to involvement of

parameter x_i. The index S_{Ti} accounts for the interaction between i-th parameter and other parameters. This can be considered as the expected portion of variance that would be left if parameter x_i is the only parameter that remains undetermined. The index S_{Ti} is useful for reducing the number of model input parameters. When a parameter does not have any effect both on its own and on other parameters, it is considered as a non-influential parameter and can be fixed at some values in its variation range. This is called Factor Fixing (FF) setting (Saltelli et al., 2004). Sobol sensitivity analysis can be conducted by using the Monte Carlo method (Homma and Saltelli, 1996). The basic idea behind the Monte Carlo method is to generate randomly sampled modeling parameters in their defined ranges, followed by estimation of $V(Y)$, V_i, and V_{-i}.

To apply the Sobol global sensitivity analysis to the Amite River, seven model input parameters closely related to SOD are selected for the sensitivity analysis, including A_s/A, T_V, D_e, μ_o, R, K_1, and L. The relative size of storage zone (A_s/A) for sandy and gravel rivers and streams was reported to vary in a wide range from 0 in the Uvas Creek (Deng and Jung, 2009) to 3.14 in the Little Topashaw Creek (Stofleth et al., 2007) with majority of A_s/A values being less than 0.5. By plotting a histogram for published A_s/A values and using the distribution fitting software EasyFit, it is found that the variation pattern of A_s/A can be best fitted with a lognormal distribution as shown in Figure 5.4. It is assumed that the variation of A_s/A for fine-grained streams also follows the lognormal distribution. The lognormal probability density function (PDF) is then employed for Monte Carlo sampling of A_s/A.

Residence time, T_V, is generally dependent on flow conditions, size of storage zone, and reactions of constituent in streams. Various tracer injection experiments were conducted to determine the residence time (Tong and Deng, 2013; Nordin and Sabol, 1974). Figure 5.5 indicates a lognormal PDF for residence time T_V for conservative tracers. It can be seen from

Figure 5. 5 that residence time can be as high as 63 hours for Missouri river (Chapra and Runkel, 1999). However, residence time for reactive constituents like dissolved oxygen has rarely been reported.

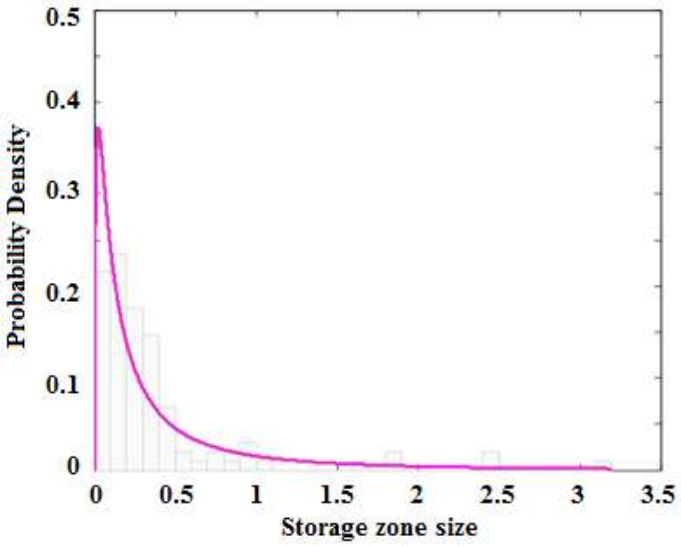

Figure 5.4- Probability density function for storage zone size

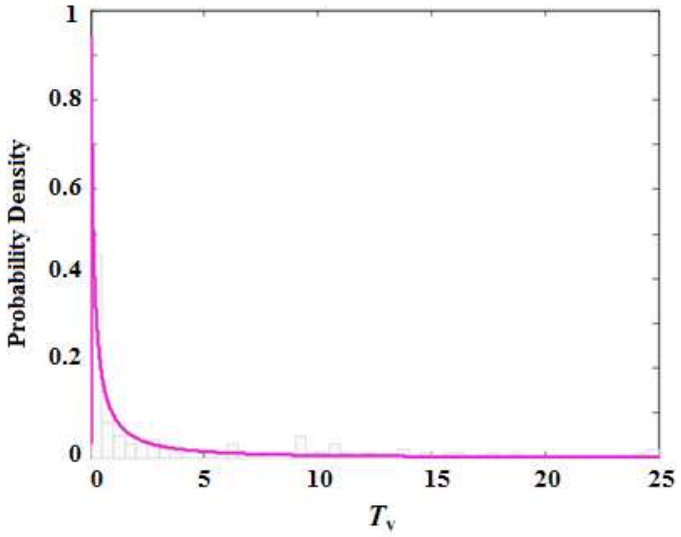

Figure 5.5- Probability density function for residence time T_V (hours)

The SOD depends on oxygen transfer (diffusion) from water column to the stream-bed sediment where microbial and chemical reactions cause the consumption of DO (Higashino et al., 2004). Therefore, μ_o (lumped reaction term), K_1 (oxidation rate of BOD), and D_e (effective diffusion coefficient) affect the SOD and they are thus included in the sensitivity analysis. Uniform distributions are used as PDFs for μ_o, K_1, and D_e. Monte Carlo method is used to sample the model input parameters using their PDFs. Then, the sensitivity indices are calculated using Eqs. (15) and (16).

5.2.6. Computation of Sediment Oxygen Demand (SOD)

Sediment Oxygen Demand (SOD) is needed in determining waste load allocations for developing Total Maximum Daily Loads and issuing NPDES (US National Pollutant Discharge Elimination System) permits. It is therefore important to understand SOD variation along the Lower Amite River. The SOD can be estimated following the method presented by Higashino et al. (2004) by considering the oxygen balance in the relatively consolidated bottom sediment. For unsteady condition, SOD is calculated as:

$$SOD = \frac{\partial}{\partial t}\int_0^{\delta} C_s(y)dy + \int_0^{\delta} \mu_o dy \tag{17}$$

where the lumped reaction term (μ_o) is usually replaced with Michaelis-Menten equation. Then, Eq. (17) can be rewritten as:

$$SOD = \frac{\partial}{\partial t}\int_0^{\delta} C_s(y)dy + \int_0^{\delta} \frac{\mu C_s}{K_{O_2} + C_s} dy \tag{18}$$

where K_{O_2} is the half-saturation coefficient for DO and μ is the biological reaction rate in sediment. It should be pointed out that the flocculent layer was not considered in the derivation

of Eq. (17). A revision to Eq. (17) is therefore needed to include the SOD in the flocculent layer in the computation of total SOD. To that end, Eq. 17 is extended as:

$$SOD = \frac{\partial}{\partial t}\left(\int_{0}^{\delta_{adv}} C_F dy + \int_{-\delta_{dif}}^{0} C_s(y) dy + \int_{0}^{\delta_{adv}} R dy + \int_{-\delta_{dif}}^{0} \mu_o dy \right) \quad (19)$$

Eq. (19) is numerically implemented by discretizing the right hand side of the equation. The SOD for each computational node *i* along the flow direction at a given time (day) *n* can be calculated using Eq. (20).

$$SOD_i = \frac{C_F(i)\delta_{adv} + \sum_{j=1}^{m}(C_{s_j}\Delta y)^{n+1} - \sum_{j=1}^{m}(C_{s_j}\Delta y)^{n}}{\Delta t} + R\delta_{adv} + \mu_o\delta_{dif} \quad (20)$$

It is clear from Eq. (20) that the SOD depends on DO concentration in both sediment layers (CF and CS), layer thickness (δadv and δdif), and the reaction (R and μo).

5.3. Results

5.3.1. Sensitivity Analysis Results

Calculated sensitivity indices for model input parameters are plotted in Figures 4.6 and 4.7. According to the first order sensitivity indices shown in Figure 5.6, the most sensitive parameter is the relative size of storage zone (A_s/A) or the relative thickness ($\delta_{adv}+\delta_{dif}$)/H. This result is easily understood since the thickness ($\delta_{adv}+\delta_{dif}$) controls SOD (Eq. (20)) and thus instream DO. It appears from Figure 5.6 that the second most sensitive parameter is the watershed BOD loading rate *L*, followed by μ_o, T_V, and K_1. It is also clear from Figure 5.6 that the parameters D_e and *R* are least sensitive.

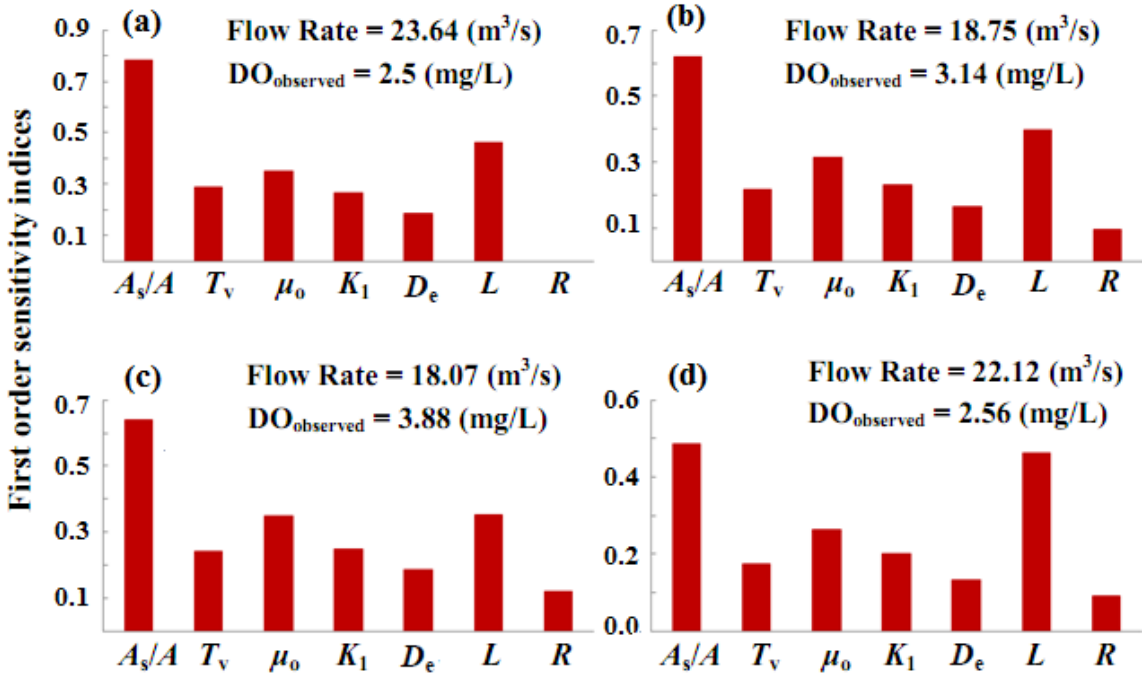

Figure 5.6- First order sensitivity indices based on DO data from first six days of July 1990

Calculated total sensitivity indices shown in Figure 5.7 further confirm that the parameter (A_s/A) or ($\delta_{adv}+\delta_{dif}$)/H has the greatest effect on simulated instream DO, followed by the three reaction parameters L, μ_o, and R. It is interesting that the parameter R is sensitive according to the total sensitivity index while it is insensitive according to the first-order sensitivity index. It appears that the result from the total sensitivity analysis is more reasonable as compared with that from the first-order sensitivity analysis. The least sensitive parameters are K_1, D_e, and T_V. As a result, the three insensitive parameters can be fixed at a value in their variation ranges without causing significant errors in simulated DO concentration in the water column. To that end, K_1 value is set to 3.2×10^{-6} (1/s) for 28°C and the calculated D_e value is 2.9×10^{-7} (m^2/s) based on the average porosity of 0.65. Although T_V does not cause any significant change in DO concentration in water column, it has great impact on DO concentration in the flocculent layer and DO profile in the diffusive bottom sediment layer. Thus, appropriate T_V value should also

yield a reasonable DO concentration profile in the diffusive sediment layer. Such a DO profile should be consistent with findings from previous studies about penetration depth (δ_{dif}).

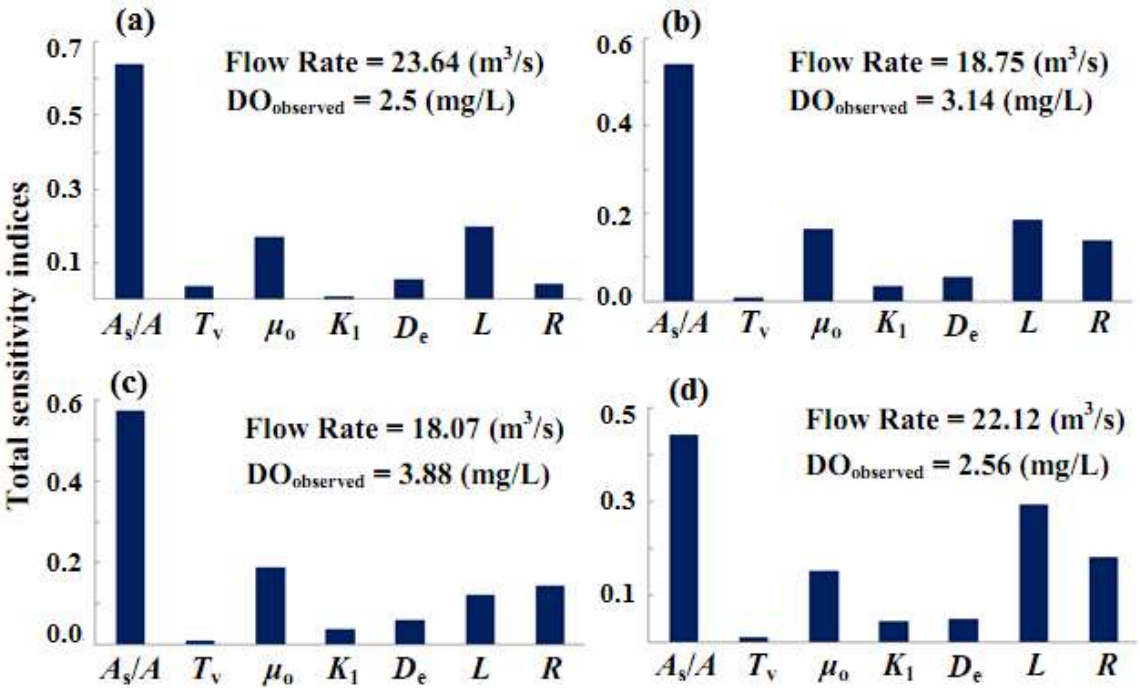

Figure 5.7- Total sensitivity indices based on DO data from first six days of July 1990

For the present study, T_V value is varied from 0.05 hours to 1.5 hours based on extensive simulation results, producing the DO penetration depth of 0.12 to 3.93 mm in bottom sediment, depending on the value of D_e and T_V. Unlike tracer materials or constituents such as nutrients that may accumulate in storage zone and get back to the main stream at later time and thus have relatively large residence time, dissolved oxygen would be promptly consumed as it reaches organic materials in bottom sediment. Benjamin (2010) mentioned that dissolved oxygen is one of the major oxidant in aquatic environments. As a result, it is expected to have relatively small residence time. In other words, a long residence time means that DO remains in the stream for a long time and therefore travels a long distance with flow. As a result, DO level in a downstream

reach should be similar to that in the upstream reach. This situation rarely happens in the Lower Amite River.

It can be seen by combining the results of both the total sensitivity analysis and the first-order sensitivity analysis that DO concentration in water column is sensitive to the parameters A_s/A or $(\delta_{adv}+\delta_{dif})/H$, L, μ_o, and R. In order to consider effects of uncertainty in the sensitive model parameters on simulated DO concentration in water column, various cases are selected and DO simulations are performed for individual cases. The cases are determined according to variation ranges of the sensitive parameters, possible DO penetration depth (δ_{dif}), and least Normalized Root Mean Squared Error (nRMSE).

5.3.2. Simulation Results for DO under High R Value Cases (Scenario 1)

Table 5.1 summarizes simulation results under the high R vale cases. Simulated DO concentrations in water column and bottom sediment vary primarily in response to variations in the sensitive parameters. If the lumped reaction term (R) in the flocculent layer is set to be as high as 28 $mgl^{-1}d^{-1}$, $L = L_{HSPF}$ (a time series), and $A_s/A = 0.15$, the DO in water column reduces from 7.9 mg/l at Denham Springs to as low as 2.85 mg/l at Port Vincent, depending on the value of μ_o.

The nRMSE between simulated DO levels and observed DO data in water column is 0.62 for μ_o = 1500 ($mgl^{-1}d^{-1}$) while nRMSE increases to 0.72 and 1.36 as μ_o reduces to 800 ($mgl^{-1}d^{-1}$) and further to 100 ($mgl^{-1}d^{-1}$), respectively. Accordingly, DO penetration depth (δ_{dif}) increases from 1.5 mm to 3 mm when μ_o decreases from 1500 to 800 ($mgl^{-1}d^{-1}$) and reaches 6 mm for μ_o=100 ($mgl^{-1}d^{-1}$). Effects of increasing BOD loading L (> L_{HSPF}) from watershed on simulate DO are shown as cases 6, 7, and 8 in Table 1. It is clear from Table 1 that both nRMSE and δ_{dif}

increase when μ_o is small (i.e. μ_o= 100 $mgl^{-1}d^{-1}$) even with L =20L_{HSPF}. For the high μ_o value of 1500 $mgl^{-1}d^{-1}$, increasing L raises nRMSE. Thus, optimum nRMSE is obtained when $L = L_{HSPF}$.

As A_s/A reduces from 0.15 to 0.1, nRMSE increases from 0.62 to 0.75 but δ_{dif} remains unchanged (Case 1 in Table 1). If $L > L_{HSPF}$ is also implemented for this case, the nRMSE reduces to 0.61 (Case 2 in Table 1). When A_s/A increases to 0.25, simulated DO concentration in water column generally underestimates observed DO at Port Vincent with high μ_o ($\geq$800 $mgl^{-1}d^{-1}$). For very low μ_o= 100 $mgl^{-1}d^{-1}$, nRMSE increases and the penetration depth in the diffusion layer becomes greater than 6 mm, making this case unrealistic. In addition, increasing L yields δ_{dif} = 0 with higher nRMSE.

Table 5-1- Results of cases in scenario 1

Case NO.	**A_s/A**	**μ ($\times 10^3 mgl^{-1}d^{-1}$)**	**δ_{diff} (mm)**	**nRMSE†**
1	0.1	1.5	1.5	0.75
2**		1.5	1.0	0.61
3	0.15	0.1	6+	1.36
4		0.8	3.0	0.72
5		1.5	1.5	0.62
6**		0.1	6+	0.80
7*		0.8	1.5	0.73
8*		1.5	1.0	0.67
9	0.25	0.1	6+	0.67
10		0.8	1.0	-0.99
11		1.5	1.0	-0.94
12**		0.1	0.0	0.94

* $L = 10L_{HSPF}$ ** $L = 20L_{HSPF}$

† negative nRMSE denotes simulated DO underestimates observed DO concentration

5.3.3. Simulation Results for DO under Moderate R Value Cases (Scenario 2)

Table 5.2 shows simulation results from cases of moderate R value (14 $mgl^{-1}d^{-1}$). The smallest nRMSE with acceptable DO concentration in diffusion layer is obtained for A_s/A = 0.15

and μ_o = 1500 $mgl^{-1}d^{-1}$. The nRMSE value and DO penetration depth (δ_{diff}) are 0.67 and 3.5mm, respectively (Case 17).

Furthermore, when increasing watershed BOD *L* is incorporated, depending on the value of *L*, nRMSE remains unchanged ($L = 10L_{HSPF}$) or increased ($L = 20L_{HSPF}$) while δ_{dif} decreases in both cases. When A_s/A reduced to 0.1 under high μ_o of 1500 $mgl^{-1}d^{-1}$, low nRMSE may be achieved with increasing *L* value.

As relative storage zone size (i.e. A_s/A=0.25) becomes larger, small μ_o values cause the overestimation of DO concentration (Cases 20) while high μ_o values result in the underestimation of DO (Case 22). Although μ_o= 800 $mgl^{-1}d^{-1}$ yields relatively small nRMSE of 0.69, DO penetration depth is unreasonably large. It means that the relative storage zone size of A_s/A=0.25 is too large to occur in fine-grained streams.

Table 5-2- Results of cases in scenario 2

Case NO.	**A_s/A**	**μ ($\times 10^3 mgl^{-1}d^{-1}$)**	**δ_{diff} (mm)**	**nRMSE†**
13	0.1	1.5	2.5	0.83
14*		1.5	2.5	0.69
15	0.15	0.1	6+	2.17
16		0.8	6+	1.41
17		1.5	3.5	0.67
18*		1.5	2.5	0.67
19**		1.5	2.0	-0.76
20	0.25	0.1	6+	1.57
21		0.8	6+	0.69
22		1.5	2.5	-0.86

* $L = 10L_{HSPF}$ ** $L = 20L_{HSPF}$

† negative nRMSE denotes simulated DO underestimates observed DO concentration

5.3.4. Simulation Results for DO under Low R Value Cases (Scenario 3)

The most feasible case under low reaction (i.e. *R*=5.5 $mgl^{-1}d^{-1}$) in the flocculent layer can be produced with small storage zone (A_s/A = 0.1), high μ_o (1500 $mgl^{-1}d^{-1}$), and high watershed

BOD loading ($L = 20L_{HSPF}$). In this case, nRMSE and δ_{dif} are 0.65 and 2.5 mm, respectively. It appears that other cases with low *R* values are less likely to occur due to either overestimation (Case 25) or underestimation (Case 31) of DO concentration in water column. Simulation results for the low *R* value cases are presented in Table 5.3.

5.3.5. Simulation Results for DO under Additional Cases

Three additional cases (33, 34, and 35) are identified and simulated separately. In the first case (33), the relative storage zone size of $A_s/A=0.0$ is considered. When A_s/A reduces to zero, no significant DO reduction is found along the Lower Amite River.

Table 5-3- Results of cases in scenario 3

Case NO.	A_s/A	μ_0 ($\times 10^3 mgl^{-1}d^{-1}$)	δ_{dif} (mm)	nRMSE†
23	0.1	1.5	3.5	0.89
24**		1.5	2.5	0.65
25	0.15	0.1	6+	2.70
26		0.8	6+	1.52
27		1.5	4	0.74
28**		1.5	3	0.74
29	0.25	0.1	6+	2.41
30		0.8	6+	1.25
31		1.5	6+	0.70
32**		1.5	3	-0.99

* $L = 10L_{HSPF}$ ** $L = 10L_{HSPF}$

† negative nRMSE denotes simulated DO underestimates observed DO concentration

The DO level at Denham Springs station is 7.9 mg/l while the DO just slightly reduces to 7.65 mg/l at Port Vincent station regardless of the magnitude of μ_o and *R*. This result is consistent with that of sensitivity analysis about the importance of storage zone size. Case 34 is designed according to previous studies by Dropp and Amos (2001) on the flocculent layer in fine-grained streams. This case is designed particularly for the Lower Amite River reach close to

the Port Vincent station. The parameter A_s/A or $(\delta_{adv}+\delta_{dif})/H$ is reduced to a small value of 0.0088, corresponding to the thickness of ($\delta_{adv}+\delta_{dif}$ = 8 + 3.5 mm) = 11.5 mm. For the very thin (8 mm) layer of sediment, the residence T_V becomes as small as 0.05 hours. With μ_o= 2000 $mgl^{-1}d^{-1}$ and R=28 $mgl^{-1}d^{-1}$, nRMSE becomes 0.72.

Measured data on BOD concentration in bottom sediment are rarely available. In addition, BOD concentration in bottom sediment may also vary along rivers. The highest R value used in the sensitivity analysis is 28 $mgl^{-1}d^{-1}$. To understand the effect of extremely high R value on instream DO level, Case 35 with R = 275 $mgl^{-1}d^{-1}$ and A_s/A =0.15 is simulated. The result indicates that dissolved oxygen is almost completely consumed in the flocculent layer ($C_F \approx 0$ mg/L) before reaching diffusion layer. In this case the parameter R is the dominant sink term and the instream DO level is independent of μ_o value. The nRMSE for this case is 0.6.

5.3.6. Simulation Results for Spatial Variations in DO and SOD

Figure 5.8 shows normalized DO concentration profiles in the overlying water column, the flocculent layer, and diffusive bottom sediment layer under Cases 5 and 34 listed in Table 1. It also shows DO penetration depth at Denham Springs station, Port Vincent station, and a third station in between that is 17 km downstream of Denham Springs Station. The overall variation trends in the vertical DO profiles particularly in the bottom sediment layer are similar to those produced by Higashino and Stefan (2011), Higashino et al. (2004), and Steinberger and Hondzo (1999) using the concept of diffusive boundary layer above the sediment-water interface. The difference is due to introduction of advection-dominated storage zone in this study with constant DO concentration throughout the flocculent layer and water column layer.

Figure 5.9 shows simulated SOD variations along the Lower Amite River under five different cases. While a constant R value is adopted in the simulation of each case, the R value

may actually vary along the river due to the change in the composition of sediment particle size and organic content in the sediment. Therefore, actual variation of SOD along the river may be a combination of the cases. The upper reach close to the Denham Springs may have a relatively low *R* value like Case 24 while the lower reach close to the Port Vincent may have a high *R* value like Case 34. Anyway, it is the SOD that causes gradual reduction in DO from the upstream Denham Springs station (DO = 7.9 mg/l) to the downstream Port Vincent station (DO ≈ 3 mg/l).

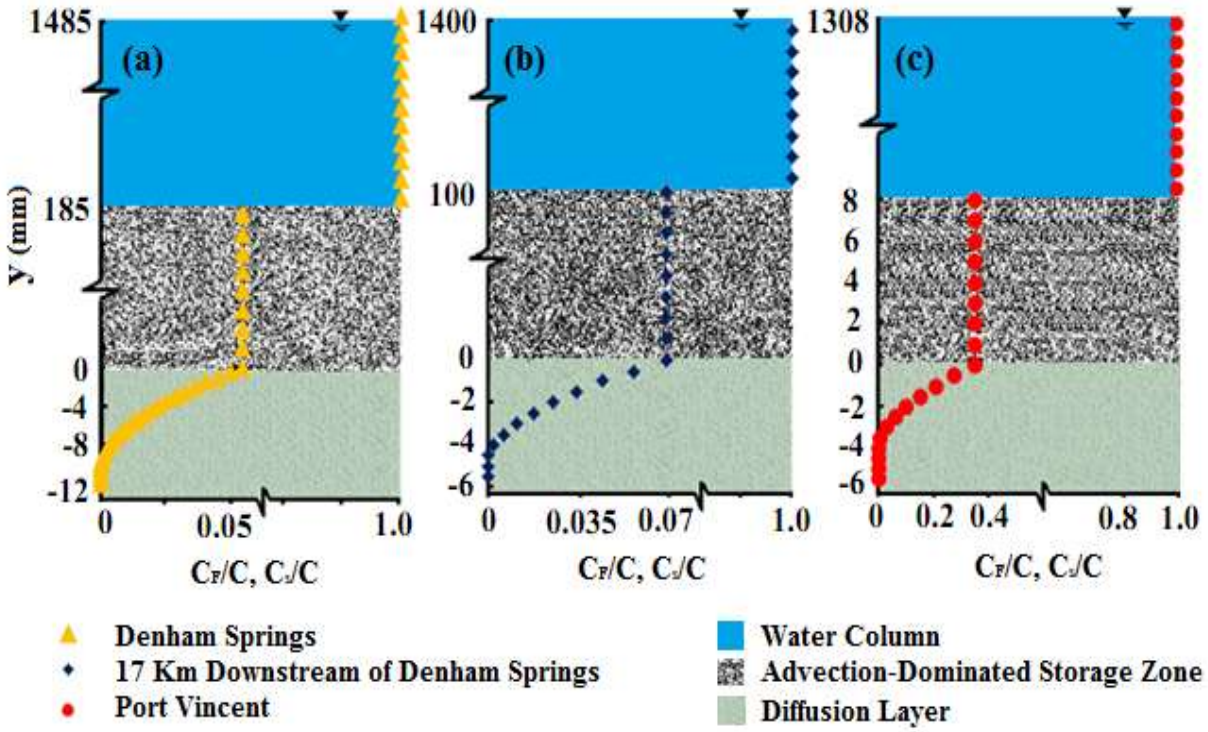

Figure 5.8- Vertical DO concentration ratio relative to DO concentration in water column at Denham Springs station (a-Case 5), Port Vincent station (c- Case 34), and a third station in between (b).

Figure 5.10 shows the DO reduction along the Amite River due to the SOD under Case 2 for four different flow conditions. The DO data observed at Denham Springs and Port Vincent stations are also included. It can be seen from Figure 10 that the DO drops rapidly in the upper

10 km and then declines slowly in the lower portion of the river reach. The slow reduction in DO in the lower reach may be due to the low DO in water column and low DO concentration gradient across the sediment-water interface. Another mechanism possibly responsible for the slow reduction in DO is the increased reaeration at water surface, balancing the DO reduction due to SOD.

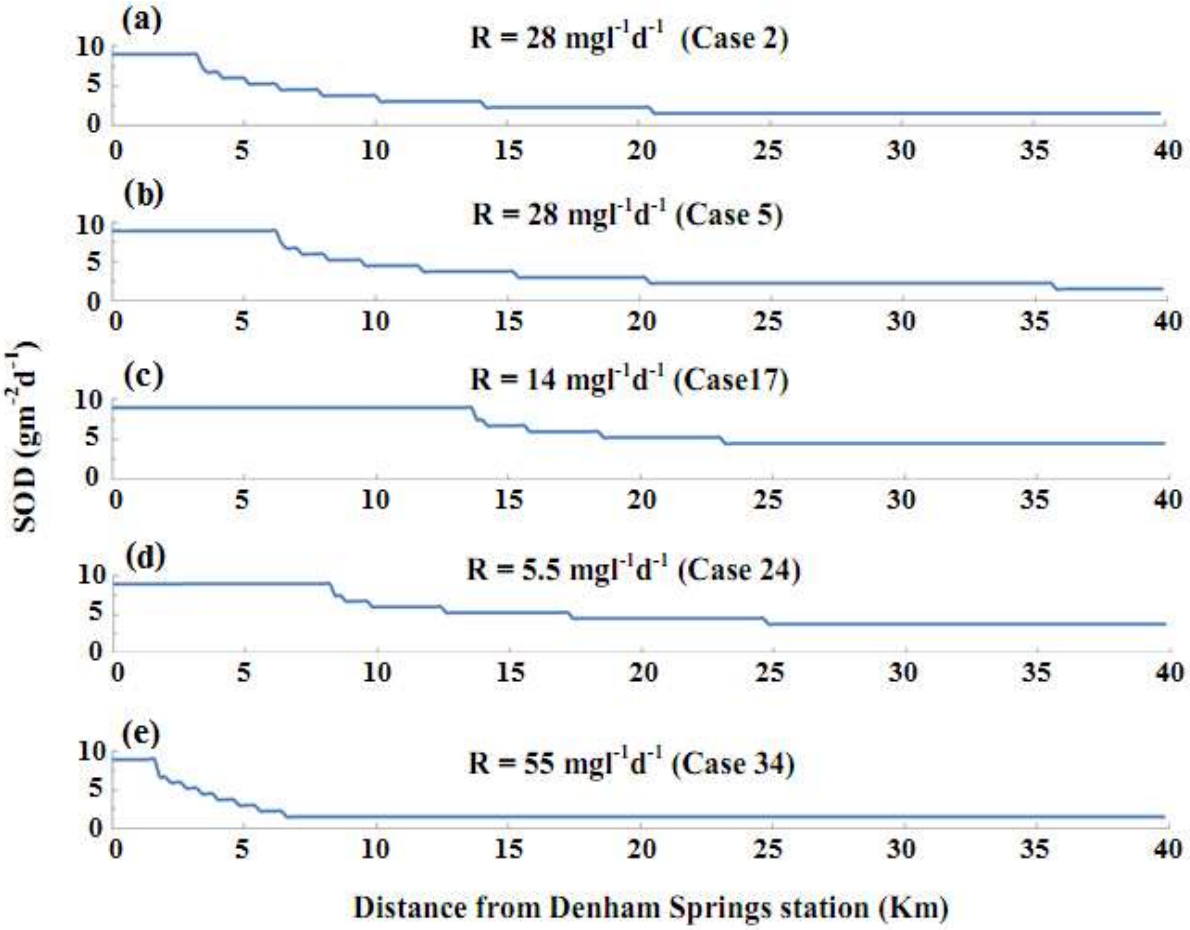

Figure 5.9- SOD variation along Amite River under different conditions

5.3.7. Mapping Longitudinal Variations in DO and SOD along Amite River

In order to better display spatial variations in DO and SOD, numerical simulation results of DO and SOD can be displayed as raster data in ArcGIS which then are used to create KML (Keyhole Markup Language) files or KMZ (Keyhole Markup language Zipped) files in ArcGIS

(Geographic Information System). The KML/KMZ files can be opened on the Google Earth to generate interactive Google maps. The Google maps can be viewed at various spatial scales (Figure 5.11 and 5.12) with different details such as river networks, cities, and land use/land cover. Figures 11 and 4.12 show Google maps for simulated variations in DO and SOD along the Lower Amite River, respectively.

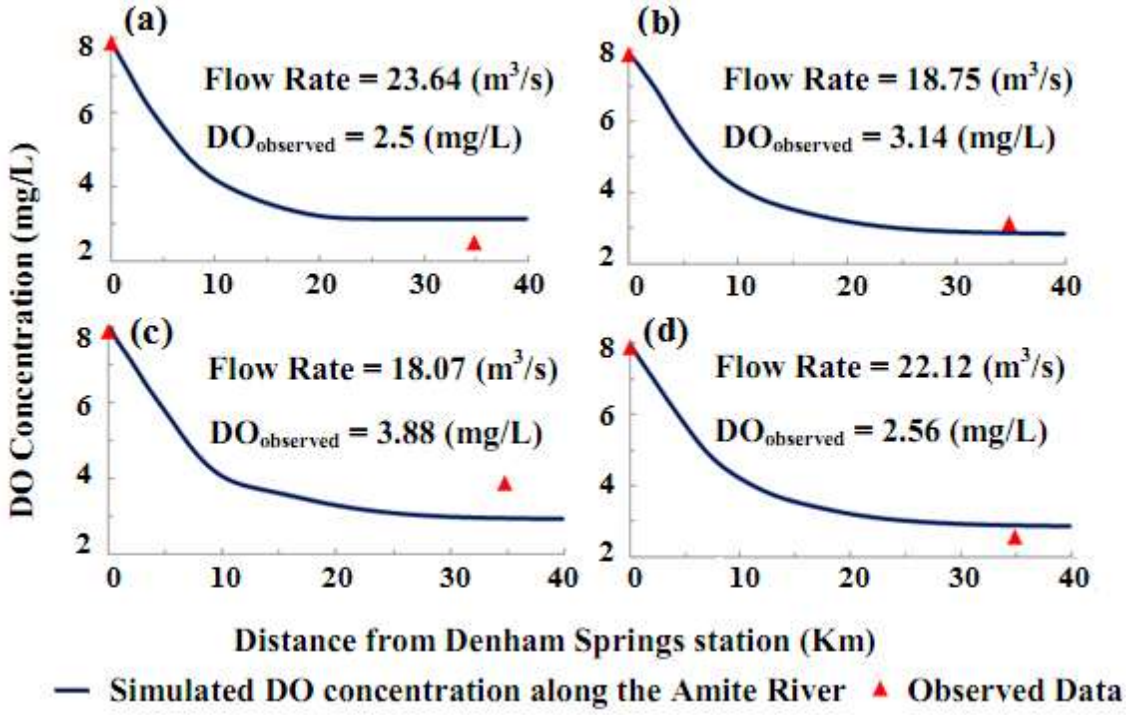

Figure 5.10- Spatial variation of DO along Amite River for case 2

It is clear from Figures 5.11 and 5.12 that DO concentration in the upper 7 km of the 40 km long river reach meets the water quality standard of 5 mg/L. The DO level drops to about 3 mg/L (in red color) in the lower 11.6 km of the river reach, where two tributaries, the Claycut Bayou and the Bayou Manchac collecting runoff from the Baton Rouge metropolitan area (Figure 5.1), join the Amite River. It appears from the maps that the Claycut Bayou and the Bayou Manchac are potentially major sources of DO pollution to the Lower Amite River. Figure 5.13 is a SOD

map showing longitudinal variation in SOD along the 40 km long river reach. The SOD is dependent on availability of DO in water column.

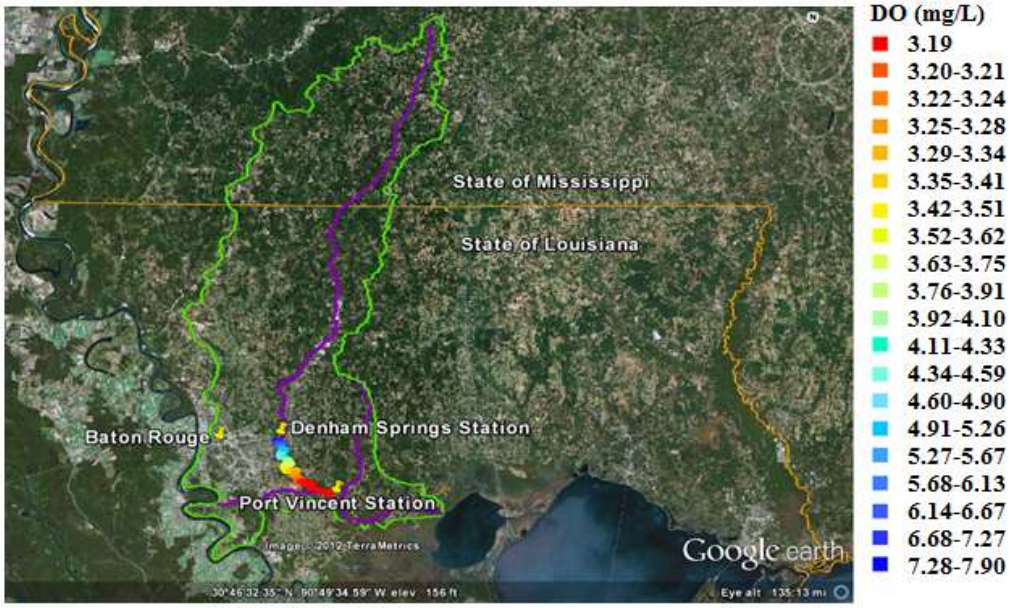

Figure 5.11- Watershed-scale map showing DO variation along Amite River

Figure 5.12- Reach-scale map showing DO variation along Amite River

The low SOD in the lower portion of the river reach is attributed to the low DO fluxes into the sediment layers due to low DO gradient across the sediment water interface. The SOD map in Figure 5.13 is consistent with the DO map in Figure 5.12.

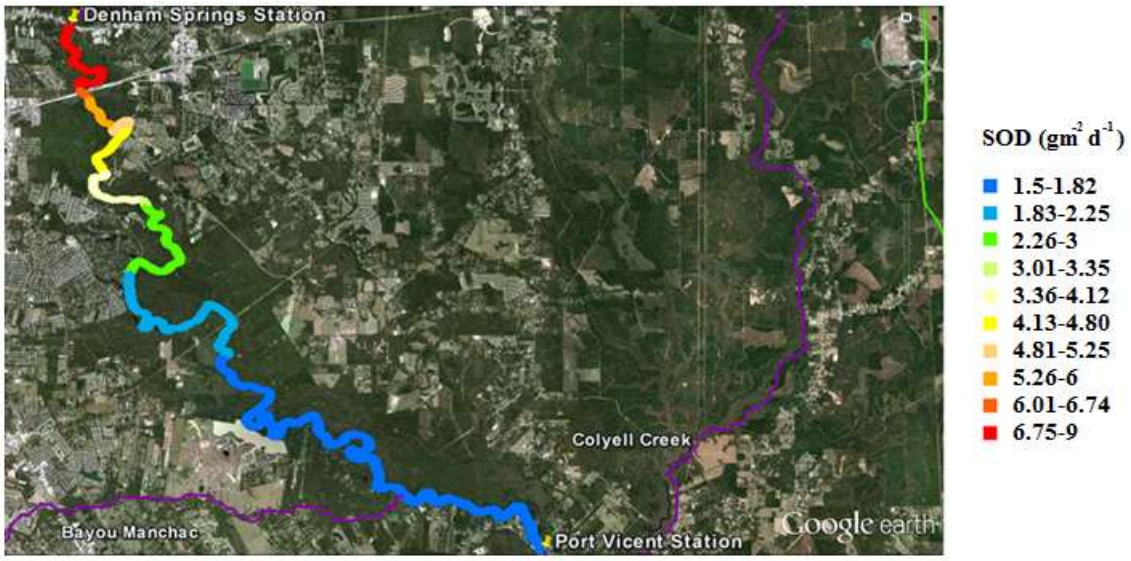

Figure 5.13- Spatial variations of SOD along Amite River between Denham Springs and Port Vincent Stations

5.4. General Discussion

Instream DO estimations were conventionally conducted under certain predefined conditions while the conditions may change significantly over time and space, causing high uncertainty in calculated DO concentrations. Therefore, it is important to recognize the uncertainty and incorporate the natural variability and associated uncertainties in model input parameters into DO simulations so that effects of the uncertainties on simulated DO concentrations could be identified and taken into account in TMDL development and implementation. This paper demonstrates how the VART DO-3L model could be employed to analyze and understand instream DO variations under uncertain environmental conditions.

It can be seen from both the sensitivity analysis and the simulation results of various cases that the relative size of storage zone (A_s/A) or the relative thickness ($\delta_{adv}+\delta_{dif}$)/H of the flocculent layer and the diffusive layer is by far the most important parameter to instream DO modeling. Unfortunately, this critical parameter, particularly the flocculent layer (δ_{adv}), is rarely taken into account in existing DO models for streams. Therefore, the incorporation of the flocculent layer (δ_{adv}) into DO modeling is a unique and important feature of the VART DO-3L model. While the ($\delta_{adv}+\delta_{dif}$)/H is the most sensitive model input parameter, the instream DO reduction is fully controlled by the three reaction terms, including the BOD in water column (L) and the SOD in the flocculent layer (R) and in the diffusive bottom sediment (μ_o). Even in the cases (e.g. Cases 30 and 31 in Table 5.3) with relatively smaller DO penetration depths, μ_o is still high, indicating high biological activities or reactions in bottom sediment. Likewise, high reaction rates (R) in the flocculent layer are also found in the simulations (Cases 2, 5, and 8 in Table 5.1). RMSEs for the three cases are 0.61, 0.62, and 0.67, respectively.

While producing low RMSE (0.61), Case 2 is less likely to occur since it requires the watershed BOD loading (L) that is as high as twenty times ($L = 20L_{HSPF}$) the BOD loading (L_{HSPF}) predicted by the HSPF model. Case 8 is based on the BOD loading rate (L) that is ten times ($L = 10L_{HSPF}$) the BOD loading predicted by the HSPF model. While the BOD loading (L) in this case is still much higher than the HSPF model prediction (L_{HSPF}), the concentration (L) is close to the BOD concentration observed during storm events in the Bayou Manchac (LDEQ, 2010), a major tributary of the Lower Amite River. The high concentration of BOD in the Bayou Manchac is attributed to growing urbanization and land use change in the Lower Amite River watershed.

According to simulation results from the VART DO-3L model, the DO level at the Port Vincent station would not drop to the observed low levels (Figure 10) under the high BOD loading ($L = 10L_{HSPF}$) alone. As a result, the parameter combination for Case 5 in Table 2 is more reasonable than other cases for the river reach close to the Denham Springs station characterized by sandy bottom sediment. The DO penetration depth for this case is 1.5 mm which is in the range of 0-3.39 mm determined from Eq. 5. For the reach close to the Port Vincent station characterized by fine-grained sediment, Case 34 seems to produce more realistic results though the nRMSE is higher than that in Case 5. Due to the transition of sediment particle size from the Denham Springs station with sandy sediment to the Port Vincent station with silt sediment, the DO variations along the Lower Amite River may better be described by combining Cases 5 and 34.

A limitation of this study is the use of constant values for the lumped reaction parameters R and μ_o along the Amite River. This, however, rarely happens in nutrient enriched rivers like the Amite River due to the change in both the composition of sediment particle size and the content of nutrients in bottom sediment. More efforts are needed to identify and describe the variability in the reaction parameters.

While this paper focuses on modeling of DO in fine-grained streams with flocculent layer, the VART DO-3L model is also applicable to sandy and gravel rivers or river reaches like the reach close to the Denham Springs station. For sandy and gravel rivers, Eq. (2) can be employed to simulate the upper sediment layer with relatively uniform solute concentration (Deng and Jung 2009) while Eq. (3) can be used for the lower diffusive layer (Figure 8 b and c). The VART DO-3L model can also be applied to simulate other pollutants and nutrients such as nitrate-nitrogen by replacing the reaction terms in Eqs. (1) – (3).

5.5. Conclusions

A new modeling tool, called VART DO-3L, is presented in this paper for simulation of instream dissolved oxygen (DO) variations. The VART DO-3L is innovative in terms of modeling the triple-layers, including water column, an advection dominated sediment layer, and a diffusion-dominated sediment layer in streams. Major findings from the VART DO-3L model application to the Lower Amite River can be summarized as follows:

1) The relative size of storage zone (A_s/A) or the relative thickness ($\delta_{adv}+\delta_{dif}$)/H of the flocculent layer and the diffusive layer is the most important parameter to modeling DO variations in nutrient enriched streams with fine-grained sediment. While the ($\delta_{adv}+\delta_{dif}$)/H is the most sensitive model input parameter, the instream DO reduction is fully controlled by the three reaction terms, including the BOD in water column (L) and the SOD in the flocculent layer (R) and the diffusive bottom sediment (μ_o).

2) DO levels in the Lower Amite River exhibits strong variations at various spatial scales ranging from millimeters in bottom sediment to meters in water column and further to kilometers in the longitudinal flow direction. In terms of longitudinal variation, the DO level decreases from 7. 9 mg/L at the Denham Springs station to about 2.89 mg/L at the Port Vincent station. In terms of vertical variation, the DO level drops rapidly from the overlying water column to the advective layer and further to the diffusive layer. The DO level in the advective layer is about 6% - 40% of that in water column. The thickness of the diffusive layer varies, depending on effective diffusion coefficient, in the range from 0 to about 10 mm.

3) Variations in SOD are controlled by the parameters R, μ_o, A_s/A, and watershed BOD loading L. The higher the R value, the steeper the slope of SOD reduction along the river. Overall, the SOD tends to approach a constant value (SOD_∞) along the lower portion of the river reach.

4) The spatial and particularly longitudinal variations in DO and SOD can be efficiently mapped using ArcGIS and Google Earth. The Google Earth map indicates that the DO level drops significantly downstream of the Claycut Bayou confluence and particularly the Bayou Manchac confluence, indicating that the Claycut Bayou and the Bayou Manchac are potentially the major sources of DO pollution to the Lower Amite River.

5) Uncertainties in model input parameters may be addressed by combining Monte Carlo method and scenario/case simulations.

6) While this paper focuses on modeling of DO in fine-grained streams, the VART DO-3L model is also applicable to sandy and gravel rivers. The VART DO-3L model can be extended to simulation of other pollutants and nutrients such as nitrate-nitrogen by replacing reaction terms in the model, providing a versatile tool for modeling stream water quality.

5.6. References

Arega, F., Lee, J. (2005). Diffusional Mass Transfer at Sediment–Water Interface of Cylindrical Sediment Oxygen Demand Chamber. J Environ Eng; 131: 755–66,

Bencala, K.E., Walters R.A. (1983). Simulation of solute transport in a mountain pool-and-riffle stream: A transient storage model. Water Resour Res; 19: 718–24.

Benjamin, M.M. (2010). Water chemistry. Long Grove, IL:Waveland Press.

Boudreau, B.P. (1996). Diagenetic models and their implication: Modeling transport and reactions in aquatic sediments.Heidelberg, Germany: Springer.

Boudreau, B.P., Joergensen, B.B., editors (2001). The benthic boundary layer. Oxford, UK: Oxford University Press.

Chan, K., Tarantola, S., Saltelli, A., Sobol, I.M. (2000). Variance-based methods. In: Sensitivity Analysis.Saltelli A,Chan K, Scott EM, editors. New York: Wiley; p. 167–197.

Corsi, S.R., Klaper, R.D., Weber, D.N., Banneerman, R.T. (2011). Water- and sediment-quality effects on Pimephales promelas spawning vary along an agriculture-to-urban land-use gradient. Sci Total Environ; 409:4847-57.

Cox, B.A. (2003). A review of dissolved oxygen modeling techniques for lowland rivers. Sci Total Environ; 314-316: 303-34.

Chapra, S.C., Runkel, R.L. (1999). Modeling impact of storage zones on stream dissolved oxygen. J Environ Eng; 125(5).

Dade, W.B. (1993). Near-bed turbulence and hydrodynamic control of diffusional mass transfer at the sea floor. Limnol Oceanogr; 38, 52-69.

Deng, Z-Q., Jung, H-S. (2009). Variable residence time-based model for solute transport in streams. Water Resour Res; 45, W03415.

Deng, Z-Q., Jung, H-S., Ghimire, B. (2010). Effect of channel size on solute residence time distributions in rivers. Advances in Water Resour; 33 (9), 1118–1127

Deng, Z-Q., Patil, A. (2011). Assessment of water quality variation in Amite River watershed under changing climate and land use. Water Quality: Current Trends and Expected Climate Change Impacts, IAHS Publ.; 348.

DiToro, D.M. (2001). Sediment flux modeling. New York: Wiley.

Droppo, I.G., Amos, C.L. (2001). Structure, stability, and transformation of contaminated lacustrine surface fine-grained laminae. J Sediment Res; 71 (5)

Droppo, I.G., Stone, M. (1994). In-channel surficial fine-grained sediment laminae (Part I): Physical characteristics and formational processes. Hydrol Process; 8 (2): 101-111.

Fesanghary, M., Damangir, E., Soleimani, I. (2009). Design optimization of shell and tube heat exchangers using global sensitivity analysis and harmony search algorithm. Appl Therm Eng; 29: 1026-1031.

Ganaoui, O., Schaaff, E., Boyer, P., Amielh, M., Anselmet, F., Grenz, C. (2007). Erosion of the Upper Layer of Cohesive Sediments: Characterization of Some Properties. J Hydraul Eng; 133: 1087–91.

Garcia, M.H. (2008). Sediment transport and morphodynamics. Sedimentation engineering: Processes, measurements, modeling and practice. Garci MH, editor. ASCE manual of practice 110. Chap. 2, 21–163, Reston, VA.

Ghimire, B., Deng, Z-Q. (2013). Hydrograph-based Approach to Modeling Bacteria Transport and Fate in Rivers. Water Res; 47: 1329-43.

Higashino, M. (2011). Oxygen consumption by a sediment bed for stagnant water: Comparison to SOD with fluid flow. Water Res;45:4381-89.

Higashino, M., Stefan, H. (2011). Dissolved Oxygen Demand at the Sediment-Water Interface of a Stream: Near-Bed Turbulence and Pore Water Flow Effects. J Environ Eng; 137: 531–540

Higashino, M., Gantzer, C.J., Stefan, H.G. (2004). Unsteady diffusional mass transfer at the sediment/water interface: Theory and significance for SOD measurement. Water Res; 38: 1-12.

Higashino, M., Stefan, H.G. (2005). Oxygen demand by a sediment bed of finite length. J Environ Eng, ASCE; 31(3).

Homma, T., Saltelli, A. (1996). Importance measures in global sensitivity analysis of nonlinear models. Reliab. Eng. Syst. Safety;52.

Hondzo, M., Feyaerts, T., Donovan, R., O'Connor, B. (2005). Universal scaling of dissolved oxygen distribution at the sediment-water interface: A power law. Limnol Oceanogr; 50: 1667-76.

House, W.A. (2003). Factors influencing the extent, development of the oxic zone in river-bed sediment. Biogeochemistry;63:317-33.

Kleeberg, A., Hupfer, M., Gust, G. (2008). Quantification of phosphorus entrainment in a lowland river by in situ and laboratory resuspension experiments. Aquatic Sciences - Research Across Boundaries; 70:87-99.

Bayou Manchac watershed TMDL for biochemical oxygen-demand substances (Phase I) (2010)- final report. Baton Rouge, LA, USA: Louisiana Department of Environmental Quality (LDEQ).

Malcolm, I.A., Soulsby, C., Youngson, A.F., Hannah, D.M., McLaren, I.S., Throne, A. (2004). Hydrological influences on hyporheic water quality: implications for salmon egg survival. Hydrol Process;18: 1543-60.

McAnally, W.H., Friedrichs, C., Hamilton, D., Hayter, E., Shrestha, P., Rodriguez, H., Sheremet, A., Teeter, A. (2007). Management of fluid mud in estuaries, bays, and lakes. I: Present state of understanding on character and behavior. ASCE Task Committee on Management of Fluid Mud, J Hydraul Eng; 133: 9–22.

Nakamura, Y., Stefan, H.G. (1994). Effect of flow velocity on sediment oxygen demand: Theory. J Environ Eng, ASCE; 120(5).

Nordin, C.F., Sabol, G.V. (1974). Empirical data on longitudinal dispersion in rivers. Water-Resources Investigations; 20-74, US Geological Survey, Denver, CO.

O'Connor, B.L., Harvey, J.W. (2008). Scaling hyporheic exchange and its influence on biogeochemical reactions in aquatic ecosystems. Water Resour Res;44, W12423.

Owens, P.N., Walling, D.E. (2002). The phosphorus content of fluvial sediment in rural and industrialized river basins. Water Res;36: 685–701.

Parr, L.B., Mason, C.F. (2004). Causes of low oxygen in a lowland, regulated eutrophic river in eastern England. Sci Total Environ; 321:273-286

Patil, A., Deng, Z-Q., Malone, R.F. (2011). Input data resolution-induced uncertainty in watershed modeling. Hydrol Process;25:2302-2312.

Runkel, R.L. (1998). One-dimensional transport with inflow and storage (OTIS): A solute transport model for streams and rivers. US Geol Surv Water Resour Invest; 98-4018.

Sobol, I.M. (1993). Sensitivity analysis for nonlinear mathematical models. Math Model Comput Exp; 1:407–14.

Saltelli, A., Tarantola, A., Campolongo, F., Ratto, M. (2004). Sensitivity Analysis in Practice: A Guide to Assessing Scientific Models. New York: Wiley.

Saltelli, A., Tarantola, S., Campolongo, F. (2000). Sensitivity analysis as an ingredient of modeling. Stat Sci; 15: 377–95.

Steinberger, N., Hondzo, M. (1999). Diffusional mass transfer at sediment-water interface. J Environ Eng, ASCE; 125:192-200.

Stofleth, J.M, Shields Jr., F.D., Fox, G.A. (2008). Hyporheic and Total Transient Storage in Small Sand-Bed Streams. Hydrol Process; 22: 1885-94.

Stone, M., Droppo, I.G. (1994). In-channel surficial fine-grained sediment laminae. Part II: Chemical characteristics and implications for contaminant transport in fluvial systems. Hydrol Process; 8:113-24.

Sweerts, J.P.R.A., Bar-Gilissen, M.J., Corneles, A.A., Cappendberg, T.E. (1991). Oxygen consuming processes at the profundal and littoral sediment-water interface of a small meso-eutrophic lake. Limnol Oceanogr; 36: 1124-33.

Taylor, K.G., Boyd, N.A., Boult, S. (2003). Sediments, porewaters and diagenesis in an urban water body, Salford, UK: impact of remediation. Hydrol Process;17:2049-61.

Todd, M.J., Vellidis, G., Lowrance, R.R., Pringle, C.M. (2009). High sediment oxygen demand within and instream swamp in southern Georgia: Implications for low dissolved oxygen levels in coastal blackwater streams. J Am Water Resour As; 45: 1493-1507.

Tong, Y., Deng, Z-Q. (2013). Moment-Based Method for Identification of Pollution Source in Rivers. J Environ Eng, ASCE (in press).

van Griensven, A., Meixner, T., Grunwald, S., Bishop, T. (2006). A global sensitivity analysis tool for the parameters of multi-variable catchment models. J Hydrol; 324:10-23.

Westrich, B., Förstner, U., editors (2007). Sediment dynamics and pollutant mobility in rivers: an interdisciplinary approach. New York: Springer.

Zahraeifard, V., Deng, Z-Q. (2012a). Modeling sediment resuspension-induced DO variation in fine-grained streams. Sci Total Environ; 441:176-81.

Zahraeifard, V., Deng, Z-Q. (2012b) VART Model-Based Method for Estimation of Instream Dissolved Oxygen and Reaeration Coefficient. ASCE J Environ Eng; 138: 518 -24.

CHAPTER 6
SUMMARY OF MAJOR FINDINGS AND DISCUSSION

6.1. Summary

The main purpose of this dissertation is to introduce a modeling framework for simulating dissolved oxygen in lowland rivers with fine-grained, organic-rich bottom sediment. Due to extremely mild (near flat) slope of lowland rivers, suspended particles/solids with high concentration in water column begin to aggregate and deposit specifically in low flow condition of hot summer time. This process eventually leads to the formation of a flocculent layer (advection dominated layer) on the top of relatively consolidated bottom sediment (diffusion-dominated layer). Based on this theory, the three-layer model, VART-DO-3L, was proposed which also includes the major physical (i.e. advection, dispersion, hyporheic exchange) and biochemical (i.e. BOD degradation, oxidation of organic materials) processes that affect DO variations in lowland rivers. The VART-DO-3L model allows the computation of spatial and temporal changes in DO in water column, flocculent layer, and bottom sediment. With the VART-DO-3L model, it is also possible to quantify sediment oxygen demand in different locations along the river at different times. The VART-DO-3L model draws a new perspective on exchange of dissolved oxygen in lowland rivers from water column to the flocculent layer (storage zone), which usually has high concentration of organic materials, and further to the bottom sediment (diffusion layer). Since detailed information about the DO consumers (i.e. BOD, algae, reduced metal ions, etc.) in flocculent layer and bottom sediment is rarely available, lumped reaction terms were used in the proposed VART-DO-3L model to represent DO consumption/uptake due to existence of various sinks. An uncertainty analysis and a scenario-based evaluation can accompany the simulations to address uncertainty in these reaction terms.

The VART-DO-3L model is also applicable to sandy/gravel rivers without any change to the structure of the model and to other constituents by considering appropriate changes to the influential processes and sink/source terms. The VART-DO-3L model was applied to the Lower Amite River in Louisiana, USA to verify its performance and demonstrate a practical application of the model. Detailed elaborations on the VART-DO-3L model were presented in Chapter 5.

The VART-DO-3L model can be simplified by ignoring DO exchange in bottom sediment especially when detailed mapping of DO concentration changes in the sediment is not required. In such circumstances, sediment oxygen demand can be considered by a lumped term defined as SOD. Furthermore, during flood events, accumulated materials (i.e. BOD, algae, and reduced metal ions) in river bed are inclined to re-suspension. Thus, beside watershed BOD, resuspension of river bed materials is an additional burden on DO concentration in water column and needs to be properly considered in simulation of DO. Therefore, the VART-DO-3L model can be modified to the VART-DOS model by keeping main processes (i.e. advection, dispersion, hyporheic exchange, reaeration, and BOD degradation) and accounting for the sediment resuspension effect. Since resuspension is very much dependent on erosion rate and thus on flow rate, during base-flow condition (lower erosion rate) the impact of sediment resuspension vanishes to minimal value in VART-DOS simulation. Effect of temperature on sediment-induced DO consumption was considered in the VART-DOS model. The VART-DOS model was calibrated and applied to the case of Amite River during high flow (Jan. 1990) and low flow (July 1990) conditions. The results showed that up to 83% of DO consumption in water column during July of 1990 can be attributed to the resuspension of bottom particles. In contrast, resuspension is ineffective in DO consumption during January 1990. Details about the VART-DOS model are given in Chapter 4.

The VART-DO-3L model can be further simplified by ignoring the exchange of DO between water column and bottom sediment to get the VART-DO model. Like the VART-DO-3L model, diurnal effects of photosynthesis and respiration are also overlooked due to the lack of detailed observed data for DO. In fact, the VART-DO model was deliberately kept simple by considering only the processes that exist in all types of rivers: advection, dispersion, hyporheic exchange (storage zone effect), BOD degradation, and reaeration such that the fundamental impact of dispersion and hyporheic exchange on reaeration coefficient (K_2) in rivers may be understood. By collecting observed DO data from river reaches that are free from BOD materials, it is possible to ignore DO consumption because of BOD degradation. The results in Chapter 2 revealed that hyporheic exchange can reduce reaeration coefficient by 30% while dispersion can increase K_2 by 50%. Generally, combined effects of storage zone and longitudinal dispersion yield reaeration coefficients that were up to six times greater than reaeration coefficients predicted by empirical equations.

Consideration of watershed contribution to in-stream DO changes was an important component of model development in this dissertation. The impact of watershed BOD, conventionally ignored in DO simulations, was captured by using watershed HSPF (Hydrologic Simulation Program-Fortran) model and integrating the results into in-stream VART series model. Thus, DO allocation to non-point source pollution is clearly addressed prior to identification of other potential sources of DO consumption.

6.2. Discussion of Future Work

Throughout present study the focus was on daily time scale simulation of DO in the river. Diurnal changes of DO, however, can be substantive in formation of DO shortage. In fact, diurnal variation of DO requires consideration of additional sink/source terms such as

photosynthesis, respiration, canopy shading. A comprehensive DO model platform should address these interactions as well.

The procedures discussed throughout this dissertation for development of modeling tools for studying DO variations in riverine environments are also applicable in development of models for other water quality indicators. The biggest shortcoming in such model development studies, however, is availability of observed data from the environment. In fact, gathering data and data analysis are primary steps in development of a new modeling tool. Furthermore, introducing a modeling platform with high predicting capability requires more reliable data for both calibration and validation. This is especially important as new contaminants, such as hormones, and pharmaceutical compounds pose threats to our water resources. Thus, as we continue to introduce new models we need to improve data gathering techniques. Sensor technologies along with sophisticated data gathering algorithms provide unprecedented data acquisition methods. Such an approach in data gathering is also helpful in conducting stochastic modeling and analysis such as Bayesian analysis in water resources planning and management. Watershed responses to climate change can seriously affect water quality parameters. Irregular flood events/drought patterns can change hydraulic and morphology of the region leading to change in water quality indicators. Thus, climate change impact should be considered in our decision making and management of water resources.

VITA

Vahid Zahreaifard was born in 1980 in Shiraz, Iran. He received his Bachelor of Science in Civil Engineering from University of Tabriz, Tabriz, Iran in 2003. He, then, pursued his graduate studies in the Department of Civil and Environmental Engineering at Shiraz University (former Pahlavi University), Shiraz, Iran. He got his Master's degree in 2006 with emphasis on water resources and hydraulic engineering. In 2008, Vahid joined the Department of Civil and Environmental Engineering, Louisiana State University. In December 2011, he got his second Master's degree in Civil Engineering prior to receiving the PhD degree in 2013.